Republic of Iraq
Ministry of Higher Education and Scientific Research
University of Misan/College of Engineering
Department of Civil Engineering

IMPROVING CARRYING CAPACITY OF REINFORCED CONCRETE BEAMS USING STEEL WIRE MESH AS SHEAR REINFORCEMENT

by

Sarah Hussain Hameed
B.Sc. in Civil Engineering, 2018

A thesis submitted in partial fulfillment
of the requirements for the Master of Science
degree in Civil Engineering
University of Misan

June2022

Thesis Supervisor: Prof. Dr. Abdulkhaliq Abdulyimah Jaafer

بِسْمِ اللَّهِ الرَّحْمَنِ الرَّحِيمِ

(يَا أَيُّهَا الَّذِينَ آمَنُوا إِذَا قِيلَ لَكُمْ تَفَسَّحُوا فِي الْمَجَالِسِ فَافْسَحُوا يَفْسَحِ اللَّهُ لَكُمْ وَإِذَا قِيلَ انْشُزُوا فَانْشُزُوا يَرْفَعِ اللَّهُ الَّذِينَ آمَنُوا مِنْكُمْ وَالَّذِينَ أُوتُوا الْعِلْمَ دَرَجَاتٍ وَاللَّهُ بِمَا تَعْمَلُونَ خَبِيرٌ)

صدق الله العلي العظيم

سورة المجادلة الآية 11

DEDICATION

To my mother

To my family

To my close friends

ACKNOWLEDGEMENTS

Praise is to Allah to give me the ability and patience to Complete this work despite all the difficulties that have faced me.

I would like to express my thanks to my supervisor Prof. Dr. Abdulkhaliq A. Jaafer for follow me in the research.

I would like to extend my thanks to Prof. Dr. Abbas O. Dawood Dean of the college of engineering, Assistant Professor Dr. Samir Mohammed chassib and I would like to express my thanks and appreciation for your great efforts in helping me Prof. Dr. Saad Fahad, Dr. Hayder AL-Khazraji and to all my teachers Prof. Dr. Ahmad Al-Shara, Dr. Faten I. Mussa, and Dr. Murtada Abass.

I would like to thank M.Sc. Hussain Sadiq, M.Sc. Ali Wathiq, and M.Sc. Saba Laith I just wanted to express how much I appreciate your supports.

Finally, special appreciation and love go to my dear mother for her love and great support which has been a source of strength and motivation.

Sarah Hussain Hameed

2022

CERTIFICATION

I certify that the thesis entitled (**Improving Carrying Capacity of Reinforced Concrete Beams Using Steel Wire Mesh as Shear Reinforcement**) which is being submitted by **Sarah Hussain Hameed** is prepared under my supervision at the University of Misan in partial fulfillment of the requirements for the Degree of Master of Science in Civil Engineering (Structures).

Signature:
Name: **Prof. Dr. Abdulkhaliq A. Jaafer**
Date: / / 2022

In view of the available recommendations, I forward this thesis for debate by examining committee.

Signature:
Name: **Assist. Prof. Dr. Samir Mohammed Chassib**
Head of the Department of Civil Engineering
Date: / / 2022

EXAMINING COMMITTTEE'S REPORT

We certify that we, the examining committee, have read the thesis titled **(Improving Carrying Capacity of Reinforced Concrete Beams Using Steel Wire Mesh as Shear Reinforcement)** which is being submitted by (**Sarah Hussain Hameed**), and examined the student in its content and in what is concerned with it, and that in our opinion, it meets the standard of a thesis for the degree of Master of Science in Civil Engineering (Structures).

Signature:
Name: **Prof. Dr. Abdulkhaliq A. Jaafer**
(Supervisor)
Date: / /2022

Signature:
Name: **Assist. Prof. Dr. Ahmed A. Hassan**
(Member)
Date: / /2022

Signature:
Name: **Assist. Prof. Dr. Hayder A. Radhi**
(Member)
Date: / /2022

Signature:
Name: **Prof. Dr. Saʾad F. Resan**
(Chairman)
Date: / /2022

Approval of the College of Engineering:

Signature:
Name: **Prof. Dr. Abbas O. Dawood**
Dean, College of Engineering
Date: / /2022

ABSTRACT

The ACI committee 549 published a general definition of ferrocement states that ‘‘Ferrocement is a type of thin wall reinforced concrete commonly constructed of hydraulic cement mortar reinforced with tightly spaced layers of continuous, small size wire mesh. Ferrocement is a construction material that proved to have superior qualities of crack control, impact resistance, and toughness, largely due to the close spacing and uniform dispersion of reinforcement within the material. The present study aims to investigate the shear behavior of beams subjected to shear failure with a number of wire mesh layers added. The experimental work consists of seventeen beams with dimensions of (150 × 200 × 1600) mm are tested under two-points load. Different parameters are examined for predicting their influence on shear behavior of beams. The parameters investigated in the experimental program includes variable shear span to effective depth ratio (a/d= 1.8 and 2.5), compressive strength (35 and 65) MPa, number of wire mesh layers (4, 8 and 10), and presence of transverse reinforcement. During the experimental work, the beam specimens are divided into five groups depending on the work parameters. Each group consisted of three beams specimens except for the third and fourth group consisting of four beams. The first, second and fifth groups have the same a/d = 2.5 and same number of wire mesh layers (4 and 8). The variable of second group and fifth group are stirrups amount and compressive strength respectively. The third and fourth groups, have the same a/d = 1.8, number of wire mesh layers (4, 8 and 10) and the same compressive strength 65 MPa. The fourth group not contain stirrups. The behavior of beams are examined by ultimate load, first crack load, load deflection response, strains distribution and failure modes. Generally, the ultimate load increases with the increase in the number of wire mesh layers compared to control beams. The addition of wire meshes improved the ultimate load by ranging from (16 to 82)%. Test results also showed that an increase in the shear span to the effective depth ratio

leads to a decrease of the ultimate load and an increase of the mid-span deflection, compared to specimens with lower shear span. Changing the compressive strength from normal to high strength increased the ultimate load of the beam containing 8 layers of wire mesh by up to 24% compared to the normal strength. As for the specimens containing stirrups with wire mesh, the ultimate load improved compared to the specimens without stirrups by up to 24.6%. The addition of the wire mesh with stirrups led to a decrease in the maximum deflection values up to 20.3%. While the beams with greater shear span showed higher ductility than the beams with less shear span up to 32%. The initial stiffness and energy absorption the values increase with increased number of layers compared to control beams by up to 56% and 52%, respectively. The beams with wire mesh achieved higher first cracking load ranging by up to 32.3% compared to the control beams. As for the failure of the specimens, the beam showed flexural failure at (4, 8 and 10) for specimens containing stirrups with wire meshes compared to control beams that failed in shear. As for the specimens without stirrups, the shear failure was observed at 4 layers of wire mesh and the flexural failure at 8 and 10 layers of wire mesh.

TABLE OF CONTENTS

LIST OF TABLES

LIST OF FIGURES

LIST OF SYMBOLES

F_t	Tensile strength in MPa
F_r	Modulus of rupture in MPa
f_y	Yield Stress MPa
f_u	Ultimate Stress MPa
f_{cu}	Cube Compressive Strength in MPa
μ	Ductility index
Δ_{max}	Maximum Deflection in mm
Δ_y	Yield deflection in mm
P_y	Yield load in kN

ABBREVIATION

RC	Reinforced Concrete
GFRP	Glass Fiber-Reinforced Polymer
FRP	Fiber-Reinforced Polymer
CFRP	Carbon Fiber-Reinforced Polymer
ACI	American Concrete Institute
LWF	Light Weight Ferrocement
FEM	Finite Element Analysis
AAC	Autoclaved Aerated Core
EFC	Extruded Foam Core
LWC	Light Weight Core
EMM	Expanded Metal Mesh
WWM	Welded Wire Mesh
FGM	Fiber Glass Mesh
ANSYS	ANalysis SYStem
FRB	Ferrocement Retrofitted Beam
FCRP	Fiber Carbon Reinforced Polymer
PMF	Polymer-Modified Ferrocement
SBR	Styrene-Butadiene-Rubber
ASTM	American Society for Testing and Materials
HRWR	High Range Water Reducers
SP	Super Plasticizers
w/c	Water to Cement ratio
LVDT	Linear Variable Differential Transforme

CHAPTER ONE: INTRODUCTION

1.1 General

Concrete is a frequently utilized building material all over the world. Though concrete relatively strong and durable material, it can deteriorate due to a variety of factors such as aging, weather effects, deterioration impacts and a lack of maintenance [1]. Shear failure in reinforced concrete beams is considered a type of failure that which has a catastrophic effect, if it occurs. Shear failure occur rapidly without warning if a reinforced concrete beam has low shear strength, whereas flexural failure happens gradually, with considerable deflections and cracks providing enough warning. As a result, reinforced concrete beams in the critical shear zone must be adequately designed and strengthened to prevent shear failure [2]. Figure 1.1 shows typical shear failure in reinforced concrete beam [3].

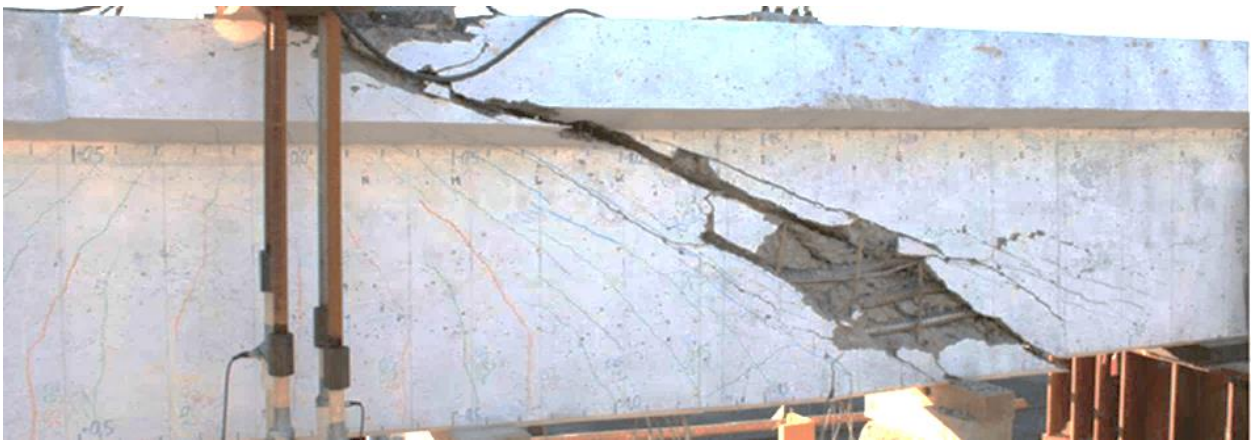

Figure 1.1 Diagonal shear crack [3].

In recent years, one of the most challenges falling civil and structural engineers has the strengthened of members against different failures. Additionally, enhancing resistance or stiffness to resist loads are possible causes for utilizing strengthening techniques, where strengthening is an effective alternative to rebuilding existing structures [4]. Hence, strengthening strength of reinforced concrete (RC) members in existing structures represent a higher important to extend

their service life, to ensure the safety and serviceability of the related components. The strengthening and restoring ability of structure must meet the codes and standards as structures erected today and in the future [5] [6]. Recently, many researchers had used modern materials such as ferrocement, glass fiber-reinforced polymer (GFRP), fiber-reinforced polymer (FRP), carbon fiber-reinforced polymer (CFRP), and steel plate jacketed for strengthened concrete structures. Many of these materials showed some flaws or shortcoming in terms of strength, cost, availability, and applicability. Hence, out of these available material options, the ferrocement had gained popularity and has becomes one of the major structural material for strengthening the concrete structure [7]. The ferrocement had taken a significant place among other materials used for construction, due to specification of durability and strength, and the small thickness, which makes it a component suitable for constructing many lightweight structures [8].

1.2 Ferrocement

Ferrocement was invented by a Frenchman called Joseph Louis Lambot, in 1848. It is a special type of reinforced concrete that was first employed in the construction of boats. Since the 1940s, the scope of ferrocement applications expanded in civil engineering [8]. ACI committee 549R defined the ferrocement as type of thin-walled reinforced concrete made of hydraulic cement mortar reinforced with tightly spaced layers of continuous, small size wire mesh. Metal or other suitable materials can be used to create the mesh. Discontinuous fibers may also be present in the matrix. Figure 1.2 shows the typical cross section of ferrocement member [8]. Ferrocement exhibits a behavior differing much from conventional reinforced concrete in terms of strength performance and prospective applications [9]. The main difference between them is mostly in size. Reinforced concrete (RC) larger size of reinforcing bars instead of wire meshes. In ferrocement the large

aggregate cannot be used as used in reinforced concrete. In sometimes, the ferrocement may contain large reinforcing as skeletal bars with layers of wire mesh [8] [10].

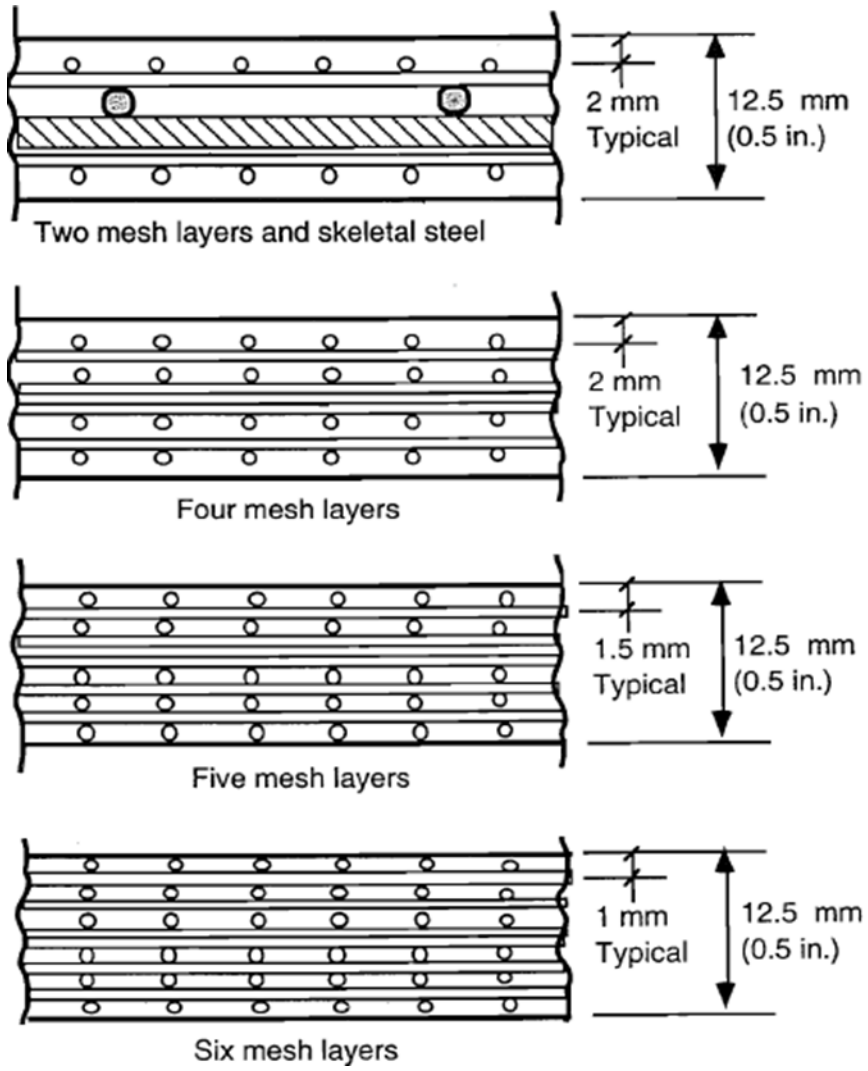

Figure 1.2 Typical cross sections of ferrocement [8].

In addition, the ferrocement can be made in any shape by unskilled labor and low technology level. The ferrocement repairs are simple and low-cost [10]. The higher characteristic and performance of ferrocement than conventional concrete make depict the most significant different them. Tensile strength behavior of ferrocement is depended on wire meshes system. The number of layers of wire mesh, the spacing between the mesh, the form of the wire mesh, and the orientation of the

wire mesh in it all affect the tensile strength of ferrocement. Ferrocement has a completely different tensile behavior than reinforced concrete because the specific surface area of the reinforcement is bigger and distributed uniformly [10] [11].

1.2.1 Mortar Composition of Ferrocement

The hydraulic cement matrix for ferrocement should be designed according to standard mix design procedures for mortar and concrete [8]. The matrix used in ferrocement consists of hydraulic cement, sand as the fine aggregate, water and various admixtures. Ferrocement often use portland cement, however the type of cement to be used should be determined by the application and the environment in which it will be utilized. Also the fine aggregate should be clean, free of organic matter, and free of clay and silt [12]. Mixing ratios of sand to cement range from (1 to 2.5). The water-cement ratio ranged between (0.25-0.6) in order to achieve an appropriate level of plasticity and make easier casting [13]. Different, additives such as fly ash, silica fume, superplasticizers, and discontinuous fibers also can be used in modern ferrocemen applications, to improve the properties of the matrix, such as its cracking behavior and shear resistance [13].

1.2.2 Mesh Reinforcement

In ferrocement industry, steel mesh can be considered as a primary type of reinforcement. The shapes of wire mesh used in ferrocement member can be classified as follows:

1. Welded meshes: it is steel wire meshes with square or rectangular apertures. Square welded wire mesh is stronger and provides more resistant to cracking [12] [13].
2. Woven wire mesh: it has similar properties of welded mesh, but it is more flexible than welded mesh and easier to work with [13].

3. Hexagonal wire mesh: commonly called chicken wire mesh and it is very flexible and may be utilized in very thin sections [13].
4. Expanded metal lath: it has almost the same strength as a welded mesh, which is made by slitting thin gauge sheets and expanding them in a perpendicular direction to the slits. This expanded takes the shape of a diamond.

Figure 1.3 illustrates the types of wire meshes used in ferrocement.

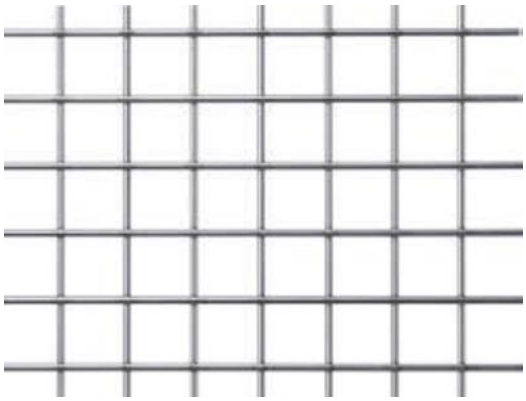

(a) Welded meshes.

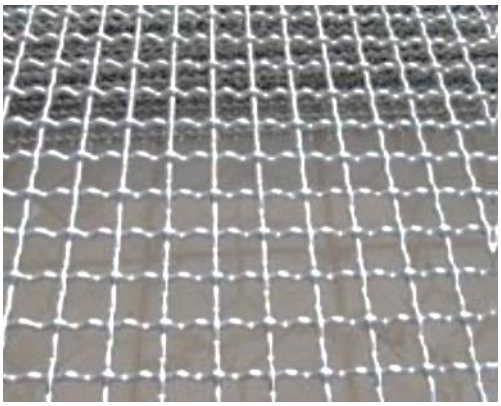

(b) Woven wire mesh.

(c) Hexagonal wire mesh.

(d) Expanded metal lath.

Figure 1.3 Types of wire meshes used in ferrocement [12].

All meshes used were preferably galvanized. In most steel meshes, whether woven or welded, it was likely that the properties (tensile strength and apparent modulus) of the mesh in the transverse direction are different from those in the longitudinal direction. The preceding remarks, also apply to hexagonal and

expanded metal meshes, since their properties were different in the two principal directions and their apparent modulus is significantly smaller than the steel modulus [8].

1.2.3 Skeletal Steel Frame

Skeletal steel is commonly employed in ferrocement construction as a welded wire fabric or as a grid of steel wires, rods, or strands , as shown in Figure 1.4. Skeletal steel is utilized to give structures their basic shape and size, around which the mesh layers will be joined later. When the thickness of the ferrocement sufficient, the use of skeleton steel can be highly cost effective [8] [12]. The skeletal steel also works as a spacer, resulting in mesh layer savings. In addition, it improves ferrocement tensile, punched shear and provide significant bending resistance [8].

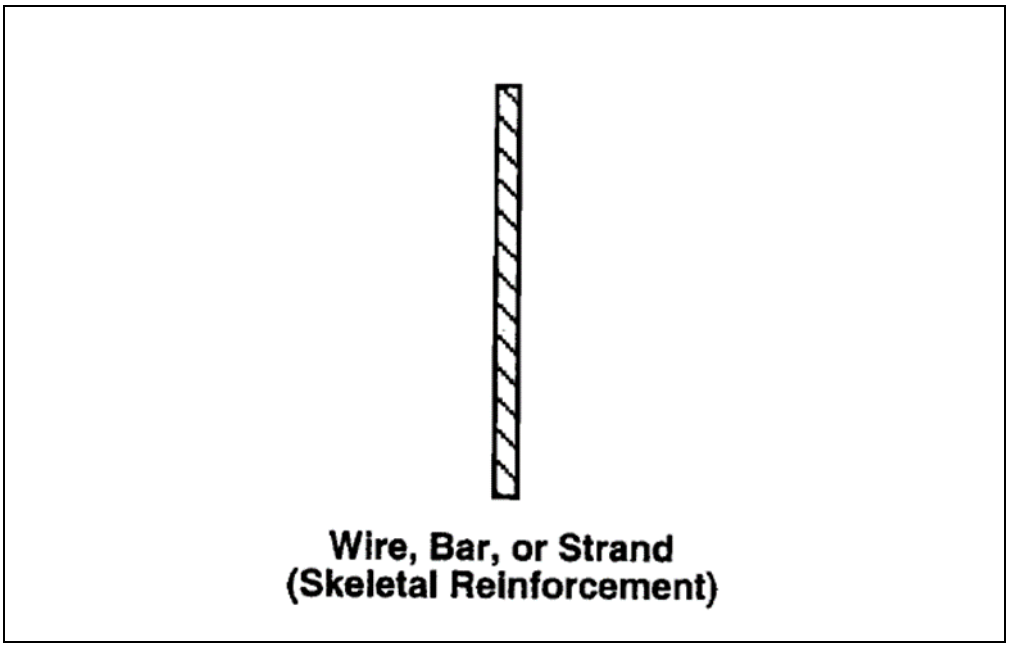

Figure 1.4 Skeletal reinforcement [8].

1.3 Applications of Ferrocement

Ferrocement contains a wide range of applications. Because of the easy availability of ferrocement materials, it can be built with very little specialized

skilled labor and very little machinery. The following are some of the applications of ferrocement [10]:

1.3.1 Marine Applications

Boats, fishing vessels, ferries, docks, cargo tugs, flotation buoys, and water or fuel tanks are all examples of marine can be constructed by ferrocement [8].

1.3.2 Terrestrial Applications

Ferrocement can be used in water supply and sanitation, housing, and rural energy. Therefore, it can be divided as [8]:

a. Agricultural applications: grain storage bins and silos, water tanks, lining for underground pits and irrigation channels pipes, shells for fish and chicken farms, and pedestrian bridges.
b. Rural energy applications: biogas digestors, biogas holders, incinerators and panels for solar energy collectors.
c. Water supply and sanitation: water tanks, sedimentation tanks, well casings, service modules, sanitary tanks, linings for swimming pools, and fuel tanks.
d. Housing applications: house, commonly centers, museums, mosque domes and other worship place, domes structures, precast housing element, wall panels, sandwich panels, corrugated roofing sheets, hollow-core slabs, permanent formwork and repair and rehabilitation of existing housing.
e. Building Industry: Roofing element, wall element, lintels, beams.

1.4 Shear in Ferrocement

There is relatively little information on the shear properties of ferrocement. Ferrocement is most commonly utilized in the form of thin elements where the span to depth ratio in bending is big enough that one-way shear does not govern the failure

mode [8]. Furthermore, ferrocement parts have a high volume fraction of mesh reinforcement, which contributes to resist dowel action in shear. Furthermore, ferrocement does not have shear reinforcement (such as stirrups), except for the ties that to join the mesh layers together [8]. Ferrocement exhibits two stages of behavior under direct shear, cracked and un-cracked, but ferrocement under flexure exhibits a third stage (ultimate or plastic stage) in addition to the un-cracked and cracked stages [14]. As a result, ferrocement is less ductile in shear than flexure. Another important characteristic to note is that ferrocement cracking and ultimate shear stresses increase as the span-to-depth ratio is decreased and volume fraction of reinforcement, strength of mortar, and the amount of reinforcement near the compression face are increased. Ferrocement beams are found to be susceptible to shear failure at small span-to-depth ratios when volume fraction of reinforcement and strength of mortar are relatively high [14]. As cited in (Al-sulaimani and Basunbul), examined the shear behavior of ferrocement under direct shear, axial load tests on direct shear specimens with dimensions of (300 × 100 × 600) mm were conducting. Most of their conclusions were similar to the effect of reinforcement on tensile response except for the fact that, in shear, there did not seem to be plastic behavior after the multiple cracking stage. Furthermore, the amount of wire mesh has little effect on shear stiffness in the uncracked stage, but it has a substantial effect in the cracked stage. But the mortar strength, affects the shear stiffness in both stages (uncracked and cracked) [8] [15]. As for the ferrocement design, one- way shear can be treated in a manner similar to reinforced concrete, using for instance. Approach to estimate the contribution of the mortar matrix, V_c, to the shear. This is achieved using for instance by the following equation **1.1**:

$$\boldsymbol{V_c = \frac{1}{6}\sqrt{f_c}} \qquad 1.1$$

where V_c is the average nominal shear strength provided by the mortar matrix, and f_c is the compressive strength of the mortar matrix obtained from cylinder tests (of dimensions 75 × 150 mm or 100 × 200 mm). For ferrocement design, the critical section for shear may be taken at a distance d_{ex} from the face of support, where d_{ex} is the distance from the extreme compression fiber to the extreme layer of mesh reinforcement [8].

1.5 Objective of the Study

The objective of this study is to examine the shear behavior of beams subjected to shear failure with a number of wire mesh layers added. The major goals of this study are,

1. To investigate the full behavior of beams under the influence of key parameters such as the shear span to effective depth ratio (a/d), the effect of compressive strength of mortar on the beam's features utilizing two types of compressive strength (normal and high strength) and ratio of the amount of stirrups.
2. To study the effect of stirrups on the behavior of beams.
3. To study the effect of number of wire mesh layers on shear strength in beams.

1.6 Thesis Layout

The following is a brief summary of each chapters substance in the thesis:

1. Chapter one (Introduction), this chapter gives a general background about ferrocement, applications of ferrocement, shear in ferrocement and the objectives of research.
2. Chapter two (Literature Review), this chapter discusses previous research works related strengthening the beams by ferrocement.

3. Chapter three (Laboratory Works), revolves around all the materials that have been used for casting specimens. Characteristics of these materials are also explained in this chapter. The experimental program, description of the tested specimens, the test program and setup, and mix design were described too.
4. Chapter four (Test Results and Discussions), this chapter illustrates the test results the specimens and discusses the obtained results from the experimental work.
5. Chapter five (Conclusions and Recommendation), this chapter includes the concluded remarks, main conclusions and recommendations drawn from this research for future works.

CHAPTER TWO: REVIEW OF LITERATURE

2.1 Introduction

The aim of this chapter is to provide a review of the available information relating to experimental and analytical works and to review the most important conclusions and findings for improving reinforced concrete (RC) beams failing in shear and flexural using wire mesh.

2.2 Ferrocement in Construction

Al-Sulaimani et al. in 1991 [16], studied the shear behavior of ferrocement box beams. The amount of wire mesh reinforcement in the webs and flanges of the beam, as well as the shear span to depth ratio (a/h) were the main parameters utilized. The beams were divided into five groups according to the quantity of wire mesh reinforcement in webs and flanges. Figure 2.1 shows details of tested specimen. Woven wire mesh of 8.4 mm square openings of 0.9 mm wire diameter was used in study, the number of layers of wire mesh was in each web (Nw = 0, 1 and 3) and in each flange (Nf = 0, 1 and 3). According to test results, the cracking and ultimate shear forces increase with was decreased (a/h) ratio and when the wire mesh in webs was increased. Wire mesh in flanges also improves shear resistance by preventing tension cracks from forming and making them finer, which indication of an increase in ductility of the beams. The ACI equation for shear strength of conventional reinforced concrete beams without web reinforcement was underestimates the cracking shear strength of ferrocement box beams. Also, a multiple regression analysis was used to establish an empirical equation to predict the shear strength of ferrocement box beams, observed when a/h reduced and increase in the amount of wire mesh reinforcement, the cracking and ultimate shear strengths of box beams improve.

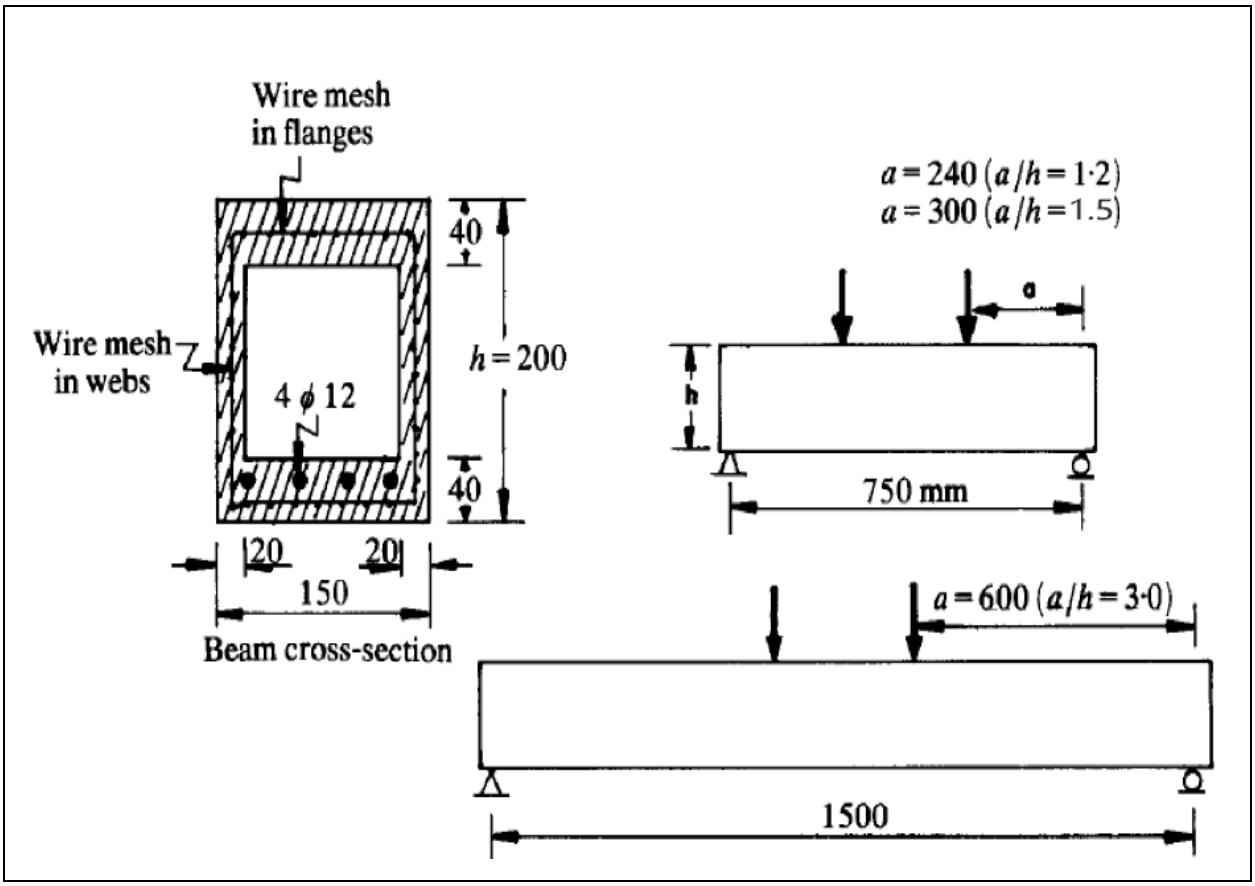

Figure 2.1 All dimensions for beams [RC] [16].

Mahmood and Majeed in 2009 [17], presented an experimental study to predict strength of folded and flat ferrocement panels reinforced with different number of wire mesh layers. Seven ferrocement pieces, each with a horizontal projection of (600 × 380) mm and a thickness of 20 mm, were built and tested. The used number of wire mesh layers were one, two and three layers. The experimental results showed that flexural strength of the folded panels increased by 90% for panels having three wire mesh layers, while for flat panel, the increase in flexural strength was 68% for panels having three wire mesh layers. The experimental and numerical results revealed that the folded panel superiority the flat panel in terms of ultimate strength and initiation of crack. Finally increasing the number of layers of wire mesh from 1 to 3 layers significantly increases the ductility and capability to absorb energy of both types of the panel.

El-Wafa and Fukuzawa in 2010 [18], examined the performance of structural behavior of lightweight ferrocement (LWF) sandwich composite beams through flexural tests. Beams performance was checked LWF and RC through fracture load, load-deflection curves, stiffness, energy absorption capacity, ductility index, ultimate flexural load-to-weight ratio, load-strain curves, crack patterns, number of cracks, average crack width, crack spacing, and failure mechanism. The test results revealed that the LWF beams perform better and had a superior advantage in terms of pre-cracking stiffness, load carrying capacity, energy absorption capacity, ductility index, and a higher ultimate flexural load-to-weight ratio when compared to RC beams. The LWF beams developed multiple cracks under flexural load in contrast to the limited number of cracks of the RC beams. The LWF beams showed remarkable enhancement in the structural behavior and potential application of lightweight ferrocement sandwich, compared to that of the RC beams.

Savale and Alandkar in 2013 [19], used different mesh patterns for studing flexural behavior of ferrocement plates. The ferrocement plates were prepared having size (490 × 230 × 20) mm. The mesh pattern was hexagonal, square and diamond. The results showed the shear strength of the plate depends upon the volume fraction of wire mesh. To attain this advantage, supports and loading points should be designed and strengthened to prevent local failure. The stress intensity was determined using finite element analysis (FEA) and compared with the available results.

Chkheiwera et al. in 2016 [20], proposed an experimental and analytical work to study the influence of mortar compressive strength and the number of wire mesh layers in web and bottom flange on the shear behavior of ferrocement slender box beams. All beams had cross section of (300 × 175) mm, length of 2000 mm, with shear span to effective depth ratio (a/d) of 2.8. The tested beams were divided into four groups, each group consists of three beams depending on compressive strength.

The first group was without wire mesh, the second group was with one layer of wire mesh in web and bottom flange, the third group was two layers of wire mesh in web and one in bottom flange. The last group was with two layers of wire mesh in web and bottom flange. The beams with mortar compressive strength (f_{cu}) of 48.3 and 60.1 MPa showed ultimate load higher from beam having f_{cu} of 37.4 MPa by a percentage 7.6% and 16.2%, respectively. The first crack and ultimate load increases with increasing the wire mesh layers in web and bottom flange. The number of cracks increases with increasing of wire mesh reinforcement. The finite element model gives good agreement with the experimental results.

Shaaban et al. in 2018 [21], focused on the study effect of different types of core materials on behavior of lightweight ferrocement composite beams. Ferrocement beams contained either an autoclaved aerated lightweight brick core (AAC), extruded foam core (EFC), or a lightweight concrete core (LWC). The beams were reinforced with either expanded metal mesh (EMM), welded wire mesh (WWM) or fiber glass mesh (FGM). The initial crack, ultimate load, deflection, ductility index, strain characteristics, crack pattern, and failure mode were investigated. The findings of the experiments showed that ferrocement beams had higher ductility indices than the control normal and lightweight test beams to different degrees. Ferrocement beams made of EFC core had the lowest ductility index, whereas beams with AAC and LWC cores had the highest ductility index. In comparison with ordinary beams, ferrocement beams showed better crack management and did not spall. Cracks appeared to form more quickly in EMM-reinforced beams, while FGM-reinforced beams had the least amount of cracks. The findings of this study suggested that ferrocement beams with light weight cores could be a feasible alternative to conventional beams, especially for low-cost residential constructions.

2.3 Strengthening of Beams Using Ferrocement

2.3.1 Strengthening of Beams Using Ferrocement (Shear)

Rafeeqi et al. in 2005 [22], conducted an experimental study on the possibility of using ferrocement in transforming brittle mode failure to ductile mode failure of RC beam. The study parameters were limited to one and two layers of woven square mesh in the form of wraps in the whole shear span and evenly spaced strips in the shear span. Beams were cast of dimension (100 × 200 × 915) mm, where the first beam was a control specimen and remaining beams were beams in which shear spans was strengthened by ferrocement. The beams were loaded up to service load, they were unloaded and strengthened and reloaded until failure. The main results revealed that strengthened beams performed better. The stiffness of strengthening beams was enhanced compared with control specimens. The increase in shear capacity was increased up to 5.8%. The strengthened specimen appeared an increase in the number of cracks and decrease in crack width. The presence of ferrocement strips and wraps, however, delayed failure, giving ample warning before failure, which was considered as the desired mode of failure.

Zhao et al. in 2012 [23], presents experimental and numerical study to evaluate the shearing performance of beams strengthened with steel wire-polymer mortar. The beams were cast from reinforced concrete with a cross section of each beam was (200 × 300) mm, the span was 2300 mm. The first Specimen served as control beam, while the remaining beams were strengthened with steel wire-polymer mortar of U-shaped. Two types of nonlinear finite element methods in software ANSYS, separated reinforcement and composite reinforcement, were used to simulate the experiment beams. Experiments showed that by steel wire mesh- polymer mortar with U-shaped, the shear strength of the beam can be improved obviously. The shear capacity of the reinforced for the second beam has improved 57% than the

unreinforced component. Reinforced concrete beam strengthened with steel wire mesh-polymer mortar can delay the cracks emergence and development. While cracks in beams by ANSYS analysis, were not very obvious.

Sun et al. in 2012 [24], introduced an efficient method for strengthening concrete beam using steel bar/wire mesh mortar to improve the shear capacity of RC beams. Rectangular beams were cast with dimensions of (180 × 300 × 1800) mm, the beams were divided into three groups. The first group was control beams and designed to fail in shear. The second group were U-shaped steel bars were used to reinforce beams. The third group were added U-shape steel bars and two wire mesh L-wraps were used in beams. The new dimensions after strengthening became (230 × 325) mm. The experimental results demonstrated that the third group was the most successful method in terms of the shear capacity and initial diagonal cracking load of strengthened beams. The cracking load increased for third group by 83%, and the ultimate load increased by 30%. This is because the wire mesh performed a better dispersion, leading to that the emergence of visible cracks was significantly delayed. The third group strengthening approach reduced the width of diagonal cracks and increases the friction of the aggregates on both sides of a diagonal crack, leading to a slight increase of shear capacity.

Hanche in 2016 [25], conducted an experimental test on strengthened twenty-four reinforced beams by ferrocement. The parameters tested in were the shear-span-to-depth ratio (a/h) which was achieved by varying the shear span to overall depth ratio from 1 to 2 at increments of 0.5, compressive strength of the mortar, and amount of reinforcement. The specimens were divided into eight series: A to H these specimens were symmetrically reinforced with four, six, eight, and ten layers of wire mesh, respectively. Series E and F were similar to series D, except for the compressive strength of the mortar. The remaining two series G and H were also identical to series D, but has difference in the amount of reinforcement in the

compression face. While the specimens in series H were reinforced with two layers of wire mesh along the compression face. The beams in series G did not contain reinforcement near the compression face. This experiment yielded the following results: the diagonal cracking strength of ferrocement increases, when the (a/h) ratio was reduced or the volume fraction of reinforcement and mortar strength were increased. The diagonal cracking strength of a beam was increased when increasing the quantity of reinforcement near the compression face.

El-Sayed and Erfan in 2018 [26], conducted an experimental and numerical study for shear behavior of beams reinforced by ferrocement. The parameters used were stirrups and wire meshes. All beams had dimensions of (150 × 150 × 1900) mm in width, depth and total length, respectively. The specimens were divided into three groups. The control specimen was in the first group. The second group contained an expanded wire mesh with dimensions (16.5 × 31) mm. The third group employed welded wire mesh of dimensions (12.5 × 12.5) mm. The results of the study showed that the ferrocement concrete specimens reinforced by expanded or welded steel wire mesh exhibit superior ultimate loads compared to the control ones under flexural loadings, where the relative ultimate load ranged from (134.74 and 135.79)%, respectively. Increasing the number of layers of expanded and welded wire meshes led to improve the ultimate load, load deflection, stiffness, toughness, and shear stress of ferrocement beams. When compared beams reinforced with steel meshes to beams strengthened with steel reinforcement, showed cracks with a greater number and narrower widths. While the analytical results showed good consistent with the experimental results.

Ghai et al. in 2018 [7], proposed a study to determine the performance of polymer-modified ferrocement (PMF) with 15% styrene-butadiene-rubber latex (SBR) polymer on strengthen predamaged beams. The main parameters of the study were shear span (1 and 3) damage level of the beams (45%, 75% and 95%). The

thickness of PMF was 20mm for all strengthening specimens, as shown in Figure 2.2.

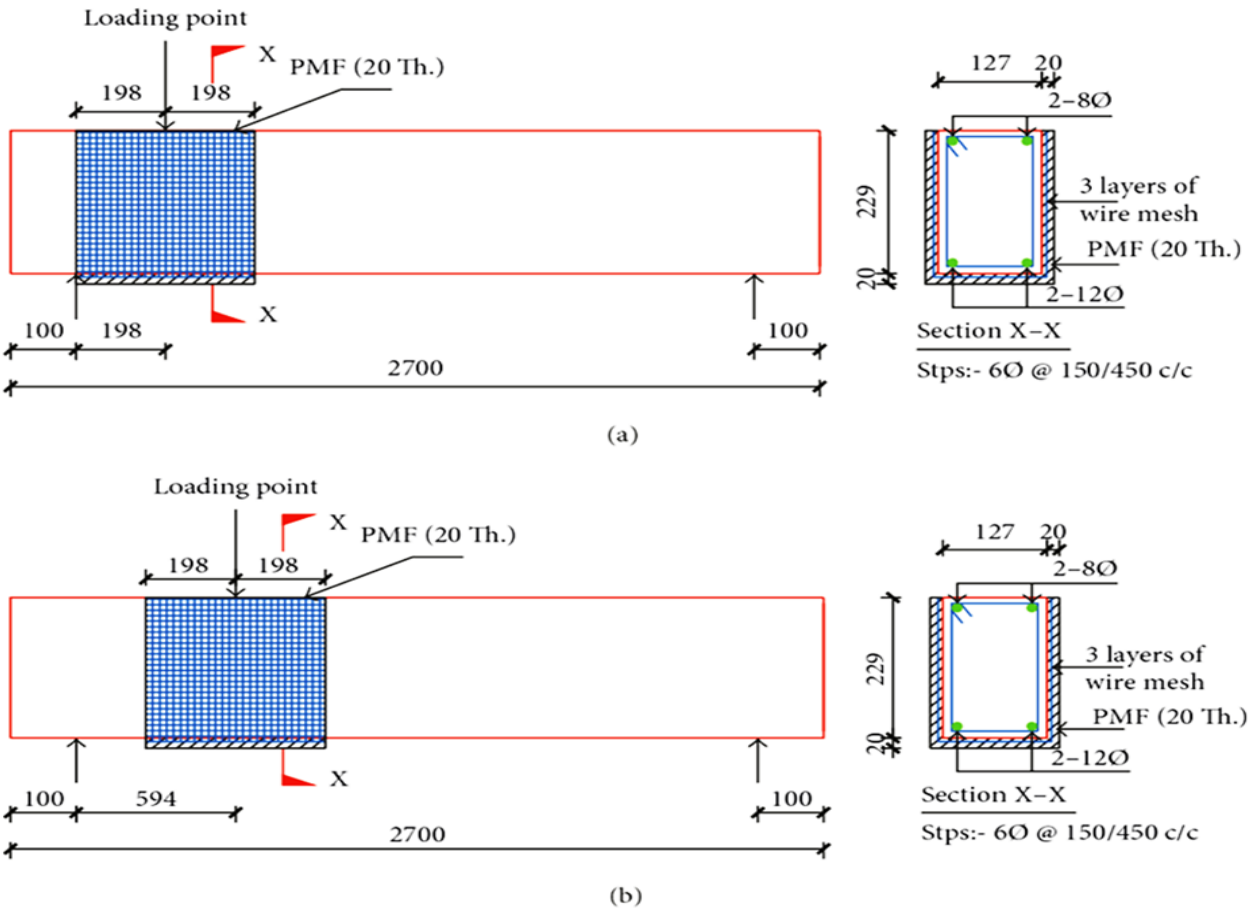

Figure 2.2 Detail of PMF strengthened beams [7].

Beams were then again tested for ultimate load-carrying capacity by conducting the shear load test. The following conclusions have been drawn from this experimental study: the PMF-strengthened beams showed restoration and enhancement of ultimate shear load-carrying capacity by 5.90% to 12.03%. The PMF strengthening technique increased the ductility of pre damaged beams and caused to delay the shear failure by resisting and distributing the applied loads. The rate of crack development was also reduced, and the strengthened beams displayed a less number of cracks as compared to the corresponding beams without strengthening.

Elavarasi and Sumathi in 2019 [27], performed the effect of using different types of transverse reinforcement on the behavior of RC beams. The transverse reinforcement employed in the study was stirrups alone, wire mesh alone and combination of wire mesh and stirrups, as shown in Figure 2.3.

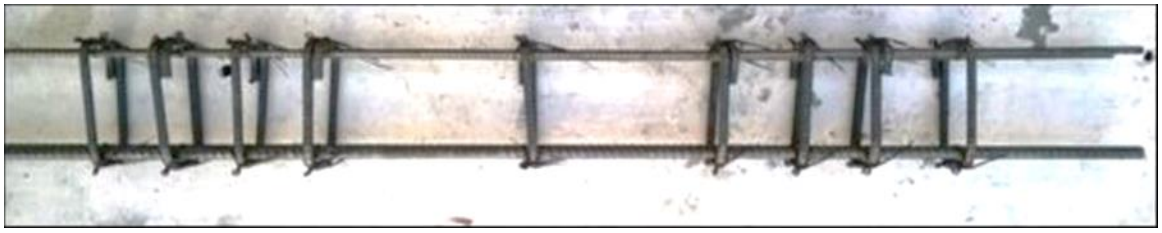

(a) Beam with stirrups as shear reinforcement.

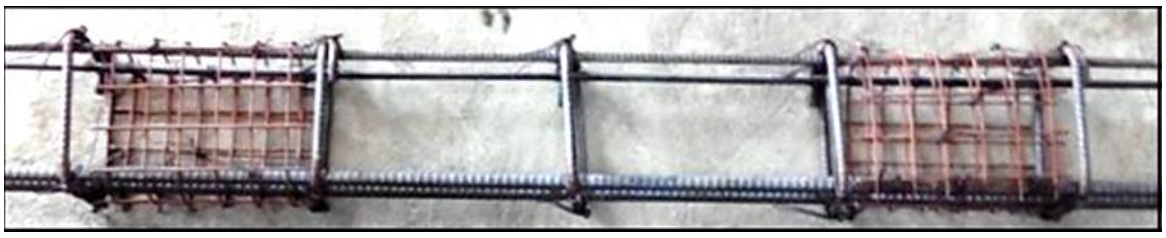

(b) Beam with wire mesh and stirrups as shear reinforcement.

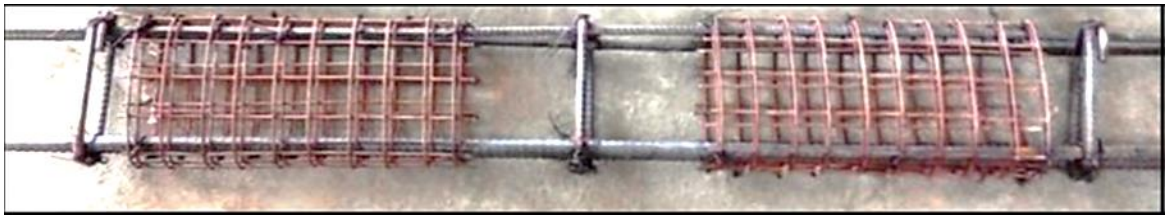

(c) Beam with wire mesh as shear reinforcement.

Figure 2.3 The reinforcement details of tested beams by stirrups and wire mesh [27].

All the beams were tested using two points loading system. The used wires were of 2 mm diameter and the spacing of interlocking links were of (34 × 34) mm. The stirrups used were of 6 mm diameter. The results showed an improvement in shear performance and bearing capacity of the studied beams. Beams with wire mesh as shear reinforcement and a combination of both wire mesh and stirrups showed an increasing of shear capacity, in comparison with beams containing stirrups alone as shear reinforcement. Furthermore, the beam specimens with mesh and specimen

with a combination of wire-mesh and steel stirrup, they had more number of cracks and reducing the crack width.

Ojaimi. in 2021 [28], the shear behavior of RC beams reinforced with four different concrete jacketing techniques was investigated. Four techniques used in this study to enhance the behavior of the beams were by using a self-compacted fiber reinforced concrete jacket without stirrups (S.-J. + Steel Fiber), a concrete jacket of self-compacted concrete with stirrups (S.-J. + Stirrups), ferrocement jacket (S.-J. + Ferrocement), ferrocement jacket with external steel reinforcing bars (S.-J. + Ferrocement + R). The dimensions of the beams were (200 × 250 × 1700) mm. All beams were tested under four-point bending. The results derived from the experimental results revealed that the used strategies improved load-carrying capacity and delayed the formation of the first crack in tested beams. In terms of stiffness and ultimate load-carrying capacity, the specimen (S.-J. + Stirrups) performed best when compared to the other strengthening strategies tested in this investigation. The ferrocement jacket (S.-J. + Ferrocement) was discovered to be the best jacketing solution for increased shear capacity in terms of cracking load. In comparison to a ferrocement jacket without steel bars, the inclusion of externally bonded steel bars under the wire mesh layers had a negative influence on the behavior of the strengthened beam.

2.3.2 Strengthening of Beams Using Ferrocement (Flexural)

Ahmed et al. in 2011 [29], studied the flexural and cracking behavior of the beams reinforced with ferrocemen. One beam was strengthened with ferrocement the other beam was without ferrocement, which act as a control beam. For the ferrocement laminates, square wire mesh with 1 mm diameter and spacing of 14 mm was used, as shown in Figure 2.4.

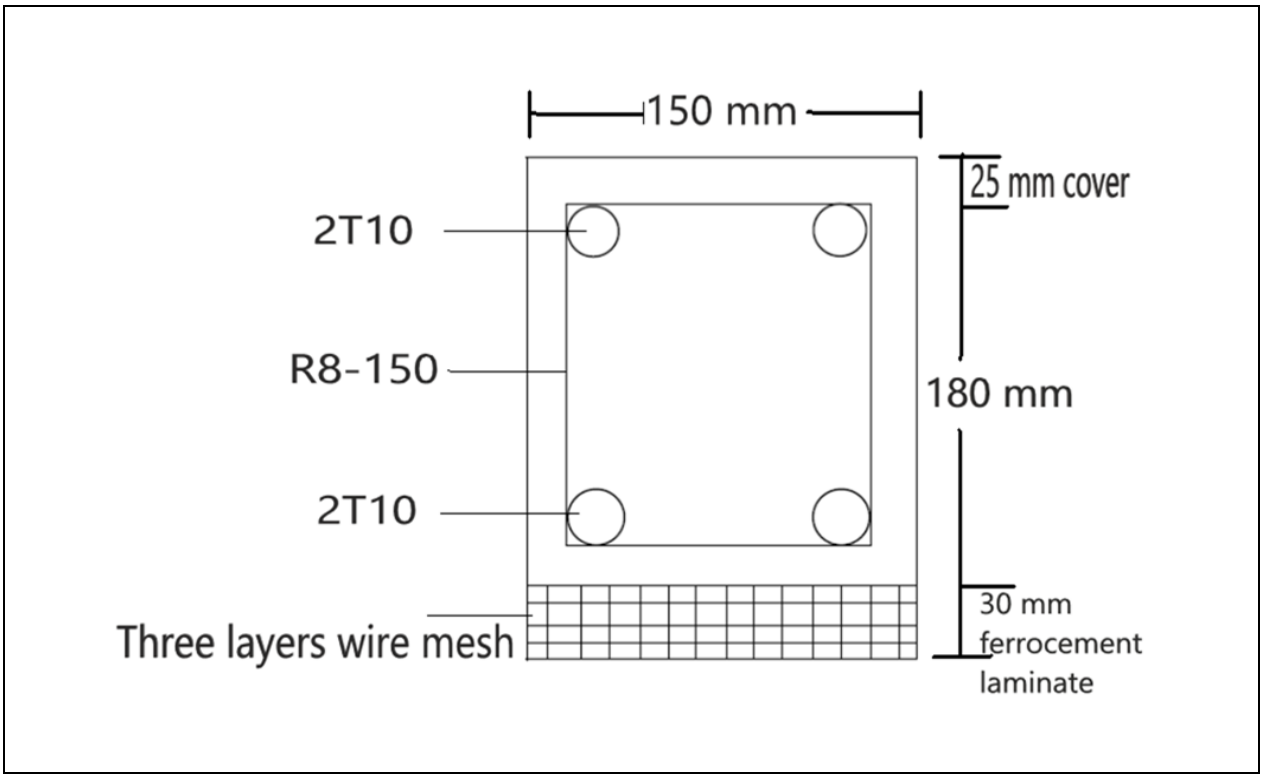

Figure 2.4 Cross-section of ferrocement beam [29].

Where the wire mesh layers were fixed to the beam using L-shaped shear connectors. Mortar is placed through hand plastering whereby mortar is forced through the mesh. Surfaces are finished to about 30mm to assure proper cover to the last layer of wire mesh. The results of the experiments demonstrated that the L-shaped shear connectors chosen were efficient in preventing ferrocement laminate from debonding. The ferrocement laminates significantly delayed the onset of the first crack and increased the flexural stiffness and load carrying capability of the strengthened beam, where the ultimate load was found to be 21% higher than that of the control beam. To assess cracking load and ultimate load for control beam and ferrocement laminates, a simplified theoretical calculation based on equivalent cross sectional analysis was performed. Theoretical and experimental results for the control beam were found to be in good agreement. As for ferrocement laminates, there were minor discrepancies between actual and theoretical results, where the ultimate load is increased by 11%.

Alam et al. in 2014 [30], suggested an experimental study to test the concrete beams retrofitted using ferrocement materials. The main parameters included in study, were the effect of the number of layers of wire meshes. Among all the sixteen beams, four beams were treated as the control beams and the other twelve beams were treated as ferrocement retrofitted beams (FRB). These twelve beams were divided into three groups (each with four beams): FRB1 (wire mesh-one layer, 12 mm thick cement mortar), FRB2 (wire mesh-two layers, 16 mm thick cement mortar), and FRB3 (wire mesh-three layers, 20 mm thick cement mortar), as shown in Figure 2.5.

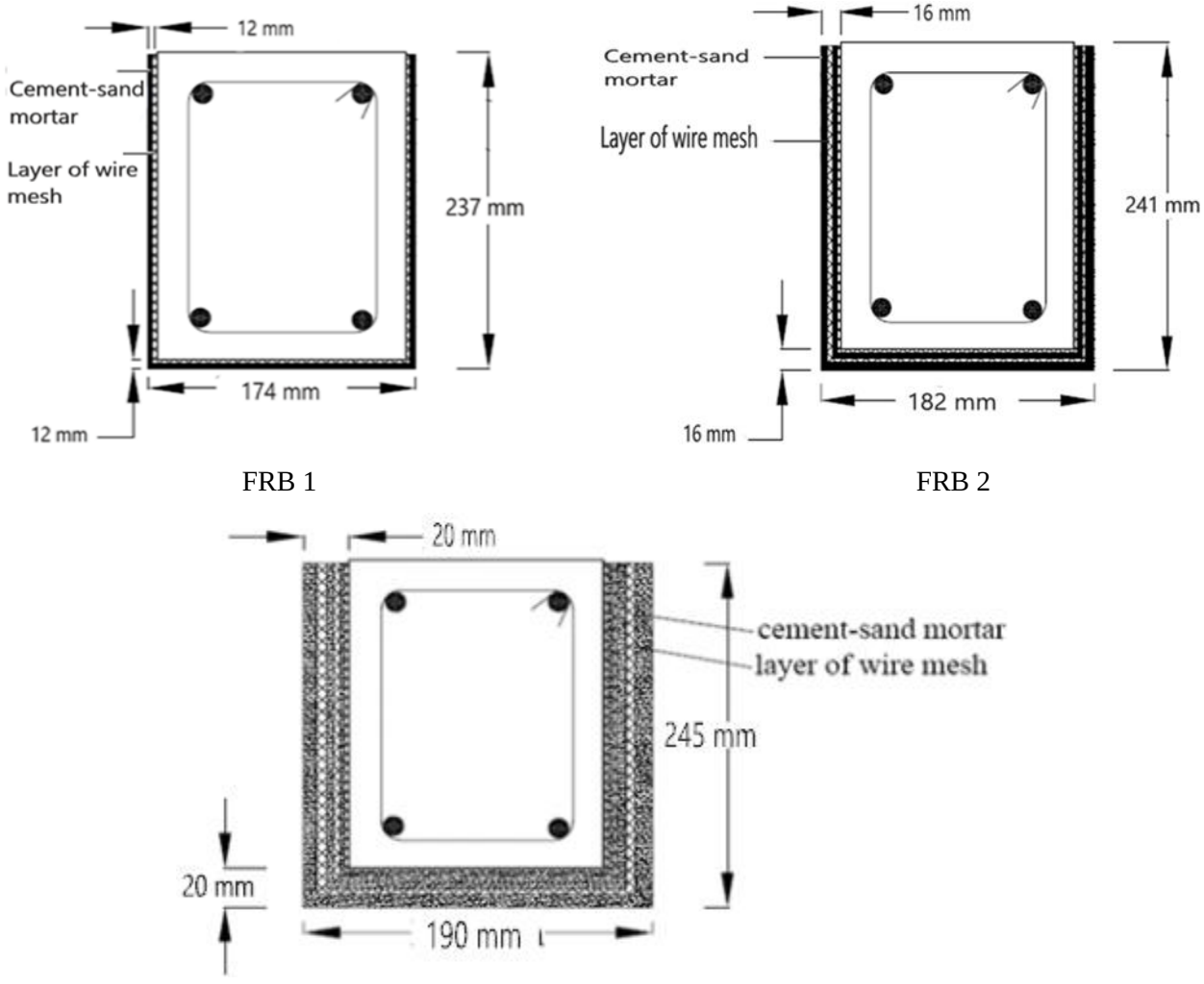

Figure 2.5 Cross-section of ferrocement retrofitted Beams [30].

Based on the test results and subsequent findings of this study, it appeared that: the first crack load increased by (14.42, 51.28, and 74.68)% for beams retrofitted with one, two, and three layers of wire meshes, respectively. The ultimate load for retrofitted beams with one, two, and three layers of wire mesh increase by (10.4, 42.4, and 58.4)%, respectively. The deflection of the ferrocement retrofitting beams with two and three layers of wire meshes was lower than the control beams. The failure of the control beams and the retrofitted beams were characterized by the formation of flexural cracks in the tension zone.

Fahmy et al. in 2014 [31], developed new types of concrete beams. In this study, precast U-shape of ferrocement forms filled with concrete with different grades was used as an alternative to the traditional concrete beams. A theoretical model was used in conjunction with an experimental program to achieve this aim. The experimental program included the casting and testing of thirty beams with total dimensions of (300 × 150 × 2000) mm, made up of permanent precast U-shaped reinforced mortar forms filled with the core material. Three types of core materials were investigated: conventional concrete, autoclaved aerated lightweight concrete brick, and recycled concrete, as shown in Figure 2.6. Two types of shear connections between the precast permanent reinforced mortar form and the core material were investigated namely: adhesive bonding layer between the two surfaces, and mechanical shear connectors. To strengthen the permanent U-shaped forms, two types of wire meshes were used: welded wire mesh and expanded steel mesh. The experimental results showed that ferrocement forms filled with concrete or recycled concrete core achieved higher first cracking load, serviceability load, ultimate load, and energy absorption compared to the control specimen irrespective of the type and number of layers of the steel mesh. Using lightweight brick core resulted in a decrease in the serviceability load and energy absorption relative to the conventional concrete beams regardless of the type of steel mesh used. The beams incorporating

thin precast reinforced mortar U-shaped forms could be successfully used as an alternative to the traditional reinforced concrete beams.

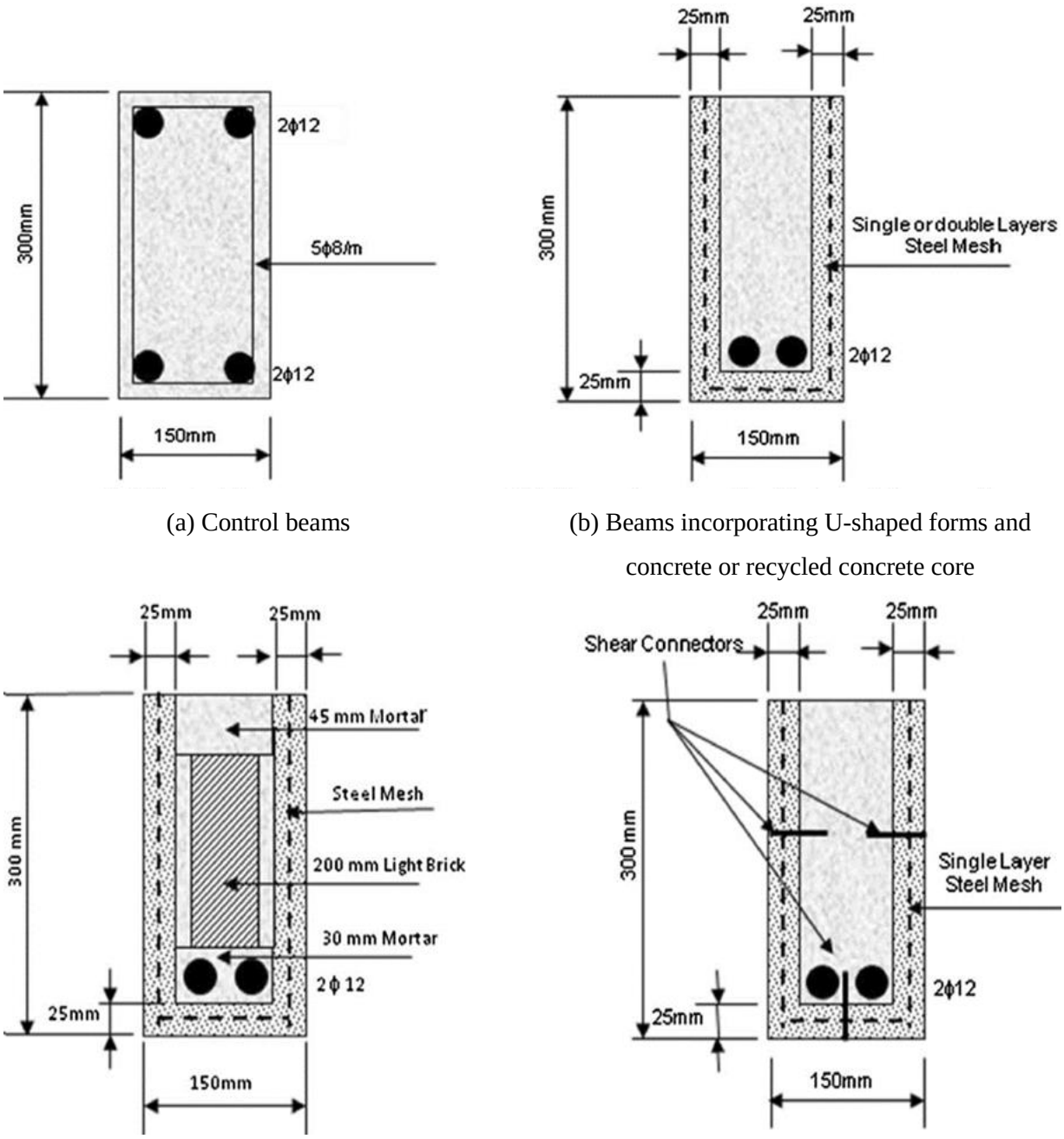

(a) Control beams

(b) Beams incorporating U-shaped forms and concrete or recycled concrete core

(c) Beams incorporating U-shaped forms and autoclaved aerated lightweight concrete brick core

(d) Beams incorporating U-shaped forms and concrete core with shear connectors

Figure 2.6 Cross section of the test beams [31].

Ganapathy and Sakthieswaran in 2015 [32], proposed an experimental study for rehabilitation and repairing of reinforced concrete beams using fibrous ferrocement laminates composites that were directly attached into the damaged tension face of the beams using epoxy adhesives. Five beams were kept to obtain for 70 % ultimate load, sixth beam used for as a control beam. Then the cracked beams were strengthened by polymer modified fibrous ferrocement composites with two different volume fractions (4.94% and 7.41%). The load deflection behavior and maximum ultimate load of all beams were determined through testing. The ferrocement laminated beam had a lower deflection value than the control beam. In conclusion, the strengthening reinforced concrete beam using fibrous ferrocement laminated to the flexural strength has increased significantly.

Ezz-Eldeen in 2015 [33], conducted a study to strengthen and retrofit reinforced concrete beams that had entirely failed to flexural failure. The strengthening technique consists of steel wire mesh with and without additional longitudinal steel angles was used. Two and three layers of steel wire mesh were used in the form of U-jacket. The investigated parameters were the size of longitudinal steel angles (10 × 10 × 3, 20 × 20 × 3, 30 × 30 × 3) mm which were added at the bottom corners of beams inside the steel wire mesh. In addition, the numbers of vertical steel clamps (2, 4 and 6) were used to fix the jacket. Twenty-four beams by the dimensions (100 × 160 × 1250) mm were cast and tested under two points loading. The results showed that reinforcing and retrofitting reinforced concrete beams with steel wire mesh, both with and without additional longitudinal steel angles, increased ultimate load carrying capacity significantly. The beam carrying capacity increased from 26.59% to 49.55% when the number of steel wire mesh plies increased with 2, 4, and 6 vertical clamps without external steel angles increases. The beam carrying capacity improved by 72.51% and 172.51% when the angle size employed at the bottom

corners of beams inside the wire mesh. On the other hand, increasing angle size, number of clamps and number of wire mesh plies decreased beams deformation.

The flexural behavior of reinforced concrete beams strengthened by ferrocement was studied by Sirimontree et al. in 2019 [34]. To conduct the experiments, three beams specimens of similar size were cast. The first beam used as a reference as shown in Figure 2.7, while the second and third beams were reinforced with ferrocement.

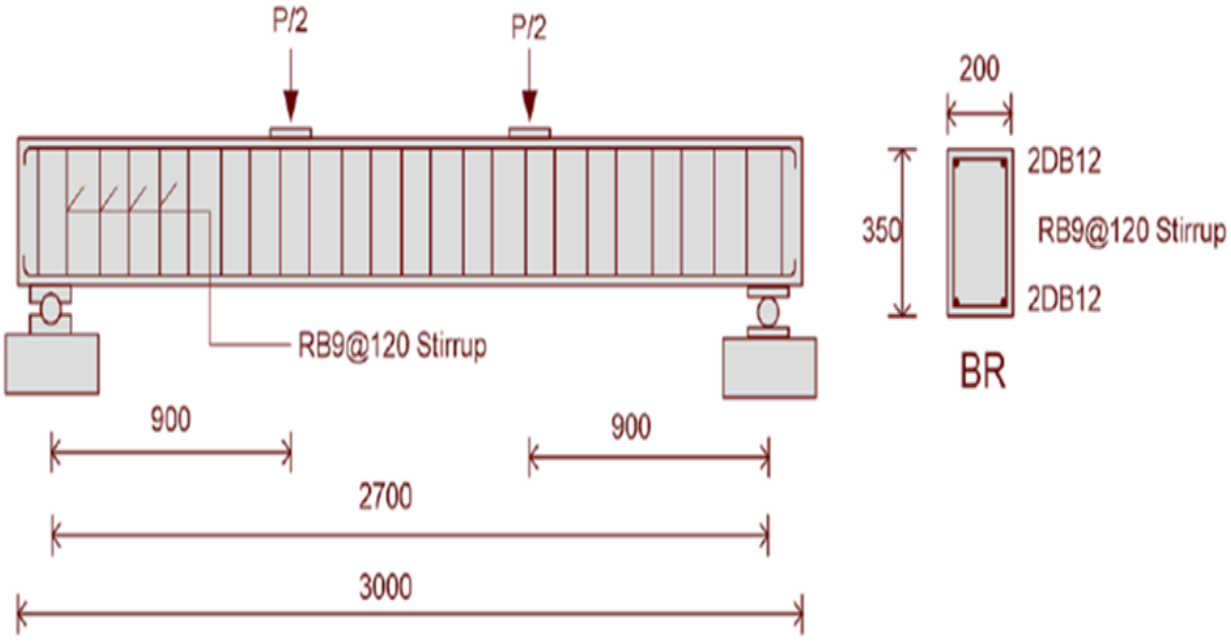

Figure 2.7 Control beam details [34].

The second beam was strengthened using wire mesh and longitudinal reinforcing bars. While the third beam was similar to the second beam but is provide the shear connecter between the beam substrate and strengthening layer, as shown in Figure 2.8. All specimens were tested under static four-point bending test. According to the results of the experiments, the ferrocement layers greatly improved the flexural capacity in terms of cracking and ultimate loads. The ductility of the beam with shear connectors was higher than that of the beam without shear connectors. The beam without shear connectors failed by the delamination between

ferrocement and beam due to the shear flow while the beam with shear connectors showed the good bond at failure between ferrocement and beam surface.

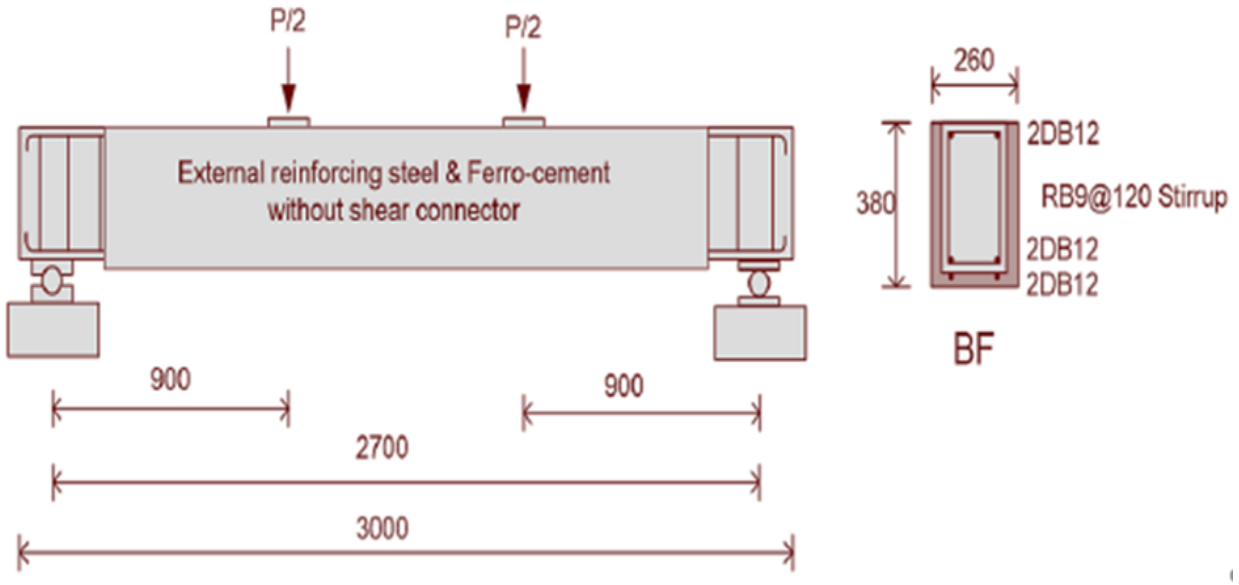

Beam strengthened by ferrocement without shear connectors.

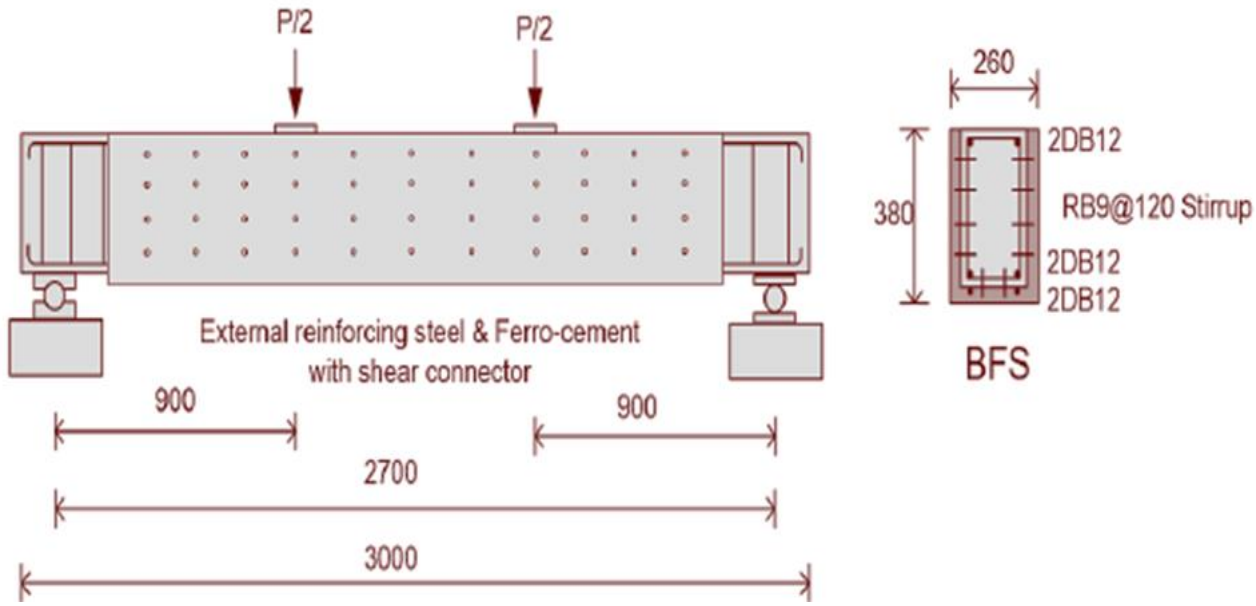

Beam strengthened by ferrocement with shear connectors.

Figure 2.8 Details of reinforcement of the beams with ferrocement [34].

Islam et al. in 2020 [35], conducted a study to evaluate the performance of flexural behavior of reinforced concrete beam with U-shaped ferrocement wrapping

and inter-surface locking. The main variables that had been worked were U-shaped ferrocement wrapping with inherent cementitious bonding, U-shaped ferrocement wrapping with epoxy bonding and U-shaped ferrocement wrapping with epoxy and screw bonding, as shown in Figure 2.9.

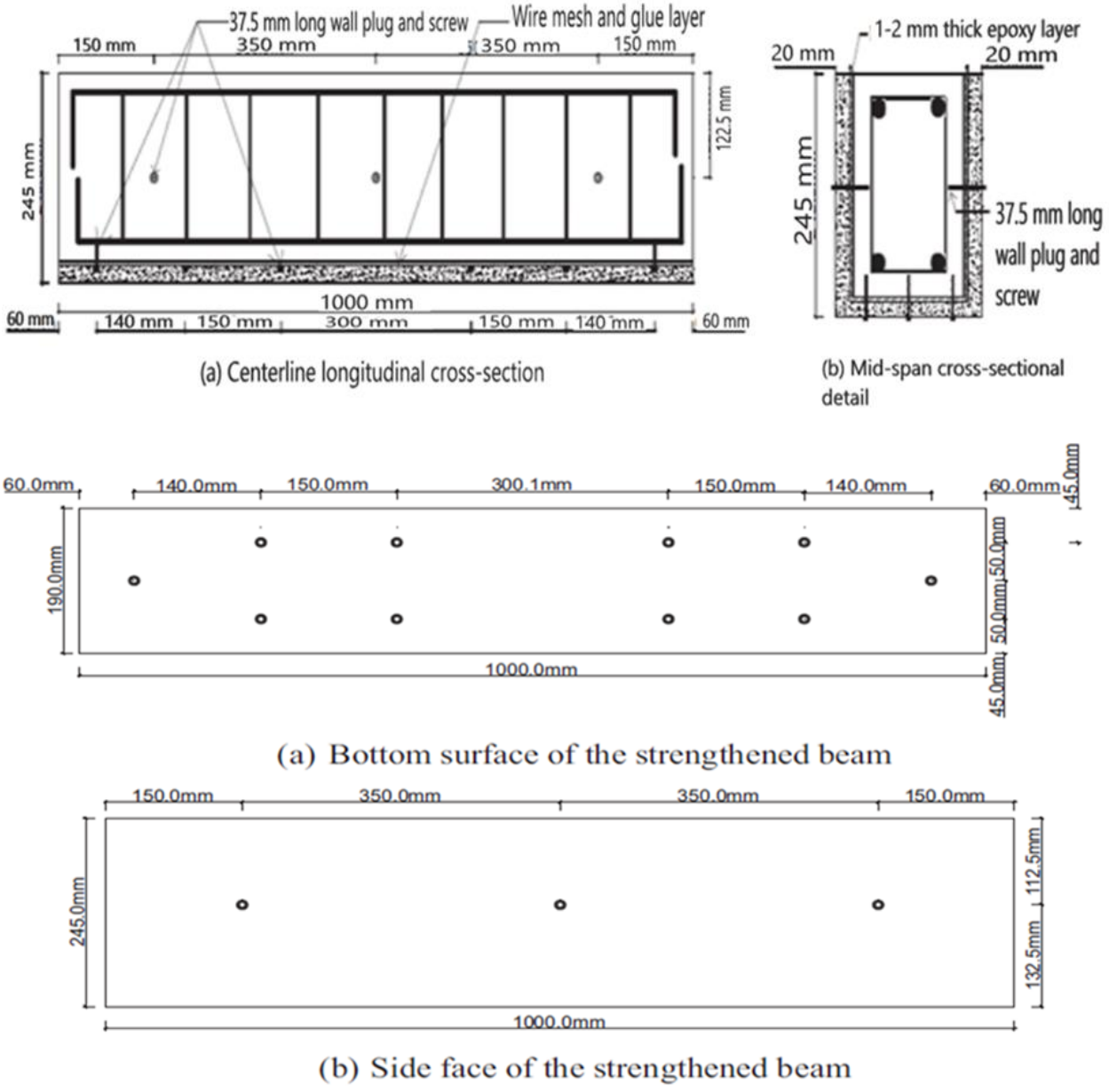

Figure 2.9 Cross sectional description of the retrofitted beam [35].

Based on the observed results, the average flexural capacity of the U-shaped ferrocement wrapping with inherent cementitious bonding was found to increased

up to 19.17%, and by enhancing the inter-surface locking between the ferrocement layer and the original beam surfaces by epoxy it increased by 35.69%. The average flexural capacity increased up to 41.29%, when the inter-surface locking was enhanced by applying epoxy and screwing together. Strengthening with varied inter-surface locking, showed a considerable increase in stiffness and energy absorption capacity. All beams developed flexural cracks without any sign of debonding of ferrocement. It can be inferred that U-shaped ferrocement wrapping successfully increased the flexural capacity of RC beams, and that this capacity may be further enhanced by enhancing the inter-surface locking between the ferrocement wrapping and the original concrete surface of the RC beam.

Amin et al. in 2022 [36], conducted an experimental study to strengthen fire-damaged concrete beams by different layers of wire mesh. After fire damaged, specimens were reinforced with ferrocement and number of wire mesh (single and double layer). A square shaped steel wire mesh having wire spacing of 10 mm and diameter of 0.6 mm was used. The results showed that the ultimate load carrying capability of single and double layers ferrocement strengthening compared to fire damaged specimens improved by 46% and 72%, respectively. The level of heating exposure considerably reduced the residual concrete compressive strength by about 46 %. In terms of load carrying capability and delayed crack formation, the ferrocement with two layers of wire mesh showed more improvement than one layer.

2.3.3 Strengthening of Beams Using Ferrocement (Shear and Flexural)

Hughes and Evbuomwan in 1993 [37], developed an experimental study for repairing of reinforced concrete beams. Five of the beams were improved from origin six, while the sixth beam, acted as the control beam. The repair material contained three types of reinforcing meshes: two layers of steel mesh, five layers of polypropylene fabric mesh, and four glass fiber rods. The results of six beams were

displayed, it can be observed that all of the reinforced beams had much higher ultimate strength than the control beam by a percentage 27%. The beams reinforced with the wire mesh showed higher strength compared to the control beam. The beam augmented with the repair material which contains polypropylene mesh showed a very large increase in deflection and hence increased ductility by over 100% compared with the control beam. This can be attributable to the polypropylene meshes high yield strain. The enhanced beams generally also exhibited higher stiffness, higher ductility and residual strength after maximum load compared to the control beam.

Fahmy and shaheen in 1995 [38], presented an experimental study to investigate the efficacy of employing laminated ferrocement for strengthening and repairing reinforced concrete beams. They used the laminated ferrocement as a suitable alternative to gluing steel plate on the cracked tension side directly with epoxy resins. Each beam was first loaded with a central point load to 67% or 85% of its ultimate load, then unloaded and a ferrocement layer was cast on the tension face or in the shape of a U around the beam. To create composite action, the ferrocement layer was connected to the beam with bent nails. In comparison to the original reinforced concrete beam, the experimental findings demonstrated that regardless of the reinforcing mesh type (woven and expanded wire mesh) and shape of the ferrocement layer, better crack and deflection control were achieved in comparison with the original reinforced concrete beam. The repaired beams reached the ultimate load 1.5 time of the control beam. This type of improvement also increased the ductility and energy absorption qualities of beams. The analytical and experimental data were evaluated and found to be in good agreement.

Bansal et al. in 2008 [39], investigated the effect of wire mesh orientation on the strength of beams retrofitted with ferrocement jackets. Dimensions (127 × 227 × 4100) mm beams were cast and tested. Two were used as control beams and tested

to failure. The other six beams were loaded to 75 % of the safe load obtained from the testing of the control beams and were then retrofitted by ferrocement jackets. The jacket was reinforced with single layer square welded wire mesh, the orientation of the three wire meshes was 0, 45, 60 degree with the horizontal axis of the member. The results indicated, wire mesh oriented at 45 degrees for retrofitting beams had the higher load carrying capacity when compared to control beams as well as the other beams retrofitted using different orientations. For all orientations, there was also a significant increase in energy absorption by a percentage for 76.27%, 73.98% and 70.42% respectively. However, the 45-degree orientation had the highest percentage gain in energy absorption, followed by the 60-degree and 0-degree orientations, respectively. All test specimens showed reduced crack width, considerable deflection at ultimate load, and a significant increase in the ductility ratio after retrofitting.

Patil et al. in 2012 [40], presented an effective method to use ferrocement for strengthening concrete beams in shear and flexure after subjected to a certain proportion of the safe load. Two of the six beams were utilized as control beams and were tested until failure in order to determine the safe load carrying capacity. The remaining four beams were stressed up to (60 and 80)% of the safe load determined by the control beams testing, and then refitted with ferrocement jackets. A double layer of (10 × 10) mm hexagonal chicken wire meshes was used to make the jacket, as shown in Figure 2.10. The main conclusions drawn based on the test results of the experimental study was retrofitted beams with chicken mesh had significant increase in the ultimate load carrying capacity. The beams stressed up to 60% and retrofit with ferrocement laminate was the highest load carrying capacity compared with that of other retrofit by 20%. All of the test specimens showed large deflection at the ultimate load after retrofitting, as well as a significant increase in the ductility ratio.

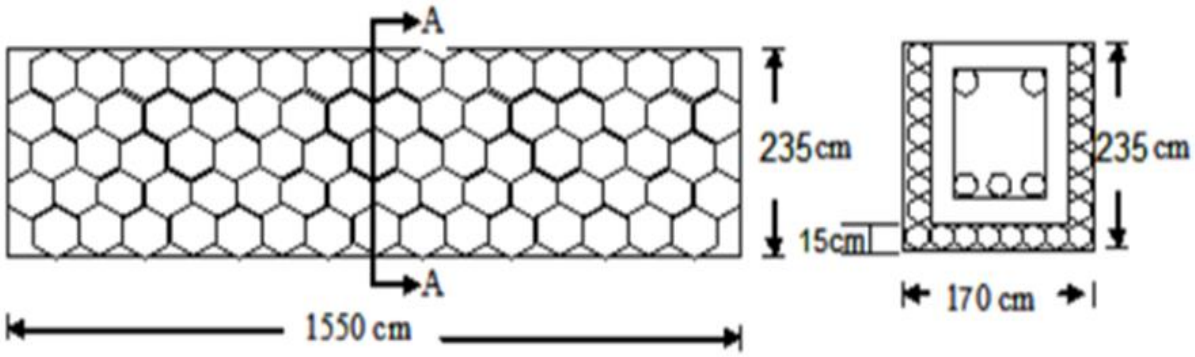

Figure 2.10 Longitudinal and cross section of retrofitted beam with chicken mesh [40].

Ladi and Mohite in 2013 [41], performed an experiment study for strengthening reinforced concrete beams in both flexural and shear using U-shape ferrocement laminated. The experimental work consisted of casting and testing the concrete beams by dimension (100 × 150 × 1000) mm. Three of the twenty-five beams were tested as a control beam to determine the beams ultimate load. Six beams were designed as shear deficient and retrofitted with single and double layers of wire mesh at 0 and 45 degrees. The remaining sixteen beams were loaded up to 60 % and 80 % of ultimate load, then retrofitted with wire mesh layers of orientations 0 and 45 degree. The conclusions obtained from the study were as follows: the flexural retrofitted beams exhibit an increase in flexural 65.18% for single layer at 45 degree and 70.61% for two layers at 45 degree. Exhibit an increase in flexural 58.28% for single layer at 0 degree and 66.66% for two layers at 0 degree. In shear retrofitting, it showed an increase in shear strength of 60.65% for double layer of wire mesh at 45 degree and 20.31% for single layer of wire mesh at 45 degree, 30.17% for double layer of wire mesh at 0 degree. After retrofitting, all the test specimens observed reduced crack widths, deflection and spacing of cracks at the ultimate load.

Majeed in 2013 [42], presented a numerical study to analysis of reinforced concrete beams strengthened with ferrocement in the form of U-jacket using ANSYS software. The study was conducted to analysis RC beams strengthened with U-shape

of different material. These materials were ferrocement jackets and carbon fiber reinforced polymers (CFRP). The predicted results were compared between the two techniques. The results showed that, the addition of a ferrocement jacket to the reference beam increased the ultimate load by about (7.5, 9 and 20)% for ferrocement had 1, 2 and 3 wire mesh layers, respectively. However, using a single layer of CFRP laminate increased the ultimate strength by 37.44%, indicating the superiority of the CFRB to that of ferrocement jacket. Strengthening the reinforced concrete beam by ferrocement jackets increased the deflection at ultimate load up to 17.5%.

Makki in 2014 [43], the flexural and shear response of RC beams retrofitted by ferrocement was investigated. The work focused on the effect of stirrups amount and different diameters of wire mesh (1.2 and 2.2) mm used in rehabilitation. The rehabilitation was applied for specimens stressed up to 50% and 70% of the control ultimate load. The experimental results showed that the rehabilitation technique of concrete beams using ferrocement system was applicable and can increase the ultimate load up to175% in case of strengthening and 125% in case of repairing in compared to control beams. The effect of wire mesh diameter on the ultimate strength of concrete beams was increased 175% without steel stirrups and 126.4% with steel stirrups. As for repairing beams, the effect of diameter of ferrocement wire mesh on the ultimate strength of concrete beams 125% without steel stirrups and 84.9% with steel stirrups. The use of ferrocement meshes as external strengthening had a considerable impact on the crack pattern of reinforced concrete beams, delaying the formation of cracks and reducing crack breadth, as well as creating high deflection at ultimate load.

Al-Rifaie et al. in 2017 [44], proposed a study to investigate the behavior of rehabilitation of the damaged reinforced concrete beams under flexural load using several techniques. Damaged beams were loaded to failure and then repaired by,

ferrocement composite, steel plate, fiber carbon reinforced polymer (FCRP), nano cement composite and the injection of a nano cement mortar were considered. The repaired beams once again tested to determine their final ultimate load carrying capacity. Deduce, the technique of employing bolts in install elements for the rehabilitation of damaged parts of loaded beams has produced good results, in which with ultimate load ratios after rehabilitation 105% and 100.8% for ferrocement and steel jackets, respectively. When epoxy was used to fix carbon polymer fibers, the ratio become 100%. The ultimate load of beam after rehabilitation was 99% of the original ultimate load when used nano ferrocement jacket for rehabilitation. Using nano materials injection technique tend to reach the ultimate load for beam after rehabilitation to 80% of the original loads.

Hassan in 2018 [45], conducted a study on the effect of using fiber wire mesh on the flexural and shear properties of concrete beams. Fiber wire mesh was applied in two manners. The first group was three layers as U shape around the section of the beam, while the second had four layers around overall section of beam. The test results indicated the used of fiber wire mesh of U-shape increases the first cracked load by 42.8 % and 41.2% for flexural and shear, respectively. While the percent increase in first cracked load of samples fiber wire mesh around overall section was 85.7 % and 76.5 % for flexural and shear, respectively. Shear failure criteria were changed from sudden to ductile when fiber wire mesh reinforcement was used.

2.4 Summary

From the previous literature review to strengthen the beams by ferrocement, the following points may be noted:

1. The main goal of the study is focused on investigating the different parameters which expected affecting the behavior of beams with steel wire mesh added. These parameters include the compressive strength, number of wire mesh

layers, shear span to effective depth ratio and presence of transverse reinforcement.

2. The beams do not contain gravel.
3. The application of the wire mesh in the form U-shaped around the steel bars along the shear span.

CHAPTER THREE: EXPERIMENTAL WORK

3.1 General

The main goal of the experimental work is to investigate the shear behavior of beams with a number of wire mesh layers added. Details of seventeen beams specimens with different parameters are presented in this chapter. The parameters investigated in the experimental program consist of variable shear span to effective depth ratio (a/d), compressive strength, number of wire mesh layers, and presence of transverse reinforcement. This chapter also describes material quantities, instruments used, and testing procedures. It also provides complete details on ferrocement beams. The experimental work and the conducted tests were carried out in the laboratories of the college of engineering at the University of Misan and Amarah Technical Institute.

3.2 Materials

The materials used in this investigation were commercially available materials, which include cement, natural sand, silica fume, water, welded wire mesh and superplasticizer. The general description and specifications for the materials used in the testing program are listed below.

3.2.1 Cement

The ordinary Portland-cement (type I) has been used to cast all specimens throughout this program. The whole quantity required was brought to the laboratory and stored in a dry place. The findings of the utilized cement's chemical and physical tests are provided in Table 3.1 and Table 3.2, respectively. These were conducted in accordance with Iraqi Standard No. 5/1984 [46].

Table 3.1 Chemical composition of the cement.

Compound composition	Chemical composition	Percentage by weight	Limits of IQS 5:1984
Lime	CaO	2.0	---
Silica	SiO_2	5.12	---
Alumina	Al_2O_3	5.99	---
Iron Oxide	Fe_2O_3	5.0	---
Magnesia	MgO	3.00	<5
Sulfate	SO_3	2.4	<2.8
Loss on Ignition	L.O.I	3.99	<4
Insoluble residue	I.R	0.7	<1.5
Lime saturation factor	L.S.F	0.66248	0.66-1.02
Main Compounds (Bogue's equation) percentage by weight of cement			
Tri Calcium Aluminate (C_3A)		7.40	
Tetra Calcium Alumina Ferrite (C_4AF)		15.20	

Table 3.2 Physical properties of the cement.

Physical Properties	Test result	Limit of IQS 5:1984
Fineness Using Blaine Air Permeability Apparatus (m^2/kg)	310	> 230
Setting time using Vicat's Instruments Initial (hrs: min.) Final (hrs: min)	 2:00 5:35	 > 45 min < 10 hr
Soundness Using Autoclave Method	0.25%	< 0.8 %
Compressive Strength 3 days (MPa) 7 days (MPa)	 19.6 31.3	 >15 > 23

3.2.2 Fine Aggregate (Sand)

The sand used in all mixtures was a natural sand, as shown in Figure 3.1. The highest grain size is 4.75 mm, with modulus of fineness of 2.73. Sand laboratory tests were carried out in accordance with Iraqi requirements No. 45/1984 [47]. The outcomes of these tests are listed in Table 3.3.

Figure 3.1 Fine Aggregate.

Table 3.3 Grading of the fine aggregate.

No.	Sieve size (mm)	% Passing by weight	
		Fine aggregate	Limits of IQS No. 45/1984-Zone2
1	10	100	100
2	4.75	97	90-100
3	2.36	87	75-100
4	1.18	70	55-90
5	0.60	47	35-59
6	0.30	18	8-30
7	0.15	8	0-10

3.2.3 Silica Fume

Very fine pozzolanic material, composed mostly of amorphous silica produced by electric arc furnaces as a by-product of the production of elemental silicon or ferrosilicon alloys (also known as condensed silica fume and micro silica) [48]. Chemical composition of silica fume contains more than 90% silicon dioxide. Other constituents are carbon, sulfur and oxides of aluminum, iron, calcium, magnesium, sodium and potassium. The physical composition of silica fume diameter is between (0.1 to 0.2) microns about 100 times smaller than average cement particles. Surface area of silica fume is about 30,000 m^2/kg and density varies from 500 to 700 kg/m^3 [49] [50]. Using silica fume with ordinary Portland cement to obtain high-performance concrete is an effective way, which mainly aims to develop properties of concrete, such as strength, permeability, sustainability, and durability [50]. Silica fume is available in markets in bags weighing 20 kg. This type of silica was used in the present work and it conforms to ASTM C 1240-04(ASTM, 2004) [48]. Table 3.4 shows the technical description of used silica fume.

Table 3.4 Technical description of Silica Fume ASTM C 1240-04 [48].

Colour	Grey to medium grey powder
Specific Gravity	2.10 to 2.40
Bulk Density	500 to 700 kg/m3
Chemical Requirements	
Silicon Dioxide (SiO_2)	Minimum 85%
Moisture Content (H_2O)	Maximum 3%
Loss on lgnition (LOI)	Maximum 6%
Physical Requirements	
Specifi Surface Area	Minimum 15 m^2/g
Pozzolanic Activity Index,7days	Maximum 105% of control
Over size Particles retained on 45 micron sieve	Maximum 10%

3.2.4 Water

Potable water was used for casting and curing the beams during work and the trial mixtures.

3.2.5 Superplasticizer

The High Range Water Reducers (HRWR) or superplasticizers (SP) are commonly used in high strength concrete, precast/pre-stressed concrete, architectural concrete, etc [51]. HRWR is can be used in concrete mixtures to increase slump, increase strength by decreasing water content and water-cementitious materials ratio (w/c), or decrease water and cement content, thus reducing temperature rise [52]. In the present work, a superplasticizer, type HyperPlast PC260 is used. This type of plasticizer conforms to ASTM C494 type (A and G) [53]. Table 3.5 shows the technical description of used super plasticizer.

Table 3.5 Technical properties of HyperPlast PC260 [53].

Technical Properties @ 250C:	
Colour:	Yellowish to brownish liquid
Freezing point:	≈ -7°C
Specifi c gravity:	1.1 ± 0.02
Air entrainment:	Typically less than 2% additional air is entrained above control mix at normal dosages
Dosage	0.5 to 3 liter per 100 kg
Storage condition /shelf life	12 months if stored at temperatures between 2°C and 50°C

3.2.6 Wire Mesh

Locally available steel wire mesh of 10 mm square opening with average wire diameter of (1 mm) has been used in this investigation. Figure 3.2 and Figure 3.3

shows the geometry and dimensions of the mesh type used throughout this work. It was decided to determine the mechanical properties of the wire mesh, by conducting a tensile test on coupon specimen using the guidelines presented by ACI committee 549, 1999 [54]. The tested specimen was prepared by embedding both ends of a rectangular coupon of mesh in mortar over a length equal to the width of the specimen, that should not be less than six times the mesh opening. The width of the specimen was taken 80 mm, and it was embedded in mortar with a length of 100 mm. The length of the tested specimen should not be less than three times its width or 150 mm whichever is larger. The length of the tested specimen was taken 240 mm. Wooden Molds were prepared to cast mortar blocks at the end of the wire mesh coupon. The dimension of the molds was in accordance with the ACI committee 549 recommendations [8]. It was 100 mm length, 80 mm width, 20 mm thick to be sufficiently attached to the testing machine clamper, and the length of the tested sample was 240 mm. Figure 3.4 shows the tested wire mesh coupon inserted in the wooden mold before applying the mortar at ends. Table 3.6 shows the geometric and strength characteristics of used wire mesh.

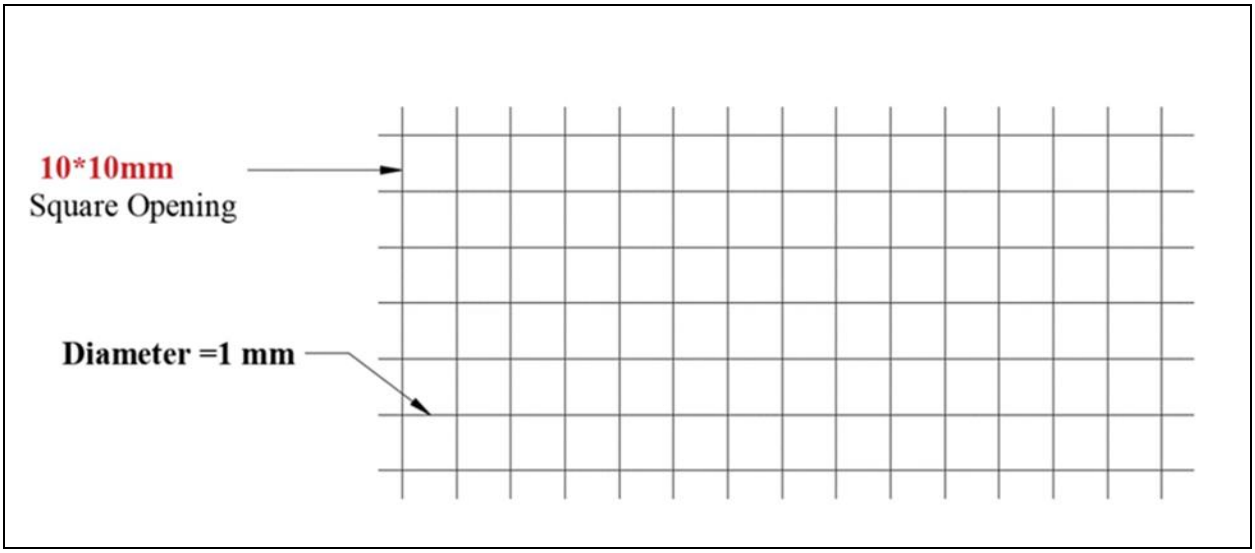

Figure 3.2 Details of steel wire mesh.

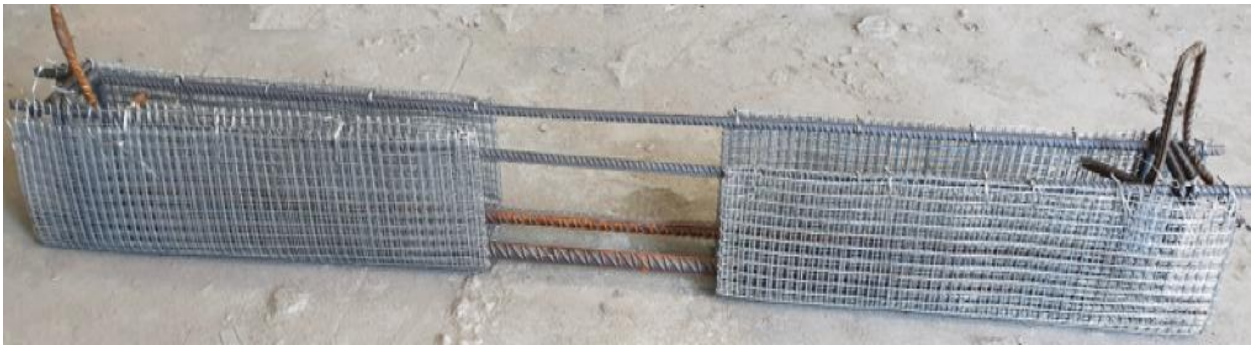

Figure 3.3 Forming the steel wire mesh.

Table 3.6 Properties of wire mesh.

Specimens	Wire diameter (mm)	f_y (MPa)	f_{ul} (MPa)
W1	1	150	290

Figure 3.4 Wire mesh tensile coupons

3.2.7 Steel Reinforcement

Grade 60 steel bars were used in this research. The steel reinforcing bars used for the construction of beams consisted of Ø10 mm diameter steel bar were used for both stirrups and top reinforcement. Ø16 mm diameter steel bar was used for main

bottom reinforcement. Three samples for each diameter were tested using the standard tension test to find the yield stress (f_y) and ultimate stress (f_u). The tests were carried out at the laboratory of Technical Institute of Amarah. Table 3.7 elucidated results of tested bars. Results were in accordance with ASTM (A615/A615-20) [55]. Figure 3.5 shows stress-strain curve of steel bar. Figure 3.6 shows tension test for reinforcement bar.

Table 3.7 Test result of steel reinforcement.

Test results				ASTM A615/A615M		
Bar size (mm)	Yield strength (N/mm^2)	Ultimate Strength (N/mm^2)	Elongation (%)	Yield strength (N/mm^2)	Ultimate Strength (N/mm^2)	Elongation (%)
10	569.0	687.0	15.6	420	550	9
16	549.8	643.6	14.9	420	550	9

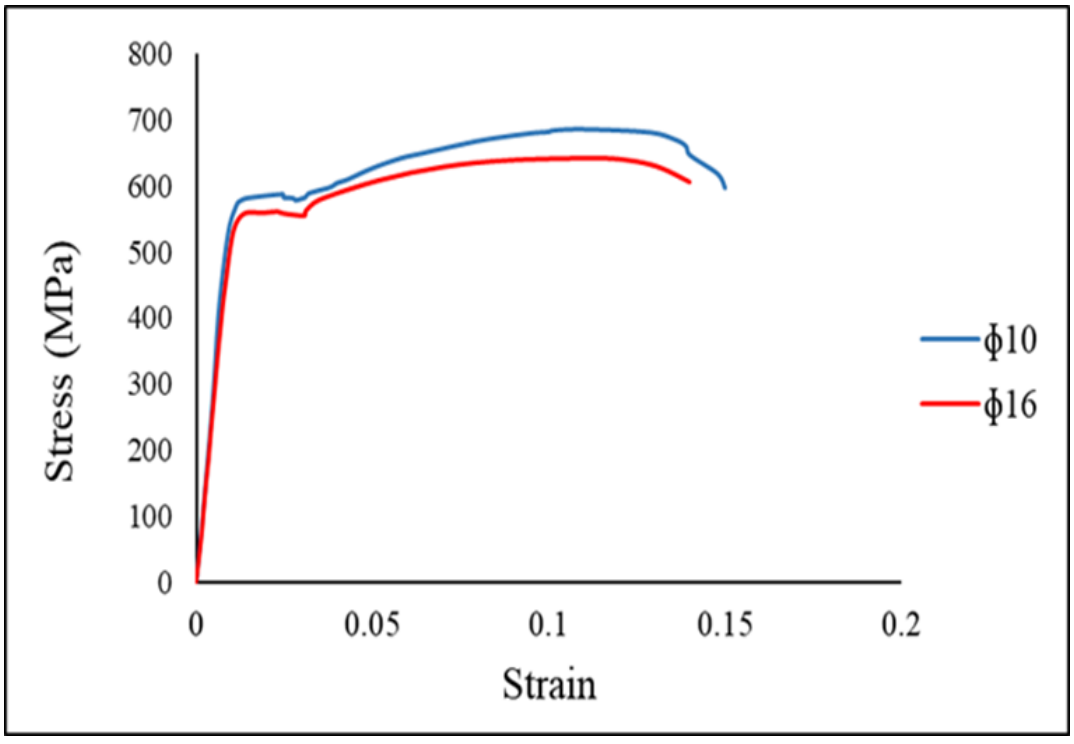

Figure 3.5 Stress-strain curve of steel bar.

(a) Test setting (b) Ø10 bar (c) Ø16 bar

Figure 3.6 Tensile strength of reinforcement test bars.

3.3 Preparation of Test Specimens

3.3.1 Mix Design

Two kinds of mortar mixes were used, which are classified depending on compressive strength values at the age of 28 days, (normal and high strength mortar).

3.3.1.1 Normal Strength Mortar

Normal strength mortar having a cube compressive strength, f_{cu} = 35 MPa was used to pour the three beams specimens. The mix proportions of mortar materials by weight were 1:2 (cement: sand). The maximum water-cement ratio (w/c) was 40% and Hyperplast PC260 superplasticizer with 0.5% of cement weight was added to the mix to improve the workability. Table 3.8 shows the mix quantities per cubic meter.

3.3.1.2 High Strength Mortar

High strength mortar f_{cu} = 65 MPa was used to pour fourteen beams. Mortar raw materials were natural sand, silica fume, portland cement, water and superplasticizer. The water to cement ratio has been reduced to 20% to produce high strength mortar and a suitable quantity of superplasticizer 2.7% was used to get good workability and silica fume 15%. The mix proportions by weight were 1:1.1 (cement: sand). Table 3.8 shows the mix quantities per cubic meter.

Table 3.8 Material quantities.

Mix No.	Cement (kg/m^3)	Sand (kg/m^3)	Water (kg/m^3)	Silica fume (kg/m^3)	Superplasticizer (kg/m^3)
1	695.80	1391.60	278.32	---	3.47
2	950.00	1050.00	190.00	142.50	25.65

3.4 Specimens Details

Seventeen beams have been cast and tested. The total length of each beam is 1600 mm with clear span 1300 mm and width 150 mm with the total depth is 200 mm. Different parameters were examined to find out their effect on the behavior of the specimen. These variable parameters were the shear span to effective depth ratio (a/d), compressive strength, and the number of layers of a wire meshes U-shaped on along the shear span, the mesh layers were tied on the steel reinforcement, in addition to the effect of stirrups amount. The effect of compressive strength (high and normal strength) were also studied.

The nomenclature used in this research to describe the specimen is as follows:

N, normal strength mortar.

H, high strength mortar.

S, stirrups.

W, without stirrups.

1, amount of (a/d) = 1.8

2, amount of (a/d) = 2.5

4, 8, 10 for number wire meshes layers.

For example 1HS10, 1: a/d = 1.8, H: high strength mortar, S: stirrups, 10: for number wire meshes layers.

Table 3.9 is elucidated the detail of all groups.

Table 3.9 Beams specimens details.

Series	ID	No. of Wire Mesh Layers	The purpose of this groups	Stirrups	ρ_v	Volume Fraction	(a/d)	f_{cu} (MPa) at 28- day
First group	2HS	0	Study the effect of stirrups with the number of wire mesh	Ø 10 @200	0.025	---	2.5	65
	2HS4	4		Ø 10 @200	0.025	0.0039	2.5	65
	2HS8	8		Ø 10 @200	0.025	0.0078	2.5	65
Second group	2HW	0	Study the effect of the number of wire mesh without stirrups	---	---	---	2.5	65
	2HW4	4		---	---	0.0039	2.5	65
	2HW8	8		---	---	0.0078	2.5	65
Third group	1HS	0	Study the effect of a/d and number of wire mesh layers with stirrups	Ø 10 @200	0.019	---	1.8	65
	1HS4	4		Ø 10 @200	0.019	0.0039	1.8	65
	1HS8	8		Ø 10 @200	0.019	0.0078	1.8	65
	1HS10	10		Ø 10 @200	0.019	0.0098	1.8	65
Fourth group	1HW	0	Study the effect of the (a/d) and number of wire mesh layers without stirrups	---	---	---	1.8	65
	1HW4	4		---	---	0.0039	1.8	65
	1HW8	8		---	---	0.0078	1.8	65
	1HW10	10		---	---	0.0098	1.8	65
Fifth group	2NS	0	Study the effect of the compressive strength	Ø 10 @200	0.025	---	2.5	35
	2NS4	4		Ø 10 @200	0.025	0.0039	2.5	35
	2NS8	8		Ø 10 @200	0.025	0.0078	2.5	35

The volume fraction of reinforcement can be calculated from the following equation 3.1

$$V_r = \frac{N\pi d_w^2}{2\,hD} \qquad 3.1$$

N = Number of layers mesh, π = 3.14, d_w^2 = Diameter of mesh

h = Thickness of ferrocement element

D = Distance center to center between longitudinal or transverse wires

3.4.1 First Group

This group was including three beams, 2HS, 2HS4, and 2HS8, with f_{cu} = 65, with a variable number of mesh layers. The first specimen represents a control beam 2HS, while a number of wire mesh layers (4 and 8) were added to 2HS4, 2HS8. The purpose of this group was to study the effect of stirrups with the number of mesh on the shear capacity of section, details of the group are in the Figure 3.7 and Figure 3.8.

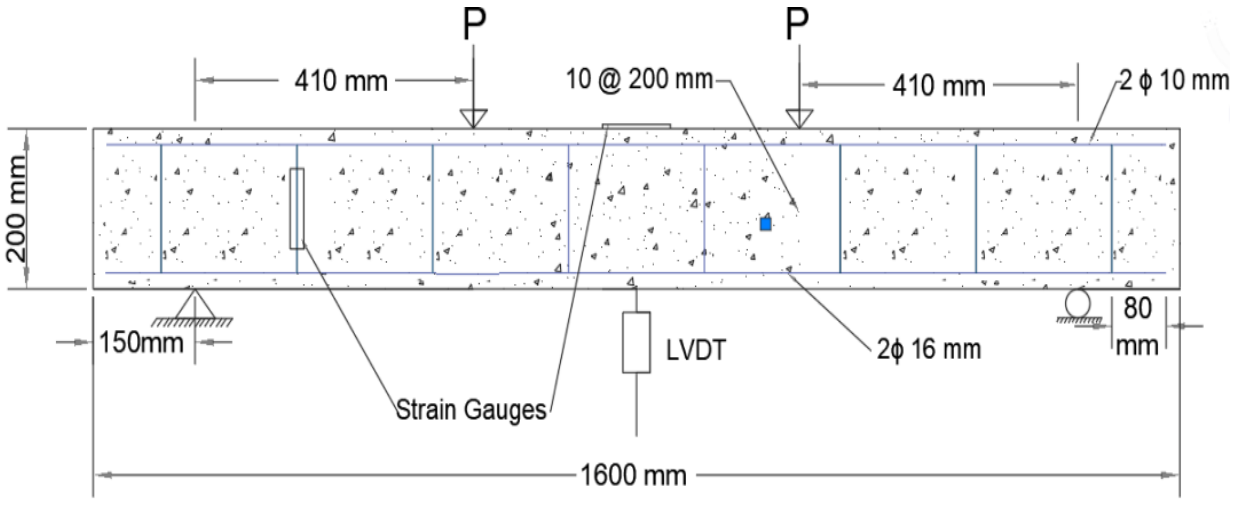

2HS specimen details.

Figure 3.7 First group details for 2HS.

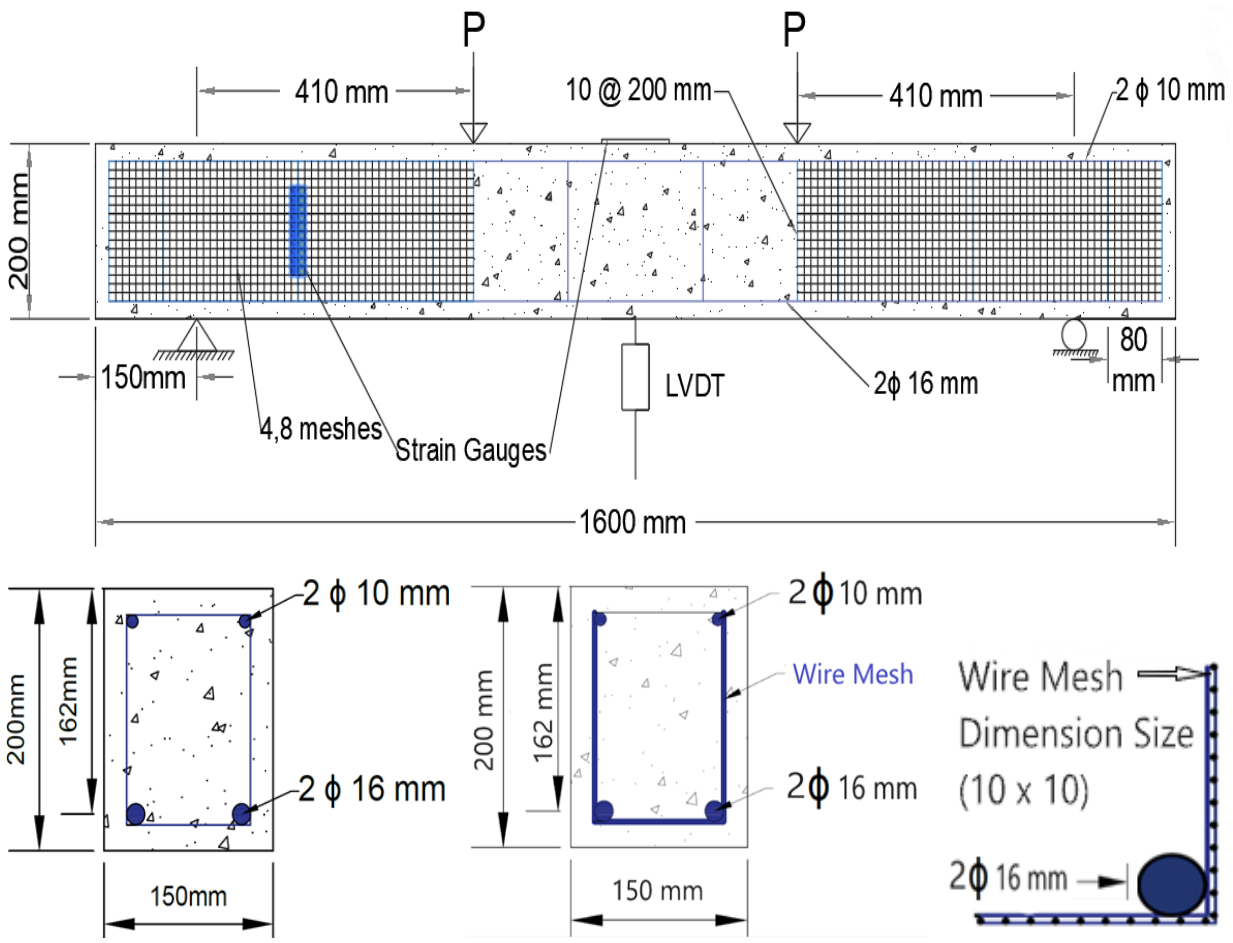

Cross-section for 2HS. Cross-section for 2HS4 and 2HS8.

Figure 3.8 First group details for 2HS4 and 2HS8.

3.4.2 Second Group

This group was including three beams 2HW, 2HW4 and 2HW8. The specimens in this groups are without stirrups. The first specimen represents a control beam 2HW, while a different number of wire mesh layers (4 and 8) were added to 2HW4, 2HW8 respectively. The purpose of this group was to study the effect of the number of mesh layers without stirrups on the shear capacity of section and compared it with the first group, details of the group are in the Figure 3.9.

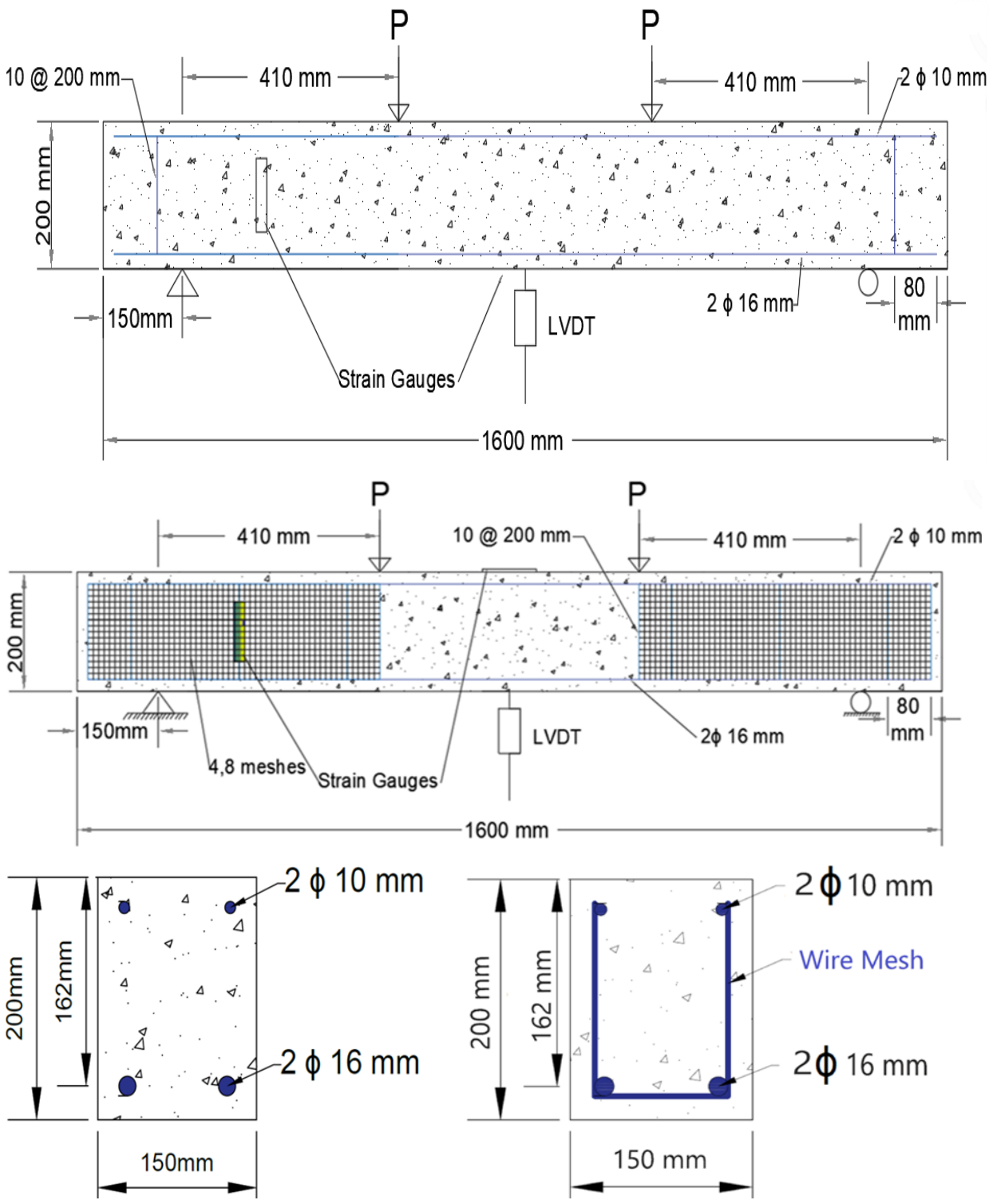

Cross-section for 2HW

Cross-section for 2HW4 and 2HW8

Figure 3.9 Second group details.

3.4.3 Third Group

Four beams belong to this group 1HS, 1HS4, 1HS8 and 1HS10. The first beam was control beam 1HS, while a different number of wire mesh layers (4, 8 and 10) were added to 1HS4, 1HS8 and 1HS10 respectively. The variable in this group is (a/d) = 1.8 while the compressive strength is kept constant. The objective of this group was to find out the effect of the (a/d) on the shear capacity. And also, the objective of this group was to make a comparison with first group to study the effect of stirrups with the number of mesh on the shear capacity of section, details of the group in the Figure 3.10 and Figure 3.11.

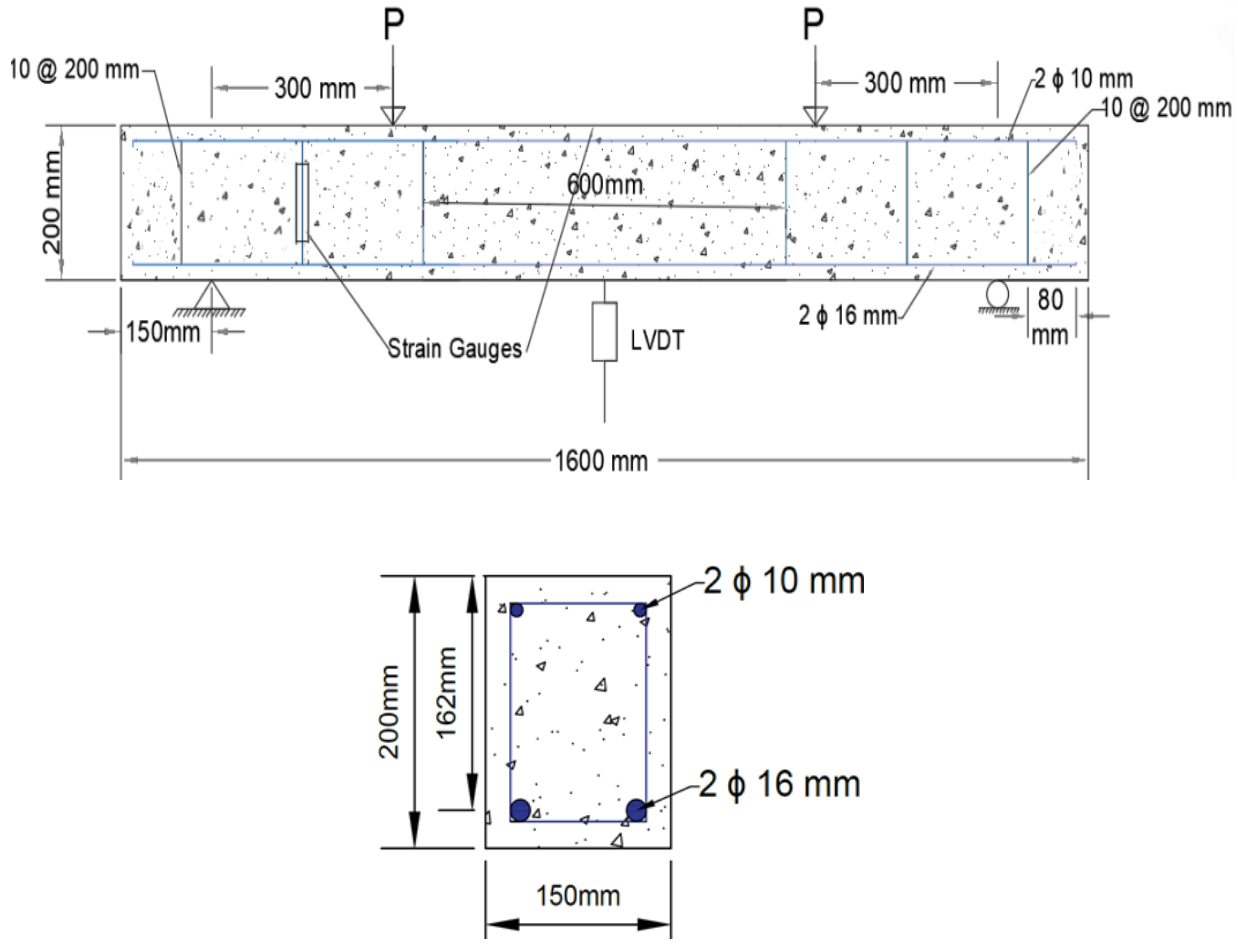

Cross-section for 1HS

Figure 3.10 Third group details for 1HS.

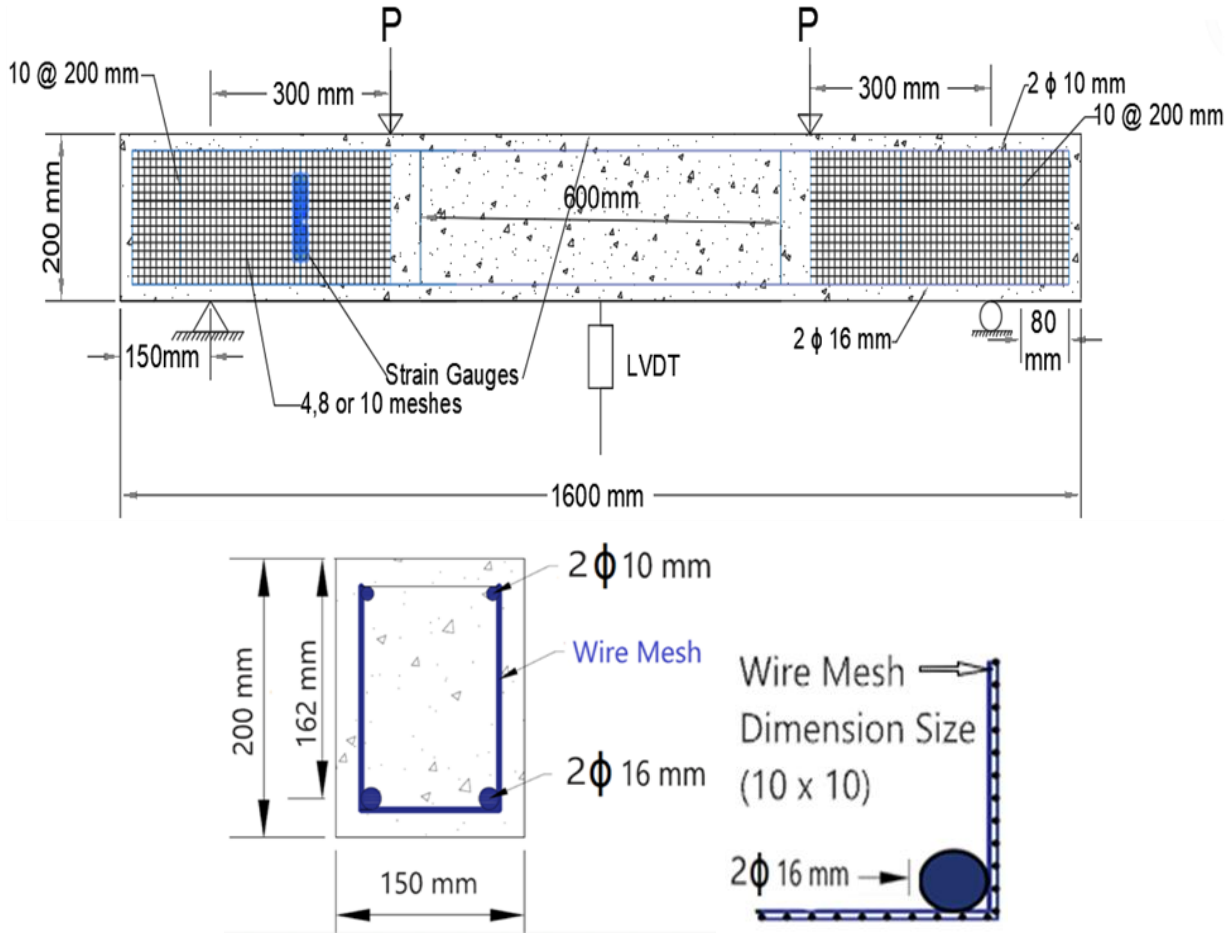

Cross-section for 1HS4, 1HS8 and 1HS10

Figure 3.11 Third group details for 1HS4, 1HS8 and 1HS10.

3.4.4 Fourth Group

This group was including four beams. The first is control beam 1HW, while a different number of wire mesh layers (4, 8 and 10) were added to 1HW4, 1HW8 and 1HW10 respectively. The variable in this group is (a/d) = 1.8 and no stirrups while the compressive strength is kept constant. The objective of this group was to make a comparison with group two and three to study the effect of the (a/d) on the shear capacity of beams and the number of mesh layers without stirrups on the shear capacity of section, details of the group are in the Figure 3.12.

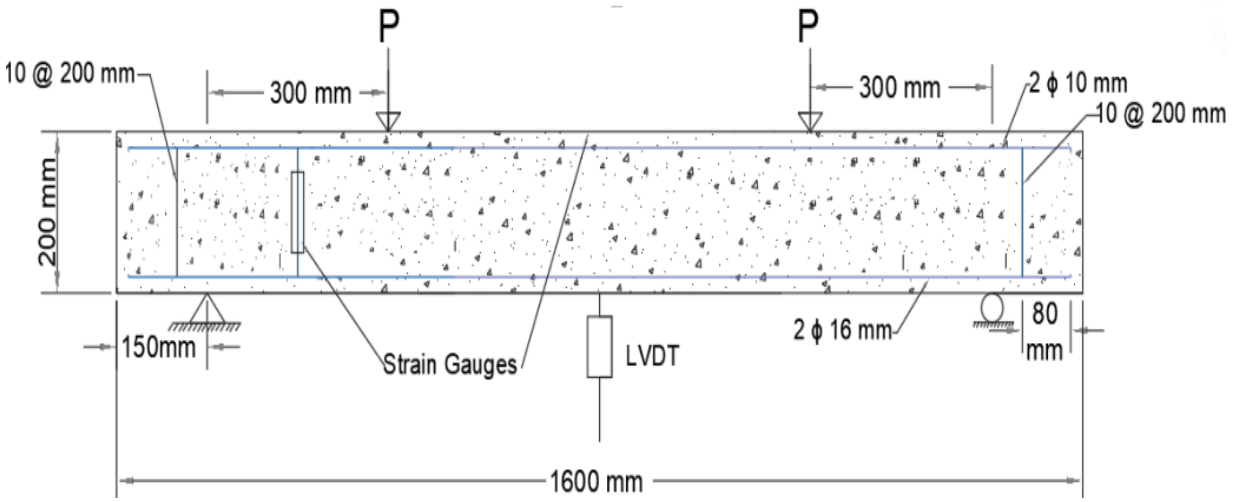

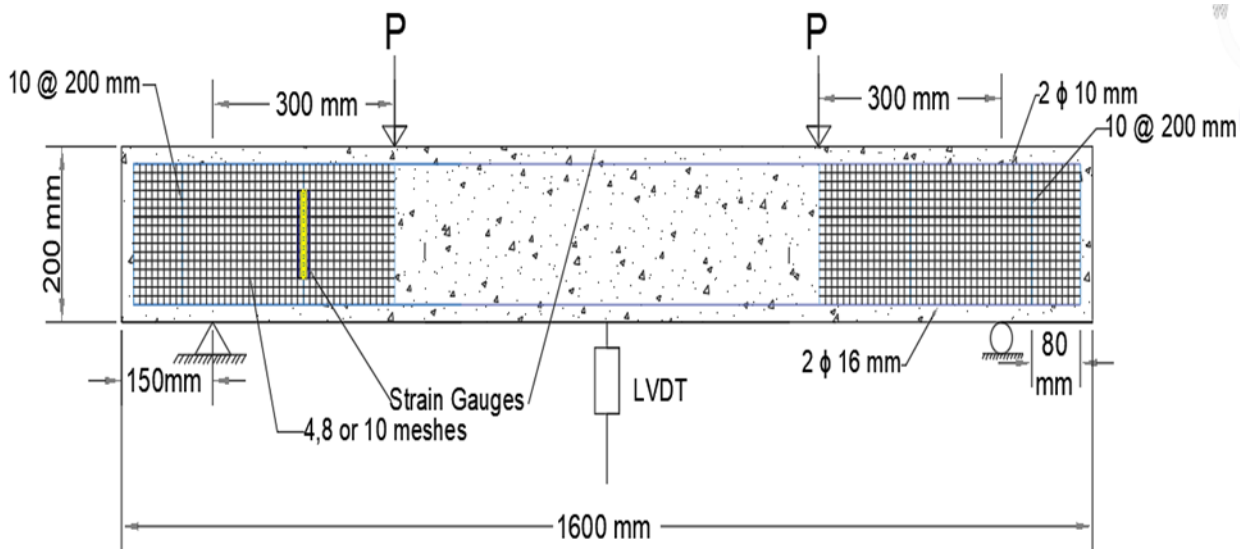

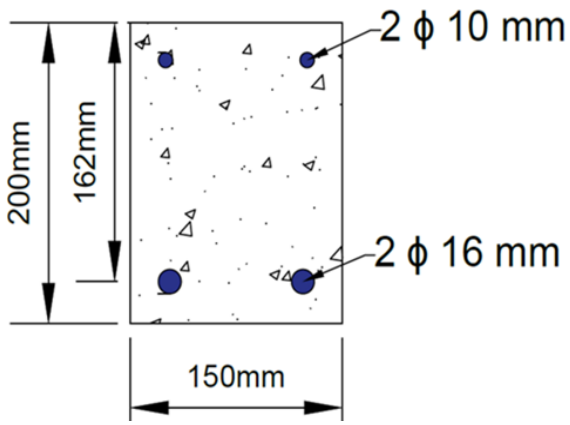

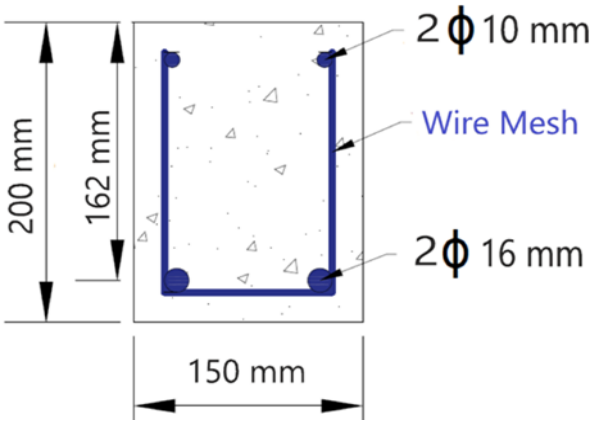

Cross-section for 1HW Cross-section for 1HW4, 1HW8 and 1HW10

Figure 3.12 Fourth group details.

3.4.5 Fifth Group

In this group there were three beams, one was control beam, and the beams 2NS4, 2NS8 as in the previous (first group). The variable in this group is the compressive strength f_{cu} = 35. The aim of this group was to study the effect of the compressive strength of beams and to make a comparison with the first group to find out the contribution compressive strength on increasing of ultimate load. Design and reinforcement details are similar to the first group Figure 3.7.

3.5 Specimens Molds Fabrication

Seventeen molds were made for ferrocement beams from plywood blocks 12 mm thickness. All molds consist of a wooden base and four movable sides connected to base with screws and nails, as shown in Figure 3.13. The dimensions of these moulds are (1600 × 200 × 150) mm. The gaps in the plywood mold were filled by silicon glue.

Figure 3.13 Plywood molds.

3.6 Casting of Specimens

In this study the mixes were mixed by utilizing 40 L pan mixer that manufactured in the local market according to the requirements, as shown in Figure

3.14. Seventeen of ferrocement beams specimens were cast. The casting of all specimens was executed at the materials laboratory of the Civil Engineering Department at the University of Misan. Before raw materials loading, the interior surface of the mixer was cleaned and moistened.

Figure 3.14 Pan mixer.

The processes of mixture are as summarized below:

1. Cement and silica fume, were mixed for (1 to 2) minutes with slow motion of mixer.
2. Sand was added slowly over cementitious material, with continue mixing the dry materials with slow motion of mixer for another (1 to 5) minutes.
3. Half of water and PC260 were mixed together, and added half of liquid to admixture slowly and continue mixing for (3 min) with increase the speed of mixer to medium motion.
4. Then the rest water was added to admixture, the mixing time of this process isn't specified due to the low w/c ratio. During this process the style of the admixture will change progressively, from a dry to a dry with balls, and finally

to be a fluid mixture. At this process the motion of mixer was at the maximum speed.

After materials loading and mixing, the mortar was transported by a wheelbarrow and placed at cleaned and oiled molds of specimens. The mortar was poured into two layers and compacted by using an electrical vibrator to secure concrete compaction and preventing of cavitation. Figure 3.15 shows the casting sequence.

Figure 3.15 Specimens casting.

3.7 Curing of Specimens

After the casting, the formworks lifted after 24 hours and the curing procedure was applied by covering by saturated burlap as shown in Figure 3.16, to prevent water loss as well as supplying additional curing water to sustain specimens. The duration of curing was continued 28 days until the required concrete properties were achieved. After 28 days, the saturated burlap is removed from the surfaces of

specimens and paint by white color to detect the crack pattern when test, as shown in Figure 3.17.

Figure 3.16 Curing of specimens.

Figure 3.17 Painting the specimens by white color.

3.8 Mechanical Properties

During casting, twelve (50 × 50 × 50) mm cubes, six (50 × 75) mm cylinders and six (40 × 40 × 160) mm prisms for each type of compressive strength were made, as shown in Figure 3.18. All molds were prepared, cleaned, and lubricated before casting. Three tests were made: flexural strength, splitting tensile and compressive strength. All the tests were executed according to (ASTM).

(a) Prisms

(b) Cylinder

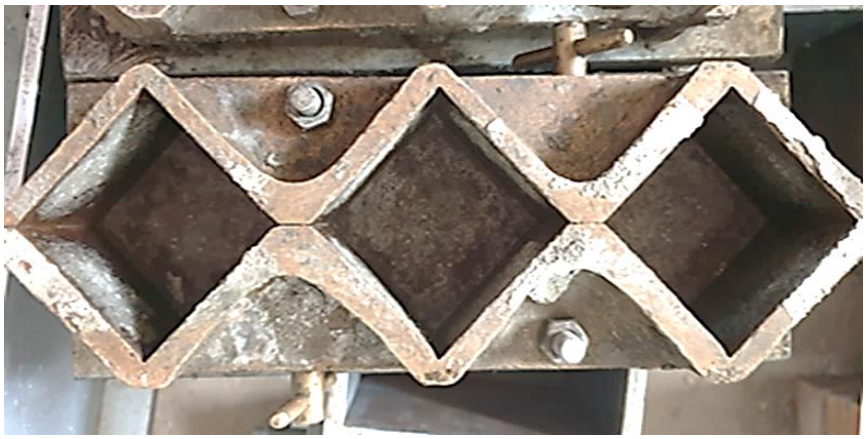

(c) Cubes

Figure 3.18 Tests tools (cubes, cylinders and prisms).

3.8.1 Compressive Strength Test

The cube compressive strength was obtained by testing cubes according to ASTM C109 – 02 [56], as shown in Figure 3.19. The test was conducted by using 2000 kN capacity compression testing machine at the laboratory of construction material of Civil Engineering Department. The tests were conducted 7 and 28 days after casting. The average compressive strength obtained of normal and high strength

are (39.3) and (72.4) MPa, respectively. The compressive strength is listed in Table 3.10.

Figure 3.19 Compressive strength test.

Table 3.10 Values of compressive strength test.

Specimens No.	High Compressive strength (MPa) at 7-day	High Compressive strength (MPa) at 28-day
1	65.6	71.3
2	64.0	72.6
3	68.0	73.4
Average	65.8	72.4
Specimens No.	Normal Compressive strength (MPa) at 7- day	Normal Compressive strength (MPa) at 28 -day
1	31.5	38.3
2	32.2	38.9
3	30.6	40.7
Average	31.4	39.3

3.8.2 Flexural Strength Test

Prisms with dimensions (40 × 40 × 160) mm were tested according to ASTM C348 [57] procedure. Six prisms were tested by flexural machine of 49 kN capacity. The values of testing specimens was at 28-day shown in Table 3.11. This test was done in the College of Engineering, Misan University, using flexural machine as shown in Figure 3.20. The test results are presented in Table 3.11. The following equation 3.2 was used to calculate the bending strength:

$$F_r = \frac{3PL}{2\,bd^2} \qquad 3.2$$

where, Fr: is modulus of rupture (MPa), P: is maximum applied load (N), L: is span length (mm), b: is average width of the specimen (mm), and d: is average depth of specimen (mm).

Figure 3.20 Flexural strength test.

Table 3.11 Flexural strength results.

Flexural strength (MPa)		
Specimens No.	Normal strength at 28- day	High strength at 28-day
1	8.9	15.1
2	9.1	15.3
3	9.4	15.6
Average at 28 days	9.1	15.3

3.8.3 Splitting Tensile Strength Test

ASTM- C 780 [58] has been adopted to check split tensile strength of concrete cylindrical specimens (50 × 75) mm. This test was done at the College of Engineering at the University of Misan by using compression testing machine with a capacity of 2000 kN as shown in Figure 3.21. The test results are presented in Table 3.12. The split tensile strength of concrete was calculated by using the following formula 3.3.

$$F_t = \frac{2P}{\pi dL} \qquad 3.3$$

where, F_t: is tensile strength (MPa), P:is ultimate failure load (N), d:is diameter of cylinder specimen (mm), and L: is length of cylinder specimen (mm).

Table 3.12 Results of splitting tensile strength.

Splitting tensile strength (MPa)		
Specimens No.	Normal strength at 28- day	High strength at 28-day
1	3.2	5.5
2	3.1	5.4
3	3.0	5.6
Average at 28 days	3.1	5.5

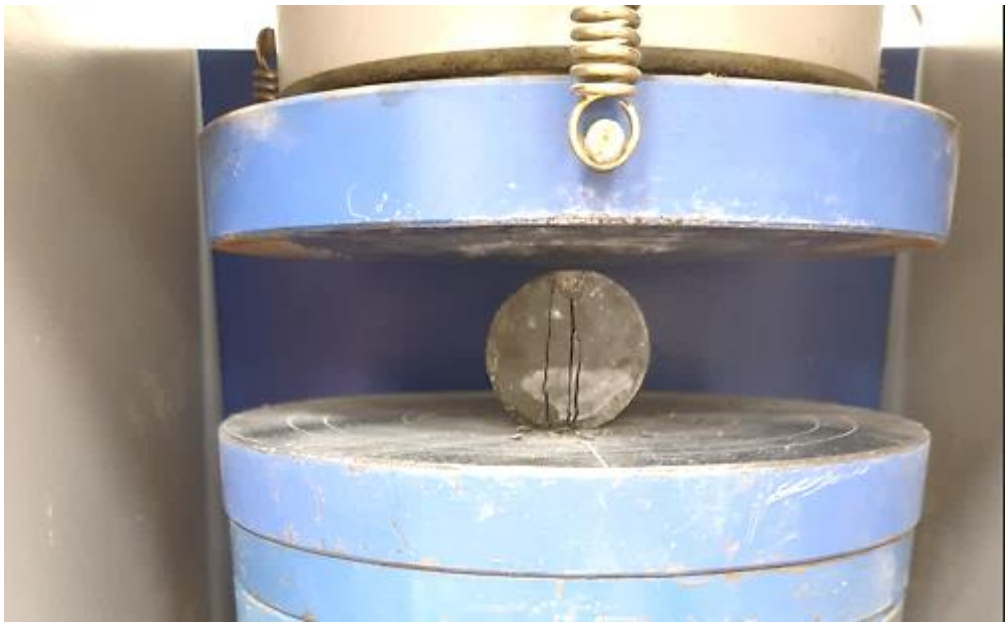

Figure 3.21 Splitting tensile strength test.

3.9 Strain Gauges

Two strain gauges of length (30 mm) used to measure strains in each specimen, as shown in Figure 3.22.

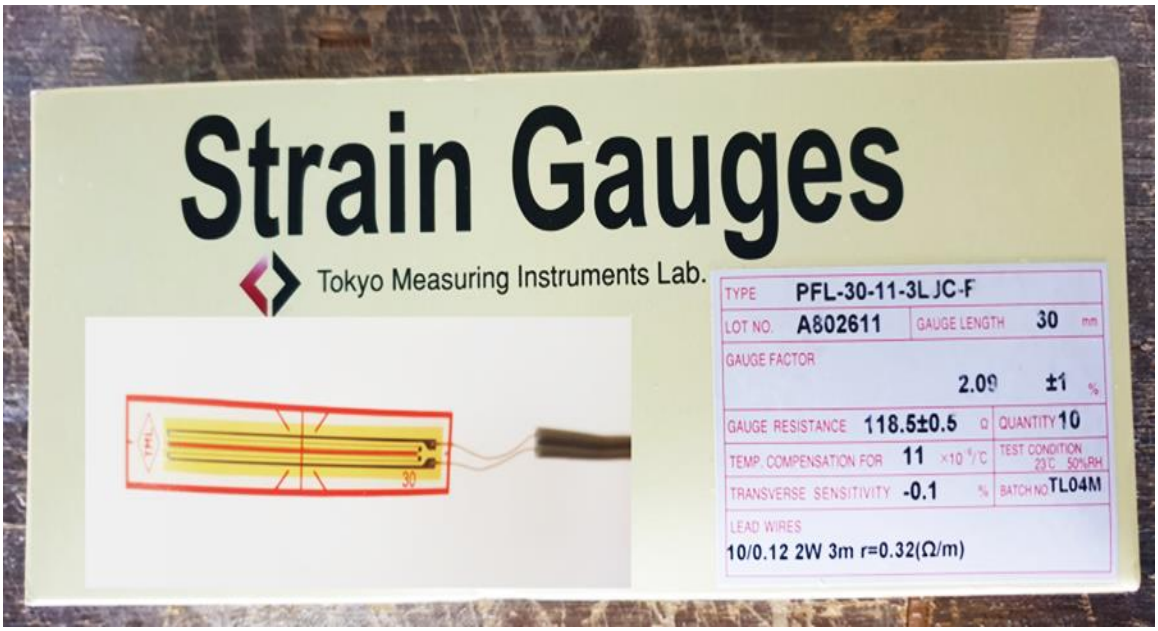

Figure 3.22 Strain gauge.

One of them was located on the upper surface of the test beam at mid span to measure compressive strain. The other was installed in the mid shear span to measure diagonal tensile strain, as shown in Figure 3.23. They were connected to data acquisition device (data logger consists of 8 channels supplied with DATACOMM software for PC data acquisition) to obtain strain reading at each load increment, as shown in Figure 3.24.

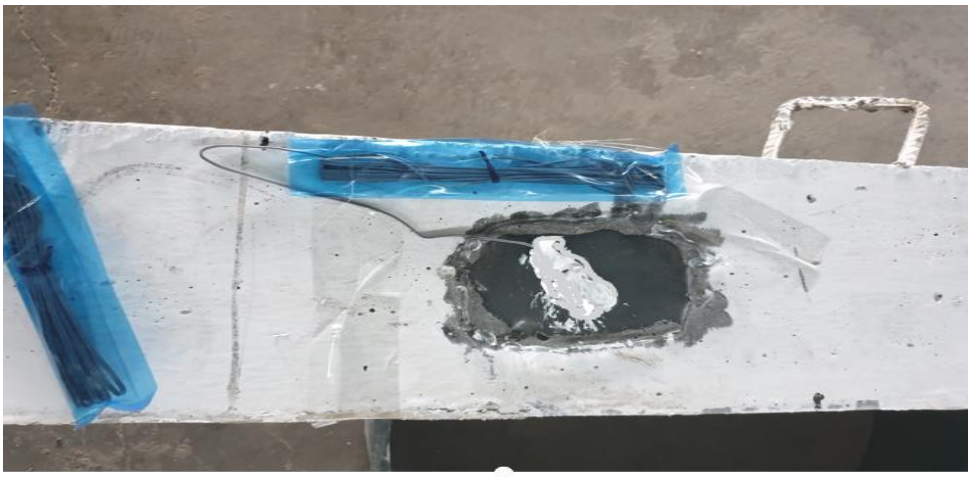

Figure 3.23 Location of strain gauges to the beam.

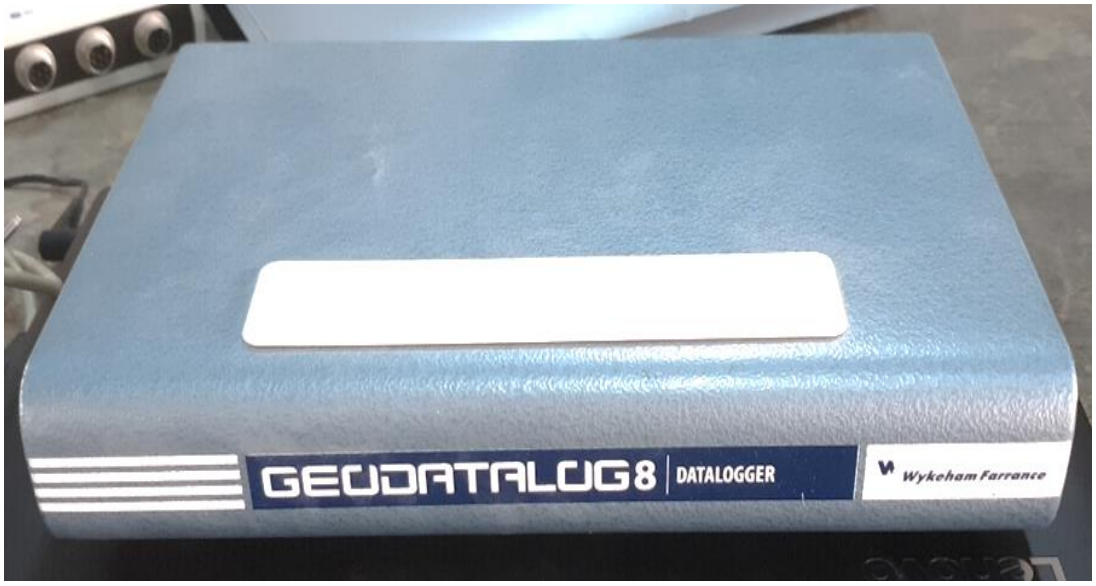

Figure 3.24 Data logger.

3.10 Deflection Measurement

The mid-span deflection of each beam was measured by using (LVDT 10 cm) with accuracy of (0.001 mm) with a magnetic base, as shown in Figure 3.25. The (LVDT) was placed at the center of span.

Figure 3.25 LVDT and the magnetic base.

3.11 Testing Procedure

The seventeen beams were tested utilizing a hydraulic machine of 600 kN capacity. This test done in the laboratory of the Technical Institute of Amarah. Static loads are applied to the beams in successive increments until they fail. The load is applied vertically at the two points load of the top face of beam (the distance between two point loads is 700 mm and 480 mm). A distance of 150 mm was left from the edge of the beam to the middle of the support when testing specimens, as shown in Figure 3.26. The mid-span deflection and corresponding applied load were taken

each 5 kN. Readings of strains are recorded by using strain gauges at each load intervals, as well as recording the first crack load and the failure load of the beam.

Figure 3.26 Test setting.

CHAPTER FOUR: RESULTS AND DISCUSSIONS

4.1 General

This chapter describes the experimental results for the beams tested in this investigation. The experimental results of seventeen beams subjected to two points load are introduced, which are divided into five groups to investigate the influence of the variables on behavior of beams. The main variables that considered in the study are the number of wire mesh, compressive strength, shear span to effective depth ratio (a/d) and presence of transverse reinforcement. Test results are analyzed by cracking load, ultimate load, failure modes, ductility index, initial stiffness, mid span deflection, and strains distribution.

4.2 Load - Deflection Response

The test results of the tested beams in terms of ultimate load, deflection and the percentage of the increase for each beam are listed in Table 4.1 and Table 4.2. The load-deflection curves for the tested beams show the behavior of beams is linear elastic till the cracks occur shear cracks in the shear span zones (edge regions), or (vertical flexural crack in the central part). As the applied load increased and the response of the beams altered, it showed a non-linear behavior of the beams response.

4.2.1 Load - Deflection to (First, Third and Fifth Groups)

Table 4.1 shows the measurement of ultimate load and deflection for the first, third and fifth groups. The load - deflection curve of specimens (2HS, 2HS4 and 2HS8) are illustrated in Figure 4.1. The specimens have the same (a/d) ratio, compressive strength and the amount of transverse reinforcement, while the selected variable is the number of wire mesh layers. They are 0, 4 and 8 layers were chosen.

Wire mesh (4 and 8) layers are added to the 2HS4 and 2HS8 beams, respectively. While the beam 2HS is a control beam.

Table 4.1 Deflection and ultimate load tested beams.

Series	ID	Deflection (mm)	Increasing ratio of deflection (%)	Ultimate load (kN)	Increasing ratio of ultimate load (%)
First Group	2HS	13.98	---	155	---
	2HS4	16.09	15	186	20.0
	2HS8	12.44	-11	248	60.0
Third Group	1HS	11.98	---	207	---
	1HS4	14.09	17.6	245	18.3
	1HS8	10.64	-11.1	271	31.0
	1HS10	9.54	-20.3	299	44.44
Fifth Group	2NS	8.76	---	137	---
	2NS4	9.87	13	159	16.0
	2NS8	8.2	-6.3	200	46.0

These beams to which the wire mesh was added showed increase of the ultimate load by percentage (20 and 60)%, respectively compared with the control beam 2HS. The maximum deflection of the beam 2HS4 is increased by 15% which contain four layers of wire mesh. While the recorded maximum deflection of 2HS8 is decreased by 11% compared by control specimen. Generally, the ultimate load increases with the increase in the number of layers compared to control beams. The addition of wire meshes improved the ultimate load well. That the increase of the number of mesh layers did not necessarily result in increasing the deflection in all specimens. The decrease of the ultimate deflection of the beams is mainly due to increasing the volume fraction. The use of a larger number of layers leads to an increase in the confining of the zone along shear span, and this in turn contributes to reducing the effective length of the beam due to the increase in stiffness. So

increasing the stiffness reduces the deflection of the beams as cited in the results (El-Sayed and Erfan [26]).

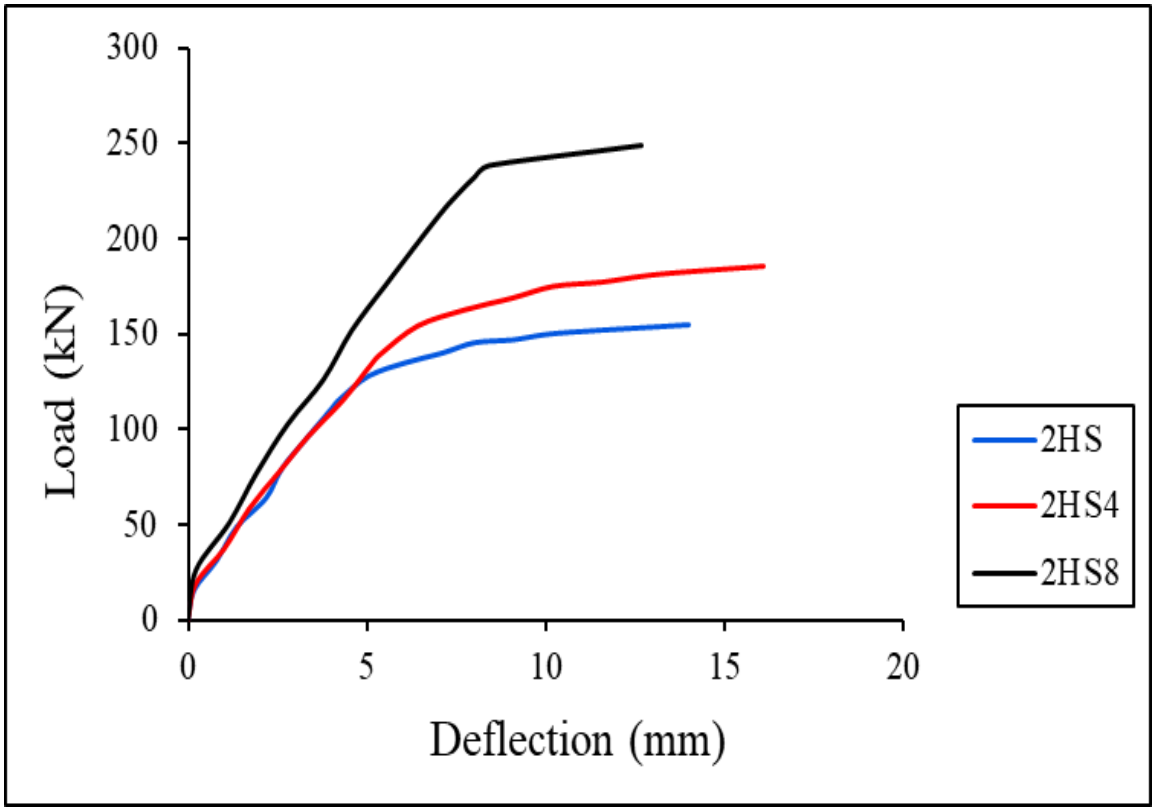

Figure 4.1 Load deflection curve for first group.

The specimens of third group (1HS, 1HS4, 1HS8 and 1HS10) have same details of the first group exept for the a/d is changed. In these specimens, the considered a/d is 1.8. The load-deflection relationships of this group are presented in Figure 4.2. The response of these specimens is similar to that of the first group. At can be observed from Table 4.1 and Figure 4.2 the ultimate strength at the specimens increased with increase the wire mesh layers. The increasing ratios are (18.3, 31 and 44.44)% for specimens 1HS4, 1HS8 and 1HS10 compared with 1HS, respectively. While the maximum deflection of these specimens showed a decrease in 1HS8 and 1HS10 by (11.1 and 20.3)% respectively. But in specimen 1HS4 the deflection increase by a percentage 17.6%, as shown in Figure 4.2. An increase in the number of layers than certain number leads to a decrease in the deflection.

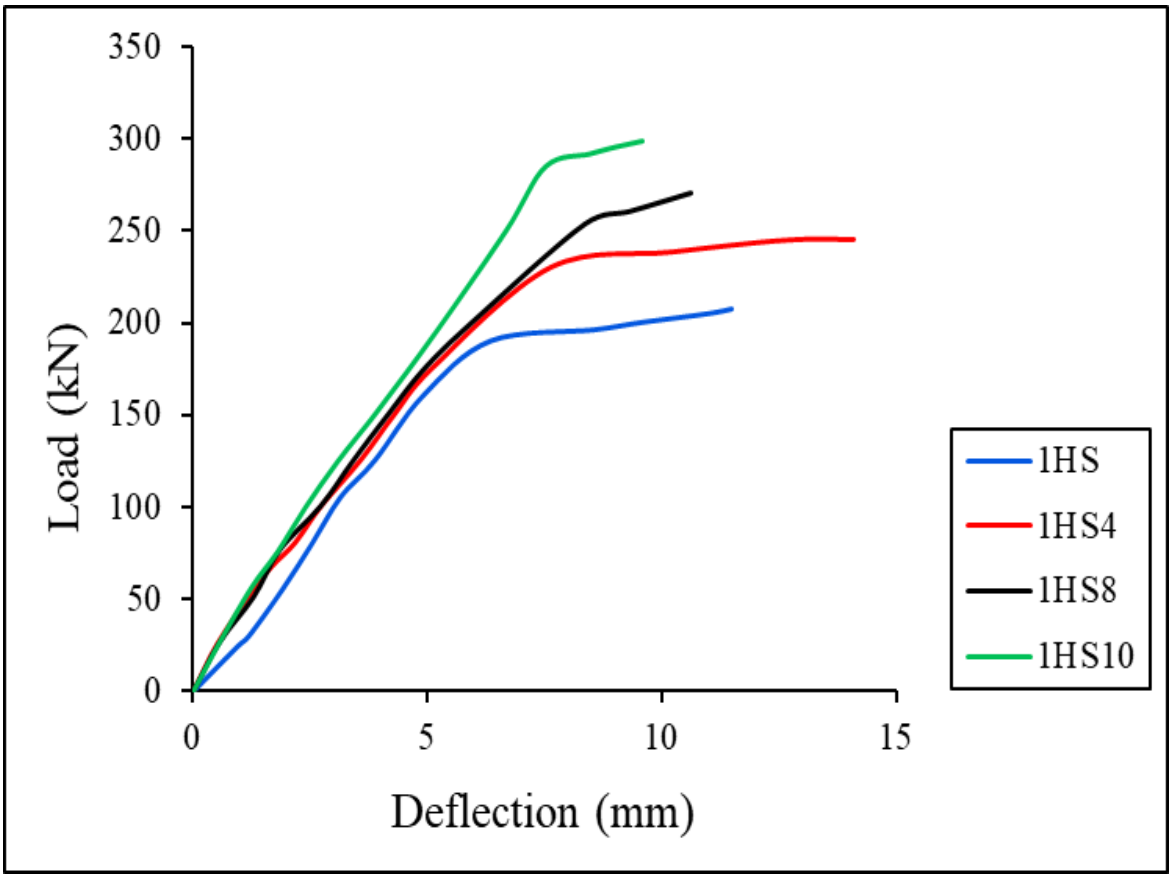

Figure 4.2 Load deflection curve for third group.

The beams tested at a/d = 1.8 showed more improvement in their ultimate load as compared to beams which are tested at a/d = 2.5, as can be seen in Figure 4.3. The ultimate load of 1HS, 1HS4, 1HS8, and 1HS10 beams is increased by 34%, 32%, and 10% compared with 2HS, 2HS4, and 2HS8 beams, respectively. It is due the shear span to depth ratio (a/d) as cited in the results (Al-Sulaimani et al. [16]). As expected, the ultimate load increase as the (a/d) ratio is decreased. The load - deflection curve of specimens in fifth group (2NS, 2NS4 and 2NS8) is shown in Figure 4.4. The specimens have the same details as the firs group, only they differ in the compressive strength of the mortar. The member 2NS4 and 2NS8 showed an increase of the ultimate load compared with specimen 2NS by 16% and 46%, respectively. The maximum deflection of specimen 2NS4 is increased by 13% while the deflection of 2NS8 is decreased by 6.3% compared with that of specimen 2NS

as can be seen clearly in Figure 4.4. The effect of compressive strength of mortar on the behavior of beams can be achieved comparison between first group and fifth group as shown in Figure 4.5. From this figure, it can be noticed that the specimens of higher strength exhibited higher ultimate load compared with specimens of normal strength. The increase of the ultimate load of member 2HS, 2HS4 and 2HS8 compared to beams 2NS, 2NS4 and 2NS8 by (13.1, 17 and 24)%, respectively. This increasing is due to the different properties of high strength mortar in terms of compressive strength, higher tensile strength, and higher stiffness than normal mortar strength. Where high mortar is superior to normal mortar in all properties, as cited in the results (Chkheiwera et al. in 2016 [20]).

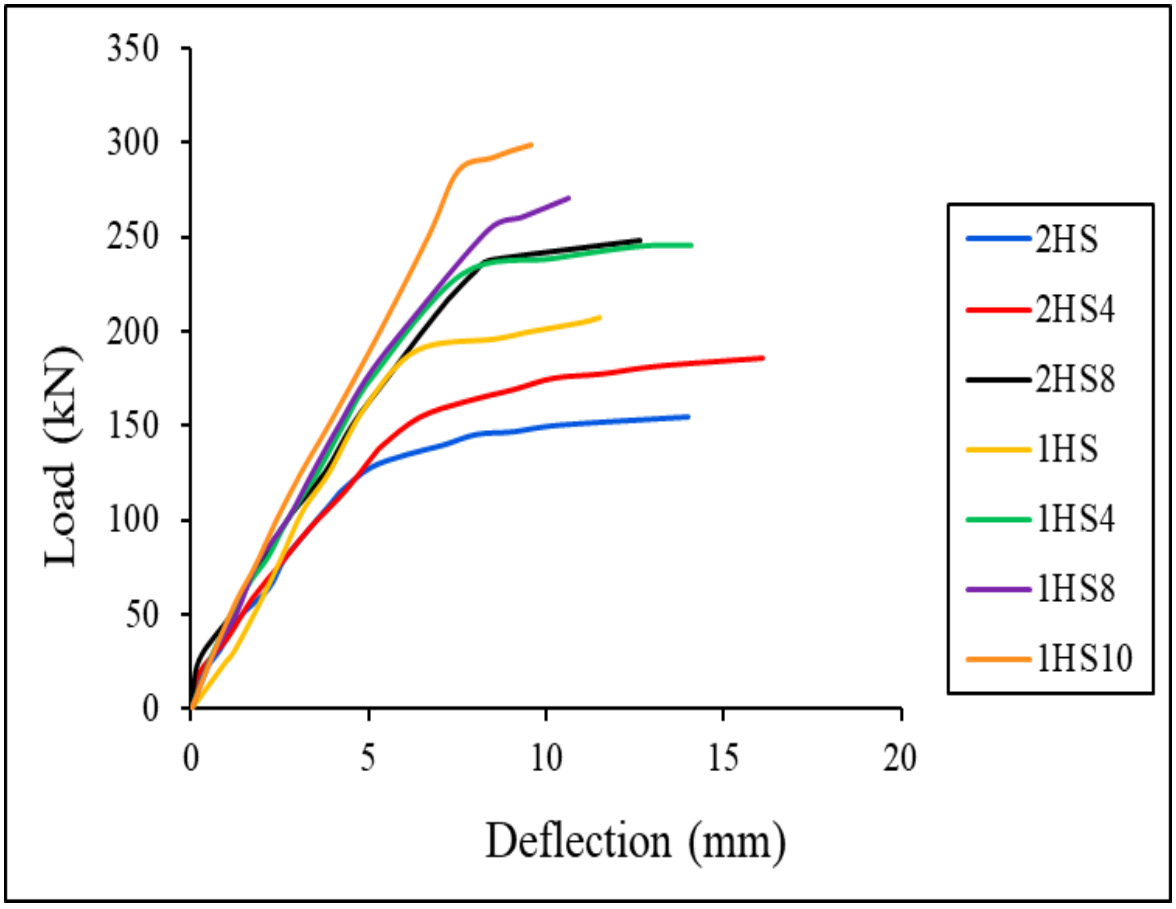

Figure 4.3 Load deflection curve for first and third groups.

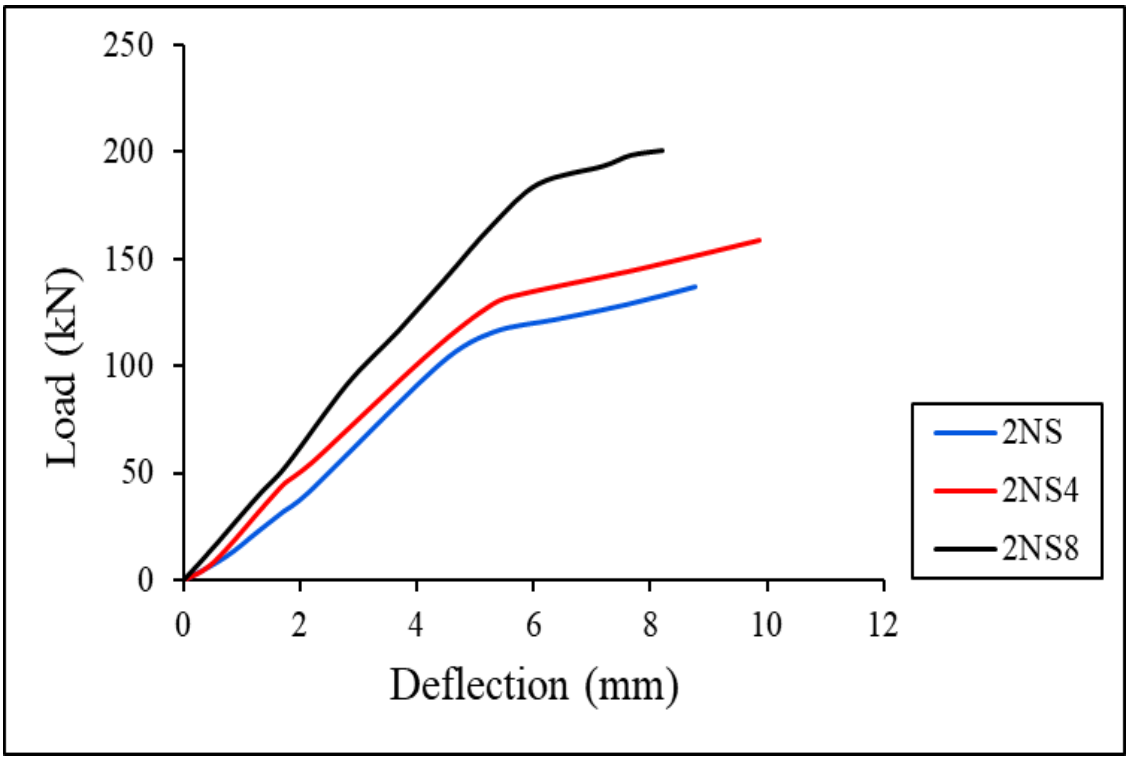

Figure 4.4 Load deflection curve for fifth group.

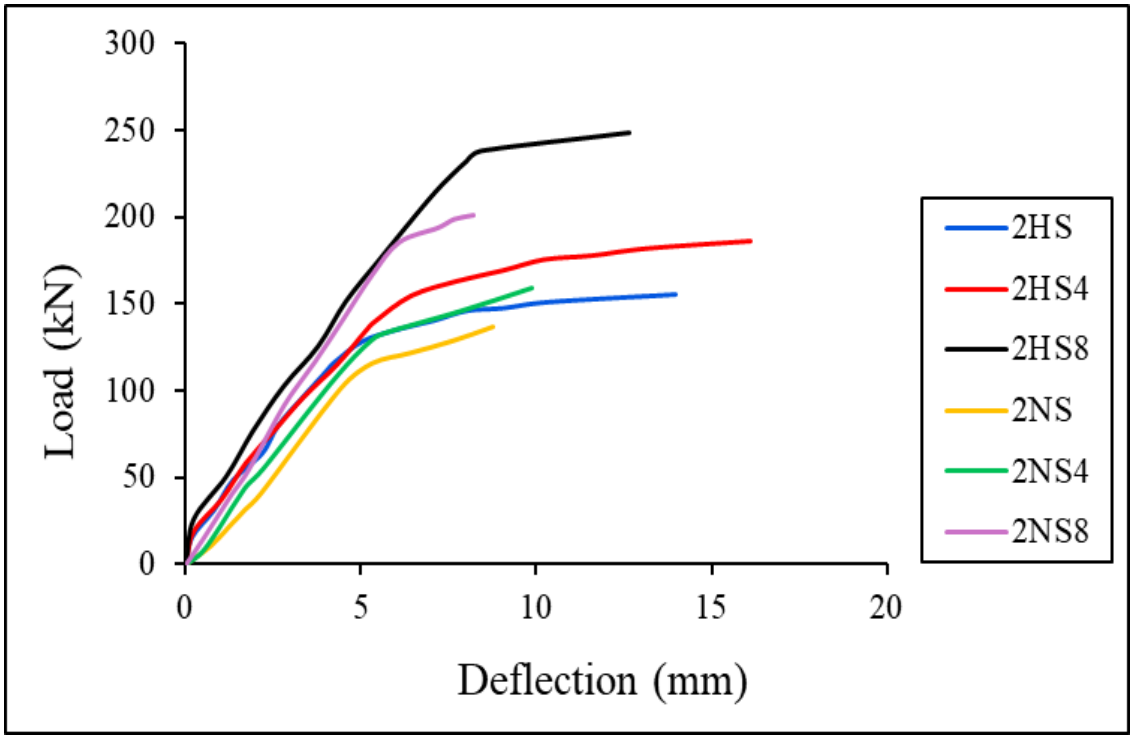

Figure 4.5 Load deflection curve for first and fifth groups.

4.2.2 Load - Deflection to (Second and Fourth Groups)

Table 4.2 shows the measurement of ultimate load and deflection for the second and fourth groups.

Table 4.2 Deflection and ultimate load for tested beams.

Series	ID	Deflection (mm)	Increasing ratio of deflection (%)	Ultimate load (kN)	Increasing ratio of ultimate load (%)
Second Group	2HW	9.5	---	120	---
	2HW4	12.8	35	161	34.0
	2HW8	11.6	22	199	66.0
Fourth Group	1HW	8.4	---	146	---
	1HW4	11	31	195	34.0
	1HW8	9.9	18	240	64.3
	1HW10	8.84	5.2	265	82.0

The specimens of second group (2HW, 2HW4 and 2HW8) have the same details of that in first group, but they not contain transverse reinforcement in shear span. The response of these specimens is similar to that of first group. It is consist of two portions. The first is the linear part which is extend until the load at which first crack is occur. While the second part characterized by slope less that of the first part and tend to non-linear can be seen in Figure 4.6. The ultimate loads of the members 2HW4 and 2HW8 are increased by (34 and 66)% compared with 2HW, respectively. The deflections at the mid-span of specimens 2HW4 and 2HW8 failure compared with control specimens are (35 and 22)%, respectively. When comparing the two groups, we notice an increase in the ultimate load and deflection for the first group by (29, 16 and 25)%, as shown in Figure 4.7. This increase could be explained by the fact that the effectiveness of the stirrups to take the shear stress coming on the beam and contributing to shear capacity improvement is higher in the presence of

transverse reinforcement going around the reinforcing steel, as cited in the results (Makki [43]).

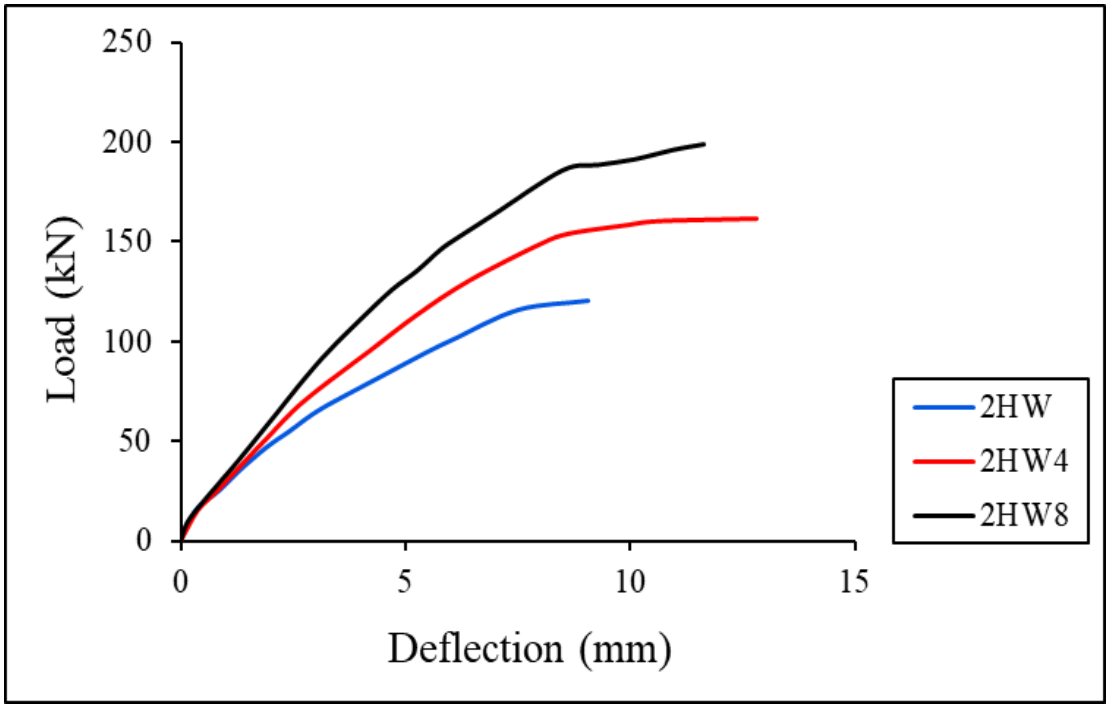

Figure 4.6 Load deflection curve for second group.

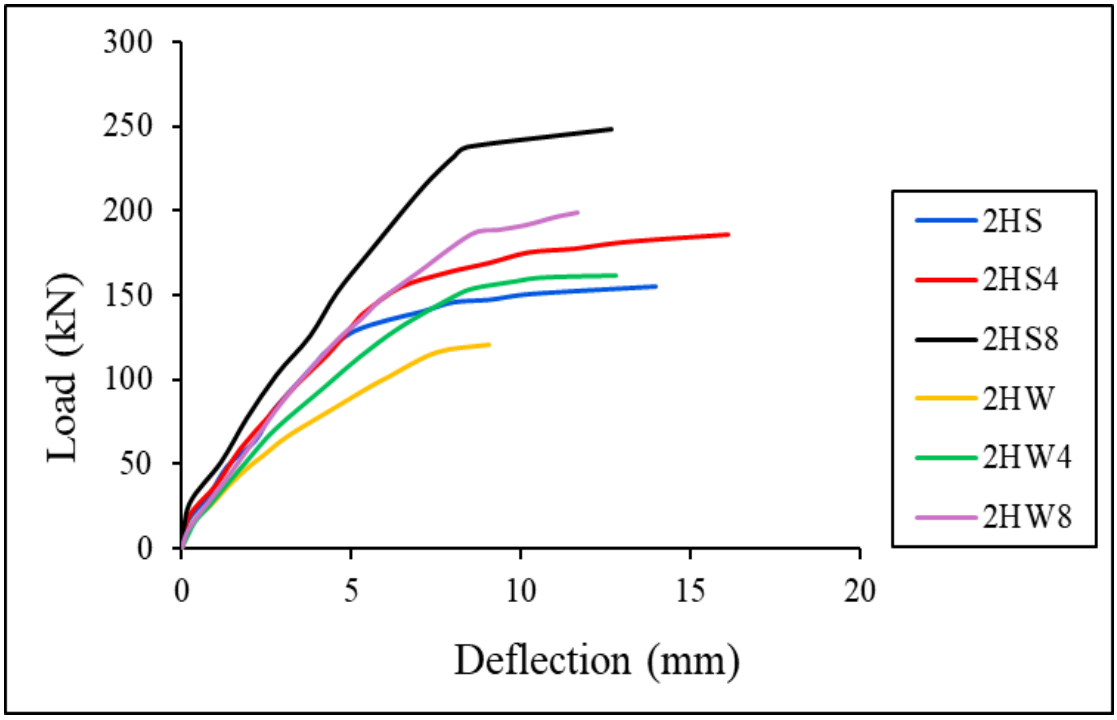

Figure 4.7 Load deflection curve for first and second groups.

The specimens of the fourth group (1HW, 1HW4, 1HW8 and 1HW10) as shown in Figure 4.8 and they are similar to the third group, except that they are without stirrups. These beams showed increase of the ultimate load and deflection by percentage (34, 64.3 and 82)% and (31, 18 and 5.2)% compared with of 2HW,respectively. When comparing the two groups (third and fourth groups), an increase in the ultimate load and deflection for the third group was observed, as shown in Figure 4.9. Where stirrups contributed to improving the ultimate load and deflection in third group compared with the fourth group by (42, 26, 13 and 13)% respectively. Also, when comparing the beams of the second group with the fourth group, it was noticed increase in the ultimate load and deflection for the fourth group specimens by (22, 21, 21)%. Because of the shear span to effective depth ratio (a/d) as the value decreases, the ultimate load increases, as shown in Figure 4.10. The beams with greater span show as in the first and second group higher deflection than the beams with less span where the distance of the load point to the support was greater which increases the deflection.

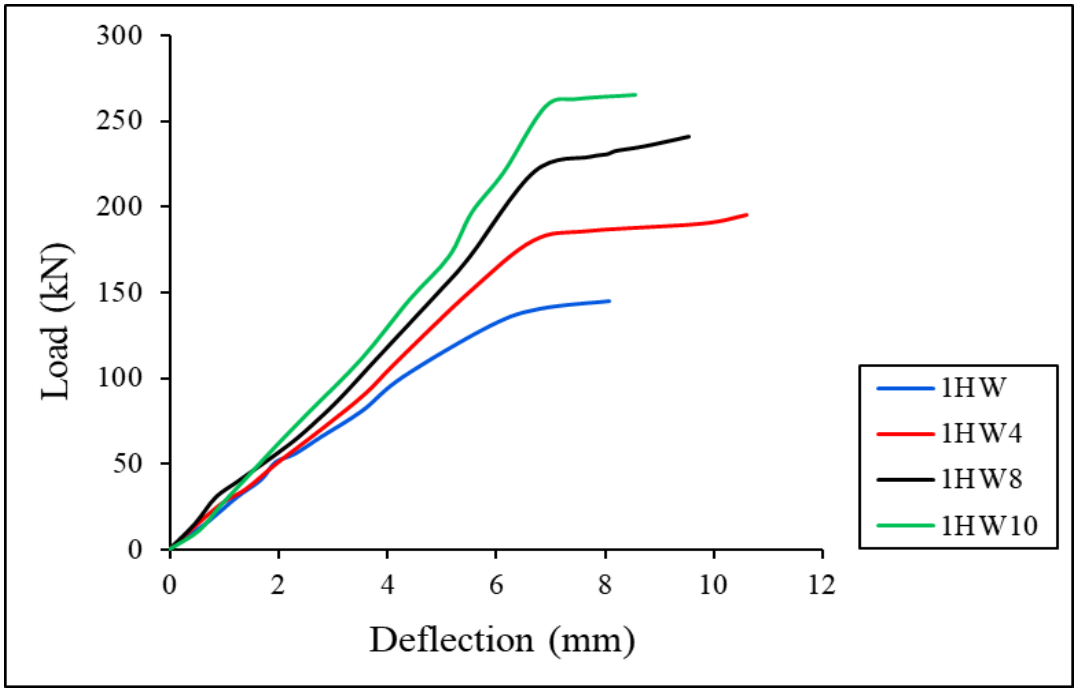

Figure 4.8 Load deflection curve for fourth group.

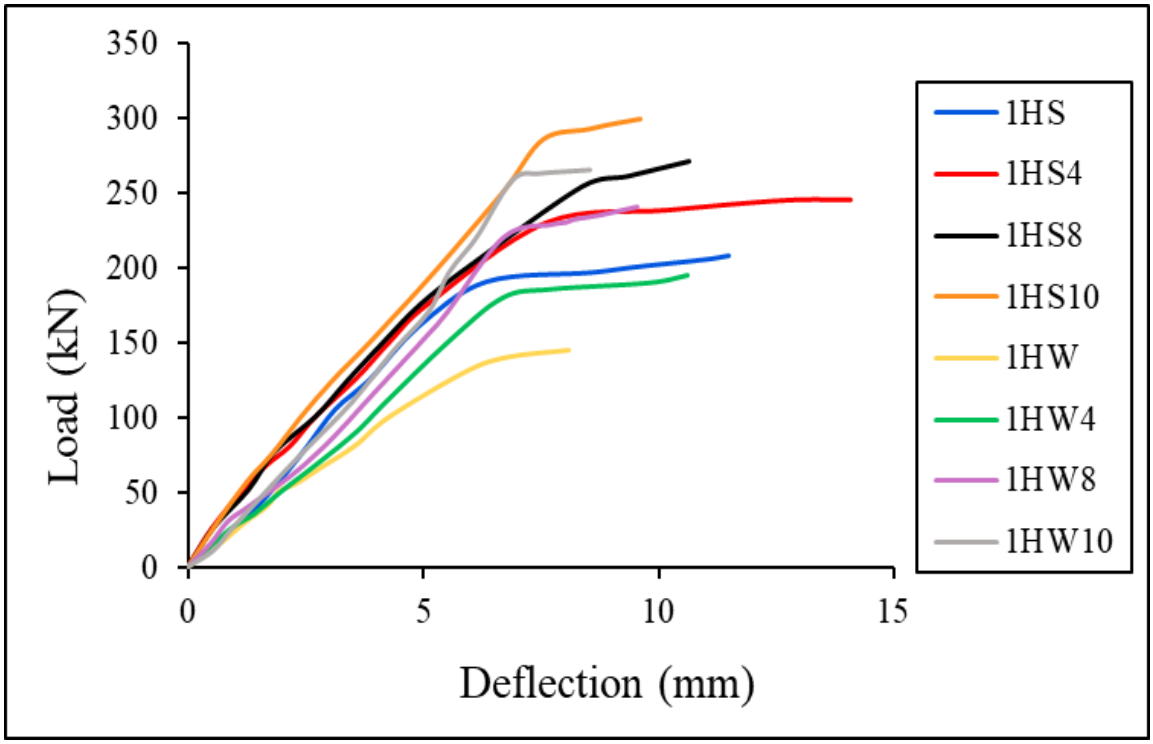

Figure 4.9 Load deflection curve for third and fourth groups.

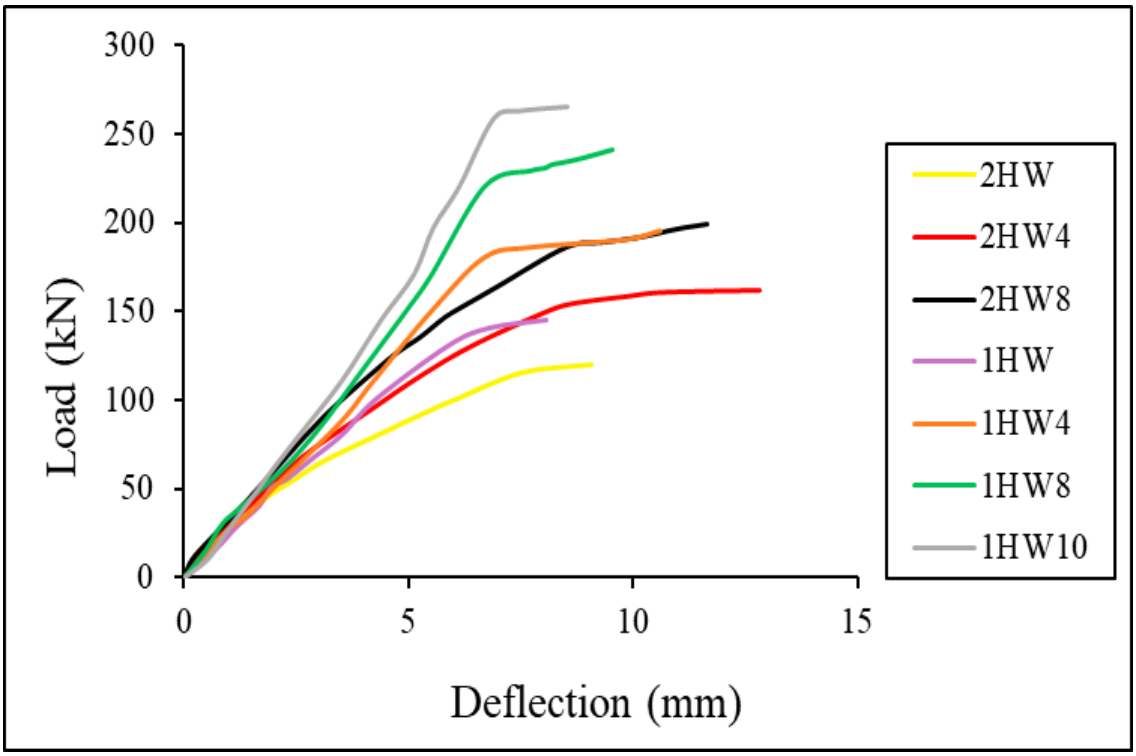

Figure 4.10 Load deflection curve for second and fourth groups.

4.3 Ductility Index

The term ductility is defined as the ability of material or member to sustain deformation beyond the elastic limit while maintaining a reasonable load carrying capacity until total failure [59]. It can determine the ductility index (μ) from the load-deflection curve, as shown in Figure 4.11. It calculated by the Equation 4.1:

$$\mu = \frac{\Delta_{max}}{\Delta_y} \qquad \textbf{4.1}$$

where μ: ductility index, Δ_{max}: maximum deflection, Δ_y: yield deflection.

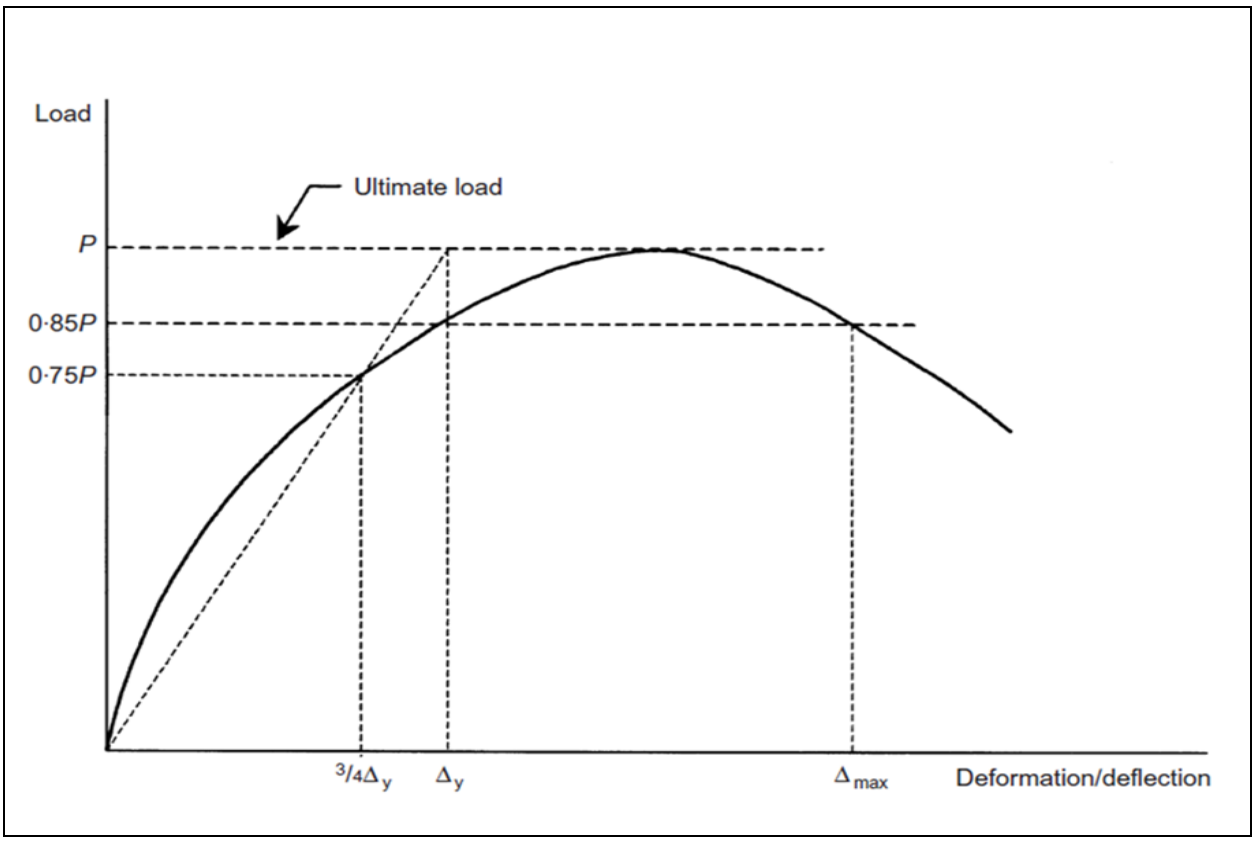

Figure 4.11 Ductility index.

Table 4.3 includes ductility index for each specimen tested in study. The ductility of beams (2HS4, 1HS4 and 2NS4) is improved when using 4 layers of wire mesh irrespective of whether the beams were tested at (a/d) 1.8 or 2.5 for first, third and fifth groups compared with the control beams (2HS, 1HS and 2NS) by a

percentage (17, 15 and 12)%, respectively. For beams (2HS8, 1HS8, 1HS10 and 1NH8) the ductility index was lower than the control beams by a percentage (7, 9, 13 and 10)%, respectively.

Table 4.3 Ductility index for all beams.

Series	ID	Ductility index	Increasing ratio in ductility (%)
First Group	2HS	3.0	---
	2HS4	3.5	17
	2HS8	2.8	-7
Second Group	2HW	1.9	---
	2HW4	2.5	32
	2HW8	2.2	16
Third Group	1HS	2.18	---
	1HS4	2.5	15
	1HS8	2.0	-9
	1HS10	1.9	-13
Fourth Group	1HW	1.7	---
	1HW4	2.16	27
	1HW8	1.84	9
	1HW10	1.8	6
Fifth Group	2NS	1.88	---
	2NS4	2.1	12
	2NS8	1.7	-10

Table 4.3 shows that the increasing number of wire mesh layers dose not lead to an increase in ductility for all beams. Hence, the ductility is decrease when increasing number of wire mesh layers especially for 8 and 10 layers. The cause of ductility decreasing is due to the members becomes higher stiffness, then for the beams tends to reduce deformation occurs. As for the specimens of second group

(2HW4 and 2Hw8) and fourth group (1HW4, 1HW8 and 1HW10), the ductility increases by a percentage (32 and 16)% and (27, 9 and 6)% respectively. When comparing the second group with the first and the fourth group with the third, the ductility increases when the groups containing stirrups by a percentage (58, 40 and 27)% and (28, 16, 9 and 6)% respectively. The examination of these specimens shows that the presence of stirrups has induced a long plastic range before ultimate failure occurred. When no stirrups are present, failure occurred only at a load less. The beams with greater shear span show higher ductility than the beams with less shear span where the distance of the load point to the support was greater which increases the deflection and therefore the observed behavior of beams was more ductility as cited in the results (Ghai et al. in 2018 [7]). When comparing the first group with the fifth group, an increase in ductility was observed by (60, 67 and 65)% for high mortar. The ductility results show with the presence of transverse reinforcement, high strength mortar becomes more ductility, even more than normal mortar. This could, once again, be explained by the better steel-concrete composition with perfect bonding between the two materials minimizing greatly the risk of any slipping movement of one material in relation to the other. This would ensure a better transmission of internal forces from one material to the other and hence a better redistribution of internal forces.

4.4 Initial Stiffness

The initial stiffness is defined as the slope of the first part of the load-deflection curve [60], as shown in Figure 4.12. It is calculated by dividing the yield load (P_y) to the yield deflection (Δ_y), in Equation 4.2 :

$$\textbf{Initial Stiffness} = \frac{\mathbf{P_y}}{\mathbf{\Delta_y}} \qquad \textbf{4.2}$$

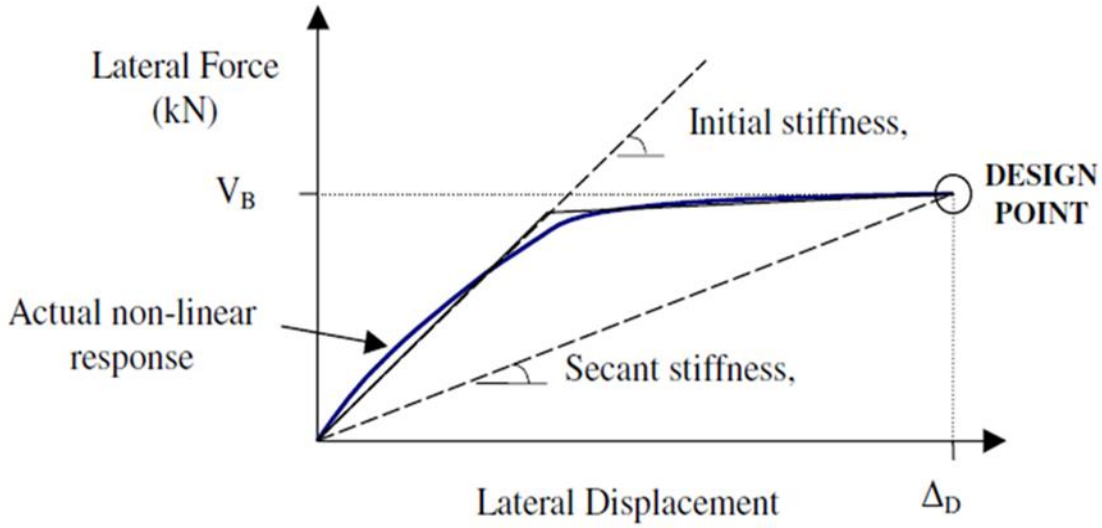

Figure 4.12 Initial-stiffness.

Table 4.4 show the initial stiffness of all specimens. It is also observed that in general, the initial stiffness increases with increased number of layers compared to control beams as cited in the results (El-Sayed and Erfan [26]). Where the initial stiffness of the first group (2HS4 and 2HS8) and third group (1HS4, 1HS8 and 1HS10) increased by a percentage (10 and 26.2)% and (11, 19.2 and 30)% compared with the control beams (2HS and 1HS), respectively. When comparing the first group with the third group, it was noticed increase in the initial stiffness for the third group specimens by (15.7, 16.5 and 10)%, respectively. Because the distance of the load point to the support for the specimens of the first group (2HS, 2HS4 and 2HS8) was greater which increases the deflection and therefore the observed behavior of beams was more ductility, the higher the ductility initial stiffness decreases. As for the fifth group (2NS, 2NS4 and 2NS8) recorded increase by a percentage of 10.2% and 33 % compared with the control beam. It was observed from the experimental data that there is an increase in the initial stiffness to beams (2HS, 2HS4 and 2HS8) compared to the beams (2NS, 2NS4 and 2NS8) by a percentage (19.6, 20 and 14)%. This increase is due to the different properties of compressive strength. Where initial stiffness of strengthened specimens increases with increasing strength of mortars.

As for the specimens of second group (2HW4 and 2Hw8) and fourth group (1HW4, 1HW8 and 1HW10), the initial stiffness increases compared with control beams (2HW and 1HW) by a percentage (14 and 44)% and (20, 42 and 56)% respectively. When comparing the second group with the first and the fourth group with the third, the initial stiffness increases when the groups containing stirrups by (40, 36 and 22.2)% and (24.6, 15.3, 5 and 6)% respectively. However, beams without stirrups show less improvement in stiffness. The stirrups also contribute in the stiffness of the beam by limiting the propagation of shear cracks. That is, the stiffness of specimens containing stirrups is higher than the stiffness of beams without stirrups.

Table 4.4 Initial stiffness for all beams.

Series	ID	Initial stiffness (kN/mm)	Increasing ratio of stiffness (%)
First Group	2HS	28.0	---
	2HS4	30.9	10.0
	2HS8	35.3	26.2
Second Group	2HW	20.0	---
	2HW4	22.8	14.0
	2HW8	28.8	44.0
Third Group	1HS	32.4	---
	1HS4	36.0	11.0
	1HS8	38.6	19.2
	1HS10	42.2	30.0
Fourth Group	1HW	26.0	---
	1HW4	31.2	20.0
	1HW8	36.9	42.0
	1HW10	40.0	56.0
Fifth Group	2NS	23.4	---
	2NS4	25.8	10.2
	2NS8	31.0	33.0

4.5 Energy Absorption

Energy absorption is the total area under the load deflection curve [61]. Table 4.5 presents the energy absorption results for all tested beams. Table 4.5 shows increase in the energy absorption of all beams with an increase in the number of wire meshes compared with control beams.

Table 4.5 Energy absorption for all beams.

Series	ID	Energy absorption (kN.mm)	Increasing ratio in energy absorption (%)
First Group	2HS	1703.00	---
	2HS4	1995.87	17.0
	2HS8	1890.00	11.0
Second Group	2HW	692.30	---
	2HW4	850.00	23.0
	2HW8	1050.00	52.0
Third Group	1HS	1682.20	---
	1HS4	1868.60	11.1
	1HS8	1795.90	7.0
	1HS10	1611.49	-4.2
Fourth Group	1HW	557.00	---
	1HW4	760.70	32.0
	1HW8	803.00	39.1
	1HW10	740.30	28.3
Fifth Group	2NS	720.84	---
	2NS4	990.60	37.4
	2NS8	940.00	30.4

The specimens of first group of a/d = 2.5 showed higher energy absorption. The increasing of energy absorption of this group for specimens (2HS4 and 2HS8) compared with control beam 2HS are (17 and 11)%, respectively. The increasing of

specimens (1HS4 and 1HS8) of third group are (11.1 and 7)% and decreases at 1HS10 by a percentage (- 4.2)% compared with 1HS, respectively. When comparing the first group (2HS, 2HS4 and 2HS8) with the third group (1HS, 1HS4, 1HS8 and 1HS10), the percentage of energy absorption for the first group increase by (1.23, 7 and 17.2)%, respectively. As for the specimens of fifth group (2NS4 and 2NS8), it recorded an increase by a percentage (37.4 and 30.4)% compared to the control beam 2NS, respectively. When comparing the first group (2HS, 2HS4 and 2HS8) with the fifth group (2NS, 2NS4 and 2NS8), the percentage of energy absorption for the first group increase by (136.25, 101.48 and 101)%, respectively. Where energy absorption increasing with increases mortar strength. As for the second and fourth groups (2HW4 and 2HW8) and (1HW4, 1HW8 and 1HW10), an increase in energy absorption was recorded (23 and 52)% and (32, 39.1 and 28.3)% compared to the control beams 2HW, 1HW, respectively. When comparing the second group (2HW, 2HW4 and 2HW8) with the first group (2HS, 2HS4 and 2HS8) and the fourth group (1HW, 1HW4, 1HW8 and 1HW10) with the third group (1HS, 1HS4, 1HS8 and 1HS10), it was noticed that the energy absorption of the specimens of the first and third group increased by a percentage (146, 135 and 127)% and (202, 145.6, 123.6 and 117.6)% compared to the second and fourth groups, respectively.

4.6 Strain Results

The diagonal tensile strain and compressive strain at failure of each specimen are summarized in Table 4.6. The beams of first group (2HS4 and 2HS8) showed an increase of the diagonal tensile strain and compressive strain in four layers by a percentage (27 and 25)%, respectively. And decreased in eight layers by a percentage (10.4 and 11)% compared with the control beam 2HS respectively, as shown in Figure 4.13 and Figure 4.14. As for the (1HS4, 1HS8 and 1HS10) specimens the third group, these specimens showed increase of the diagonal tensile

strain and compressive strain in four layers by percentage (40 and 27)% respectively compared with the control beam 1HS. While the strain showed a decrease in eight and ten layers by (12, 15.4 and 19.4, 24)% respectively, as shown in Figure 4.15 and Figure 4.16.

Table 4.6 Strain at failure load for all beams.

Series	ID	Diagonal tensile strain	Increasing ratio in strain %	Compressive strain	Increasing ratio in strain %
First Group	2HS	1.34×10^{-3}	---	2.24×10^{-3}	---
	2HS4	1.7×10^{-3}	27.0	2.8×10^{-3}	25.0
	2HS8	1.2×10^{-3}	-10.4	2×10^{-3}	-11.0
Second Group	2HW	1.06×10^{-3}	---	1.59×10^{-3}	---
	2HW4	1.36×10^{-3}	28.3	1.95×10^{-3}	23.0
	2HW8	1.15×10^{-3}	8.4	1.7×10^{-3}	7.0
Third Group	1HS	1.01×10^{-3}	---	1.42×10^{-3}	---
	1HS4	1.33×10^{-3}	40.0	1.8×10^{-3}	27.0
	1HS8	8.91×10^{-4}	-12.0	1.2×10^{-3}	-15.4
	1HS10	8.14×10^{-4}	-19.4	1.08×10^{-3}	-24.0
Fourth Group	1HW	6.41×10^{-4}	---	8.72×10^{-4}	---
	1HW4	8.43×10^{-4}	32.0	1.06×10^{-3}	22.0
	1HW8	7.3×10^{-4}	14.0	9.52×10^{-4}	9.1
	1HW10	7.01×10^{-4}	9.3	9.4×10^{-4}	8.0
Fifth Group	2NS	9.82×10^{-4}	---	1.04×10^{-3}	---
	2NS4	1.09×10^{-3}	11.0	1.38×10^{-3}	33.0
	2NS8	8.7×10^{-4}	-11.4	9.5×10^{-4}	-9.0

When comparing the first group (2HS, 2HS4 and 2HS8) and third group (1HS, 1HS4, 1HS8 and 1HS10) together, it was noticed that in the first group the strains increased by (33, 28 and 35)% and (58, 56 and 67)% compared with third group,

respectively. Where the strains increase the diagonal tensile strain and compressive strain with (a/d) increase. That is, the specimens with most ductility show the more strains.

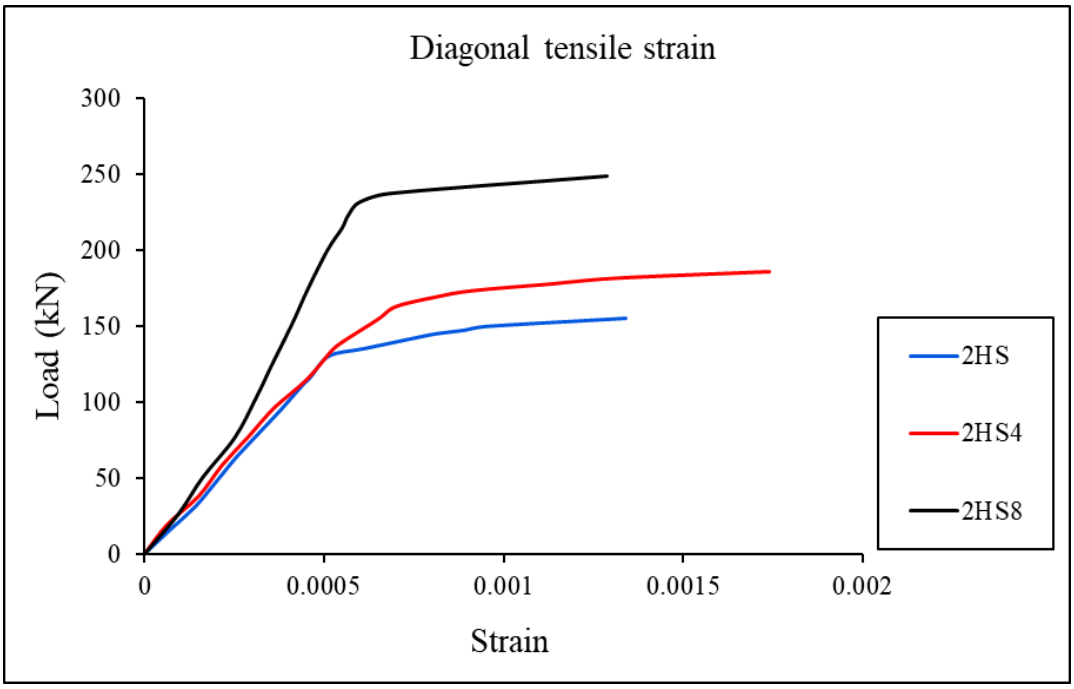

Figure 4.13 Diagonal tensile strain for first group.

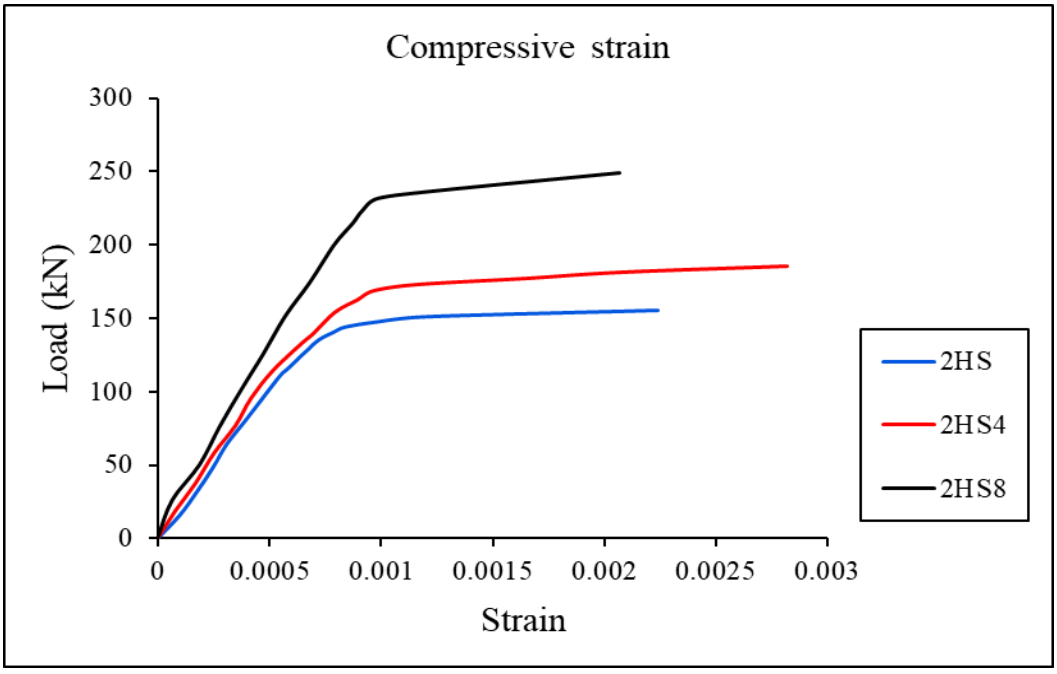

Figure 4.14 Compressive strain for first group.

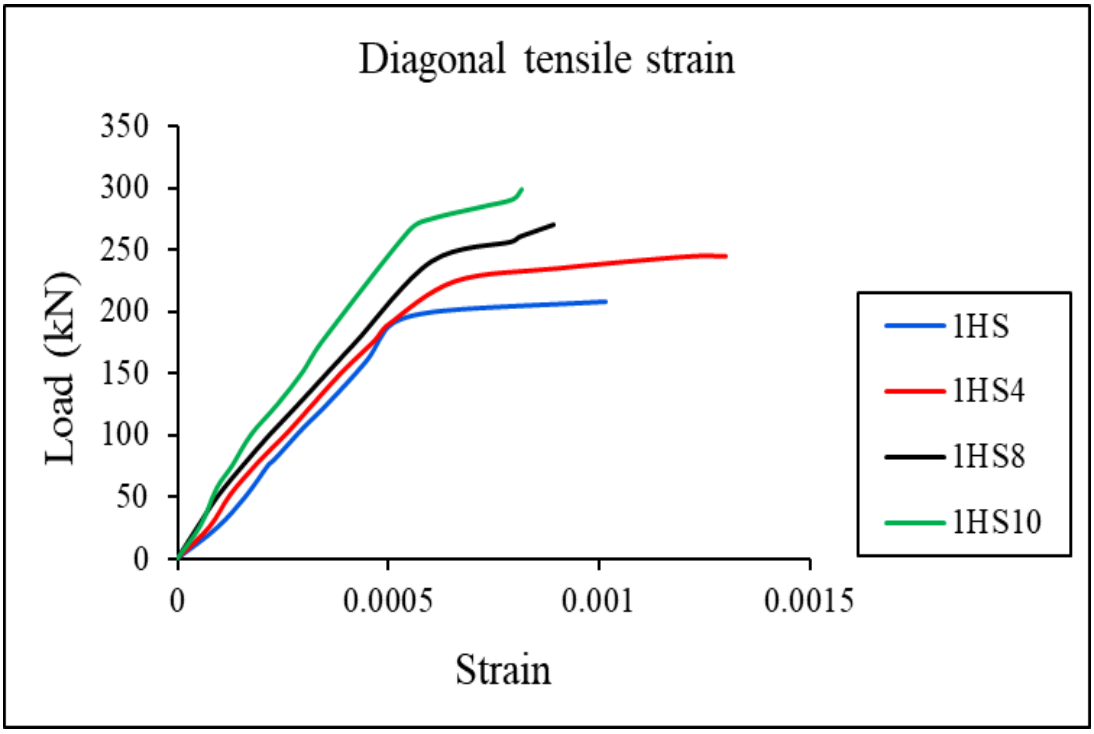

Figure 4.15 Diagonal tensile strain for third group.

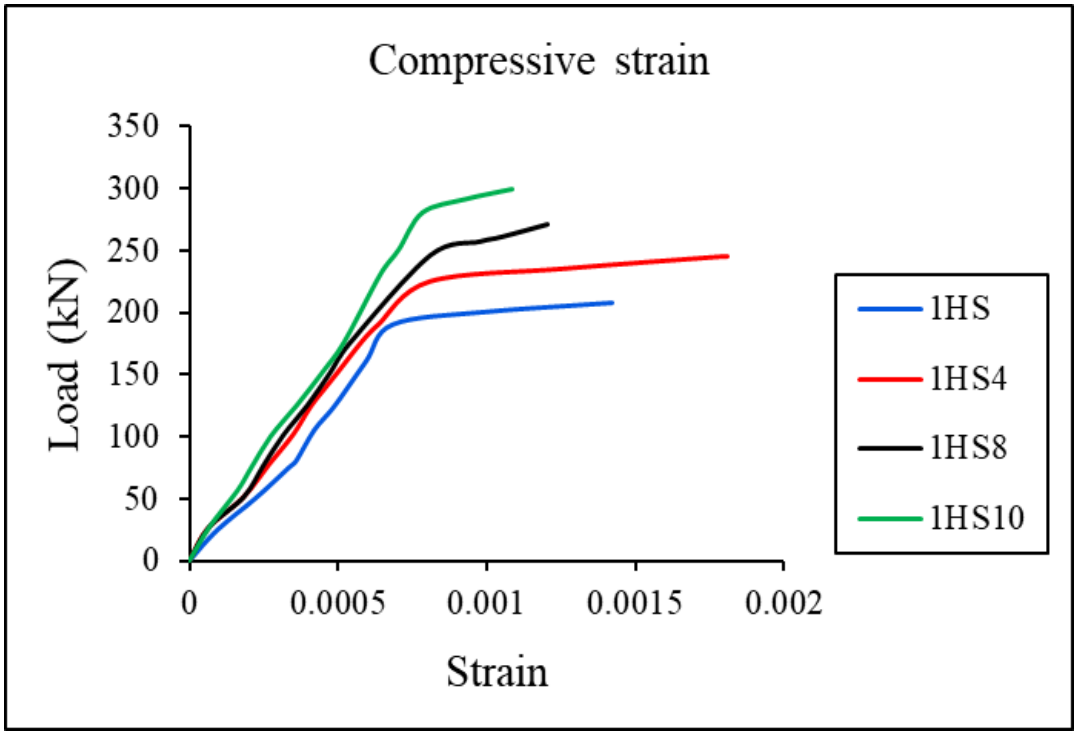

Figure 4.16 Compressive strain for third group.

The specimens of fifth group (2NS4 and 2NS8) showed similar behavior to the first and third groups, where the strain increased at 4 layers by (11 and 33)% and decreased at 8 layers by (11.4 and 9)% compared to the control beam 2NS respectively, as shown in Figure 4.17 and Figure 4.18. A decrease in the strains is observed with the increase in the number of wire mesh. Because the higher the stiffness, the less deformation of the specimens (that is, have a lower strain). When comparing the first group with the fifth, it was noticed that the strains of the first group increased by (36.4, 56 and 38)% and (115.3, 103 and 117.3)% compared with fifth group, respectively. Due to the different characteristics of the compressive strength, where the strains tend to increase with the increase in mortar strength.

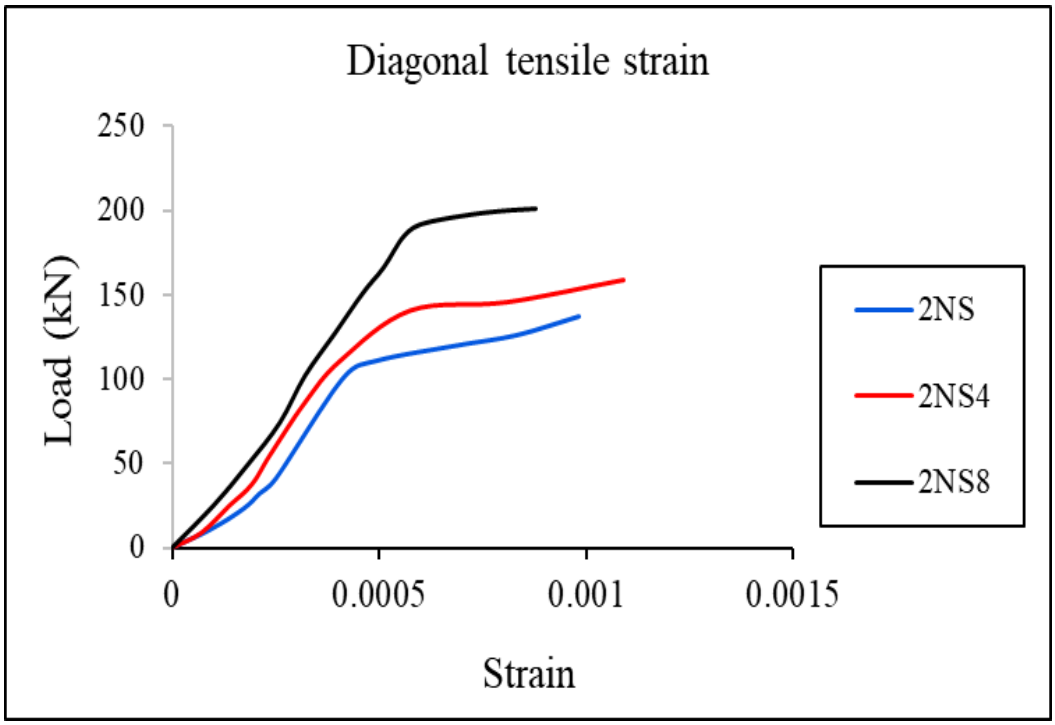

Figure 4.17 Diagonal tensile strain for fifth group.

For the specimens of the second group (2HW4 and 2HW8) showed an increase in the diagonal tensile strain and compressive strain in four and eight layers by (28.3, 23 and 8.4, 7)% compared to the control beam 2HW respectively, as shown in Figure 4.19 and Figure 4.20. As for the specimens of the fourth group (1HW4,

1HW8 and 1HW10), the percentage increase was at 4 layers (32 and 22)%, while at 8 and 10 layers the percentage increase was (14, 9.1 and 9.3, 8)% respectively, as shown in Figure 4.21 and Figure 4.22. When comparing the first group with the second and third with the fourth, an increase in strains was observed in the first and third group. Because the first and third groups contain stirrups, where the strains increase with the presence of stirrups.

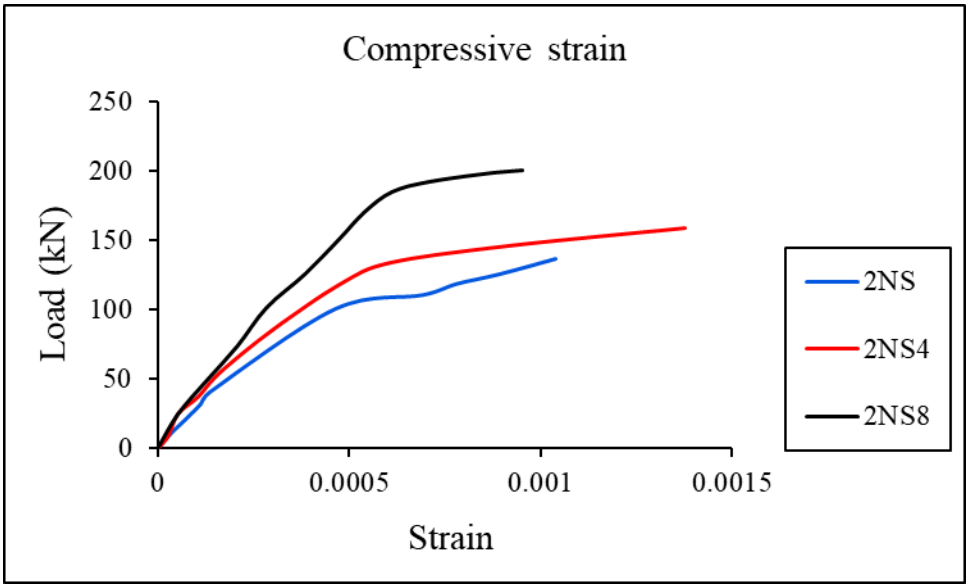

Figure 4.18 Compressive strain for fifth group.

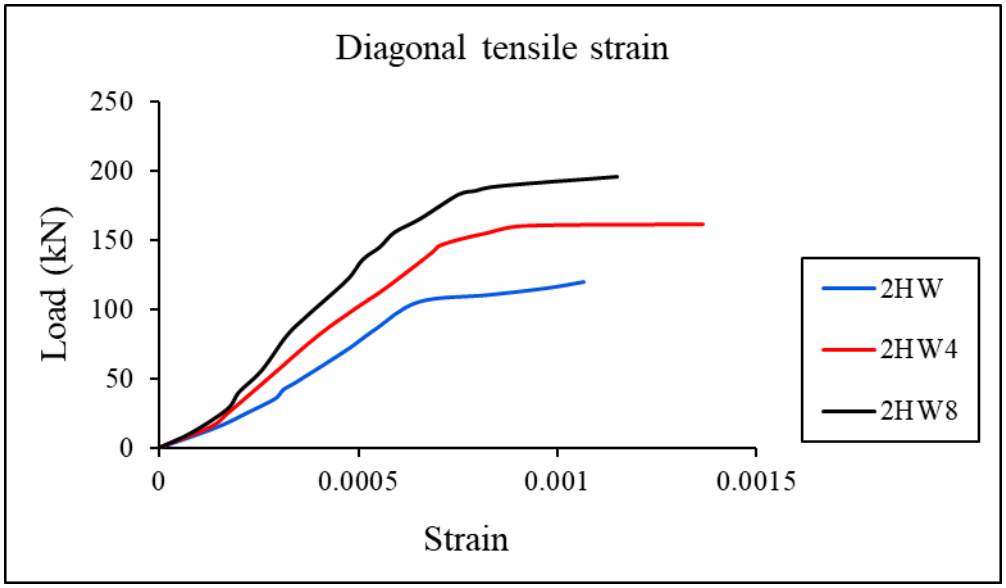

Figure 4.19 Diagonal tensile strain for second group.

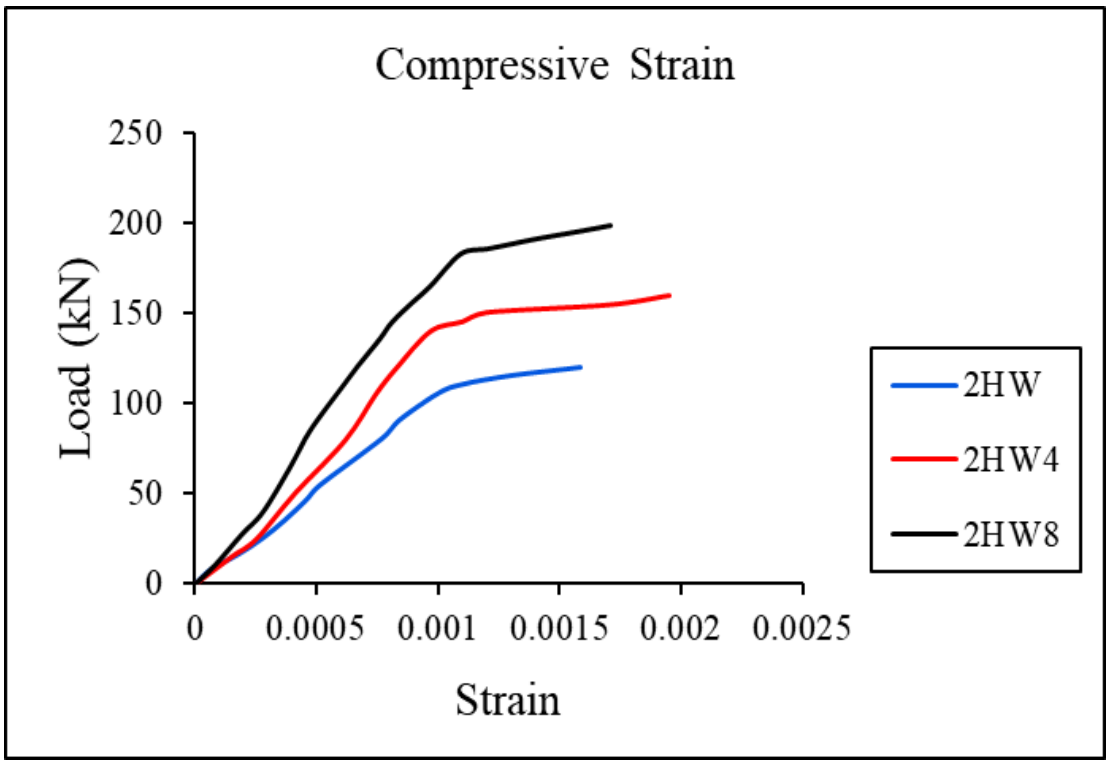

Figure 4.20 Compressive strain for second group.

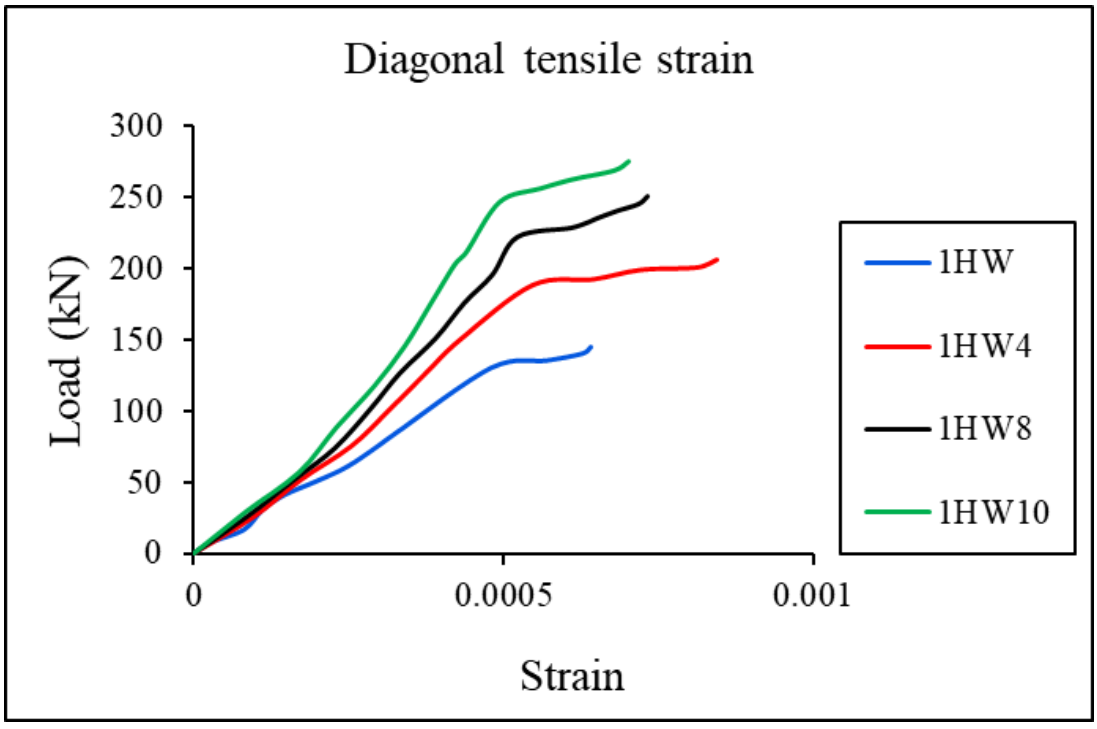

Figure 4.21 Diagonal tensile strain for fourth group.

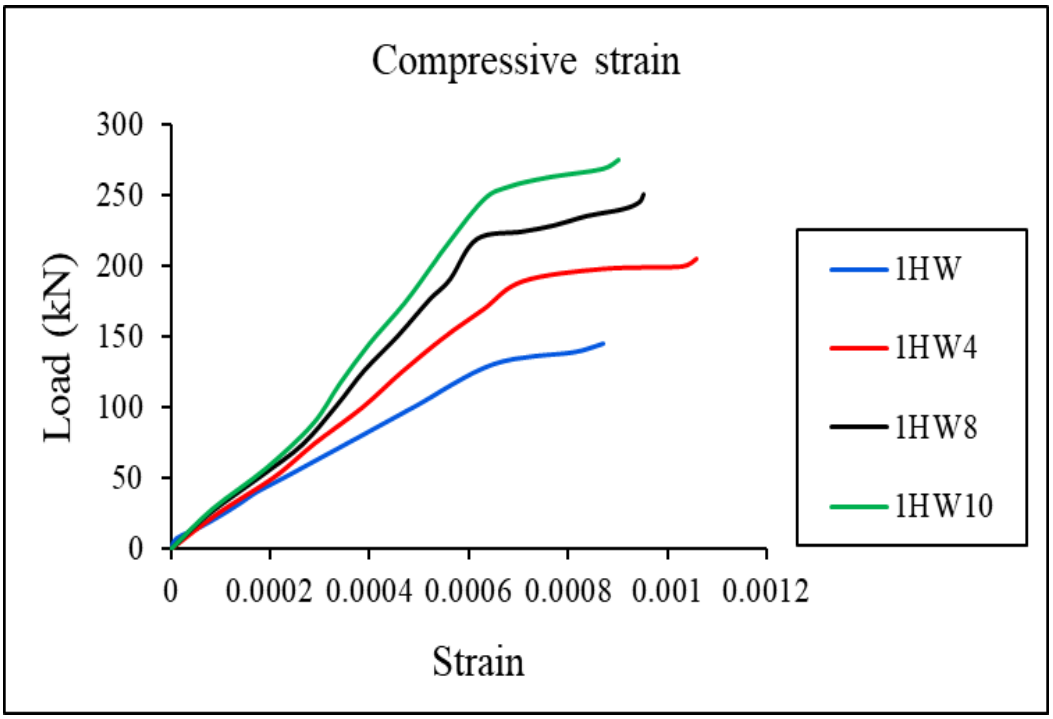

Figure 4.22 Compressive strain for fourth group.

4.7 Crack Propagation and Modes of Failure

Table 4.7 shows cracking load values for all beams. For all group the control beams show diagonal shear failure mode. For the control beams (2HS, 1HS and 2NS) showed a diagonal shear failure mode the first diagonal shear crack started in when load (42, 53, 31) kN, respectively. The crack began near the support and extending at a 45^{o} angle towards the loading point region. the crack widened and stretched more as the load increased, causing the beam to failure when the load (155, 207 and 137) kN respectively, as shown in Figure 4.23, Figure 4.24 and Figure 4.25. After adding the wire mesh to the beams (2HS4, 2HS8, 1HS4, 1HS8, 1HS10, 2NS4 and 2NS8) the specimens showed flexural failure, the cracks began to appear when load (46, 51, 59, 65, 68, 36 and 41) KN, respectively. The first flexural crack initiated in the central zone of the specimens (between two points load). When the load increases, cracks extended toward the top and followed by other small flexural cracks appear in the same region. Later, the beams failed due to the developing one

flexural crack in the middle region of the beam, as shown in Figure 4.26, Figure 4.27, Figure 4.28, Figure 4.29, Figure 4.30, Figure 4.31 and Figure 4.32. It was observed for the specimens containing the wire mesh that the cracks appeared delayed by (10, 21.4, 11, 23, 28.3, 16.1 and 32.3)% than the control beams, respectively. The meshes contributed to the delay in the appearance of cracks as the specimens became more stiffness.

Table 4.7 Crack load for all beams.

Series	ID	First crack load (kN) (Pcr)	Increasing ratio of First Crack load (%)	Failure load (kN) (Pu)	Mode of failure
First Group	2HS	42	---	155	Shear
	2HS4	46	10.0	186	Flexural
	2HS8	51	21.4	248	Flexural
Second Group	2HW	36	---	120	Shear
	2HW4	39	8.3	161	Flexural - Shear
	2HW8	45	25.0	199	Flexural
Third Group	1HS	53	---	207	Shear
	1HS4	59	11.3	245	Flexural
	1HS8	65	23.0	271	Flexural
	1HS10	68	28.3	299	Flexural
Fourth Group	1HW	45	---	146	Shear
	1HW4	51	13.3	195	Flexural - Shear
	1HW8	55	22.2	240	Flexural
	1HW10	58	29.0	265	Flexural
Fifth Group	2NS	31	---	137	Shear
	2NS4	36	16.1	159	Flexural
	2NS8	41	32.3	200	Flexural

Figure 4.23 Diagonal shear failure for beam 2HS.

Figure 4.24 Diagonal shear failure for beam 1HS.

Figure 4.25 Diagonal shear failure for beam 2NS.

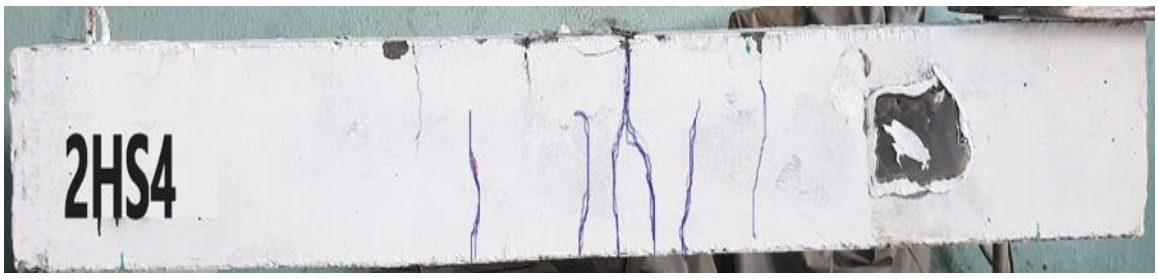

Figure 4.26 Flexural failure for beam 2HS4.

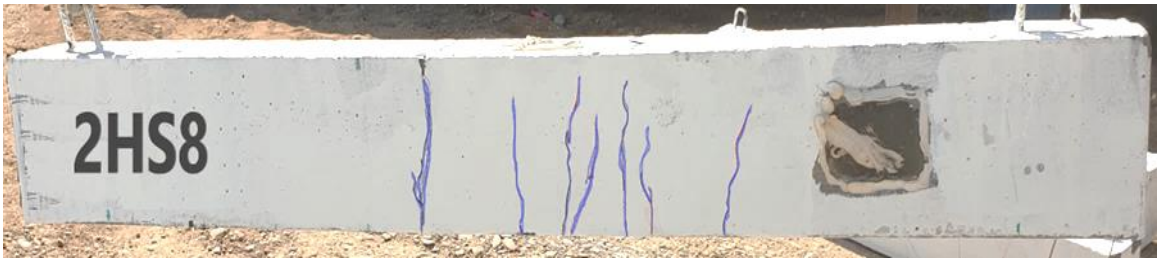

Figure 4.27 Flexural failure for beam 2HS8.

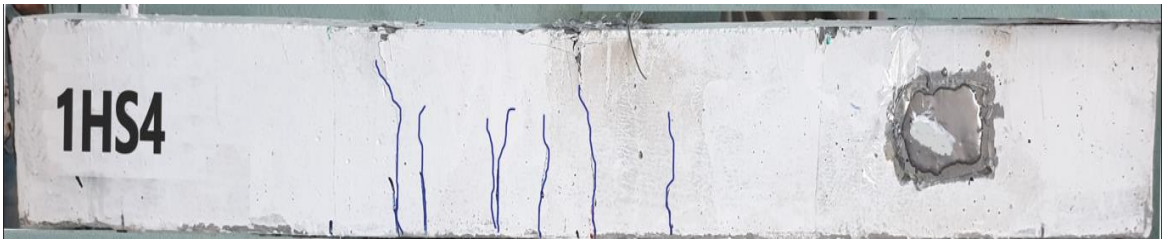

Figure 4.28 Flexural failure for beam 1HS4.

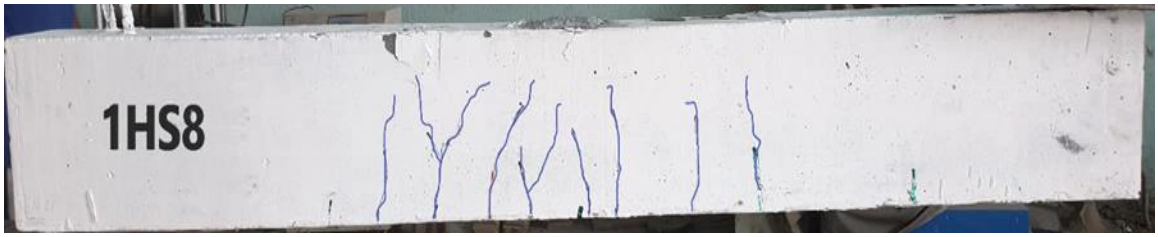

Figure 4.29 Flexural failure for beam 1HS8.

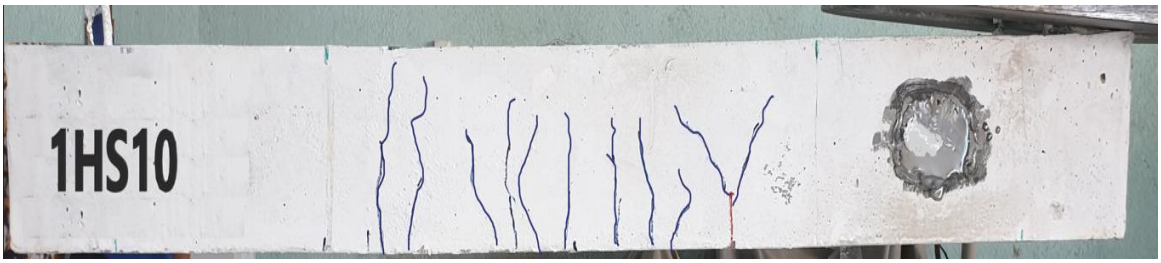

Figure 4.30 Flexural failure for beam 1HS10.

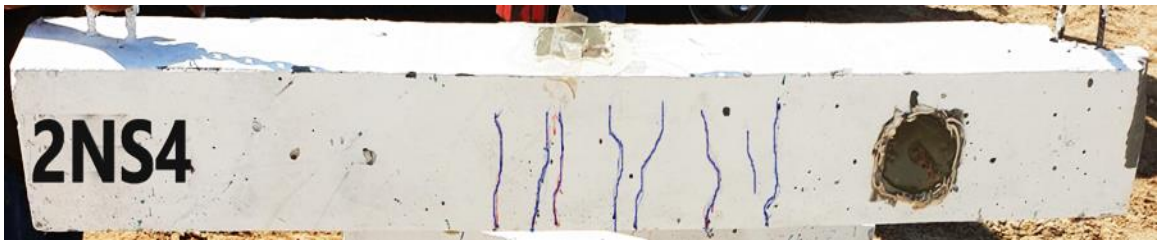

Figure 4.31 Flexural failure for beam 2NS4.

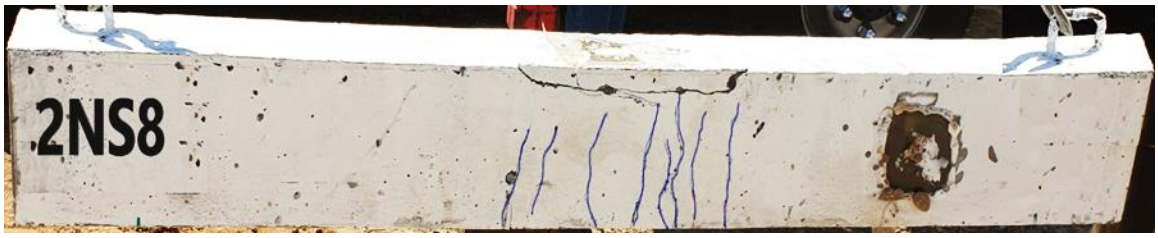

Figure 4.32 Flexural failure for beam 2NS8.

When comparing specimens (2HS, 2HS4 and 2HS8) made of high-strength mortar, the delay in cracks appearance was observed compared to (2NS, 2NS4 and 2NS8) specimens made of normal strength mortar. As for the control beams (2HW and 1HW) that without stirrups, the diagonal shear failure appears in a brittle manner with the formation of a large diagonal crack of greater width compared to the control beams containing stirrups, where the first incision started at the load (36 and 45) kN, respectively. The crack began near the support and extending at a 45o angle towards the loading point, the crack widened and stretched more as the load increased, causing the beam to failure when the load (120 and 146) kN respectively, as shown in Figure 4.33 and Figure 4.34.

Figure 4.33 Diagonal shear failure for beam 2HW.

Figure 4.34 Diagonal shear failure for beam 1HW.

After adding the wire mesh to the specimens (2HW4 and 1HW4) with four layers, the first crack appears at (39 and 51) kN in the shear zone. When the load increased, the flexural cracks began to appear and eventually the samples failed due to the development of the diagonal crack at the ultimate load (161 and 195) kN respectively, as shown in Figure 4.35 and Figure 4. 36.

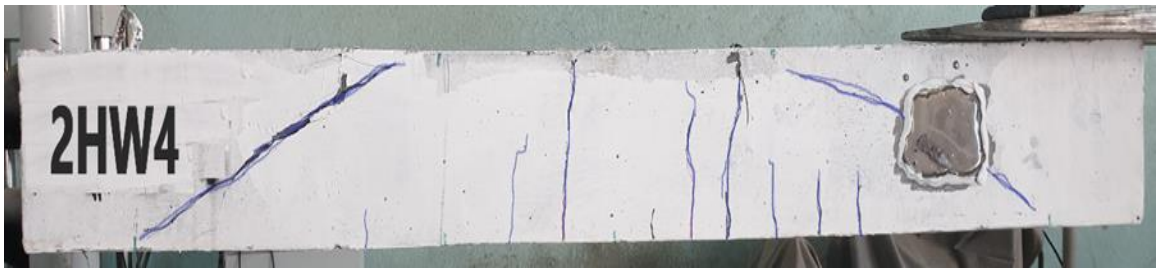

Figure 4.35 Flexural-Shear failure for 2HW4.

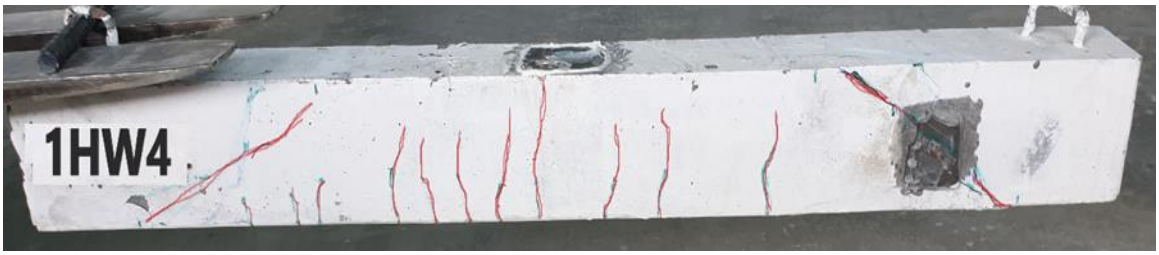

Figure 4.36 Flexural-Shear failure for 1HW4.

As for the specimens (2HW8, 1HW8 and 1HW10) cracks began to appear in the flexural zone when load (45, 55 and 58) kN, when the load was increased the cracks extended towards the top and failed due to the development of one of the flexural cracks at load (199, 240 and 265) kN respectively, as shown in Figure 4.37, Figure 4.38 and Figure 4.39. When comparing specimens containing stirrups with specimens without stirrups, the delayed appearance of cracks was observed in the specimens containing stirrups with wire mesh as the stirrups contributed to making the specimen more strength and make it more stiffness. Also, with the stirrups the diagonal crack is relatively narrower at formation.

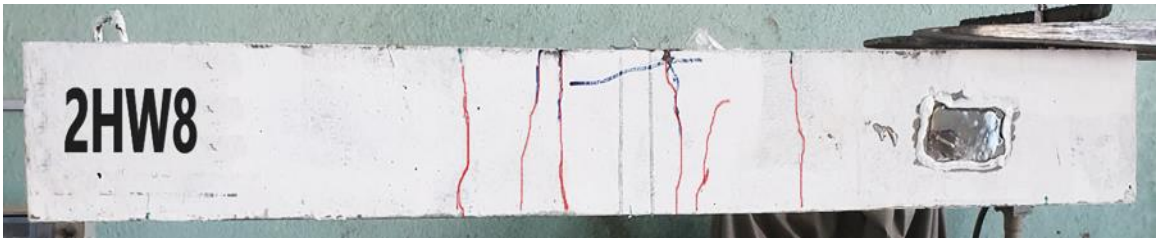

Figure 4.37 Flexural failure for beam 2HW8.

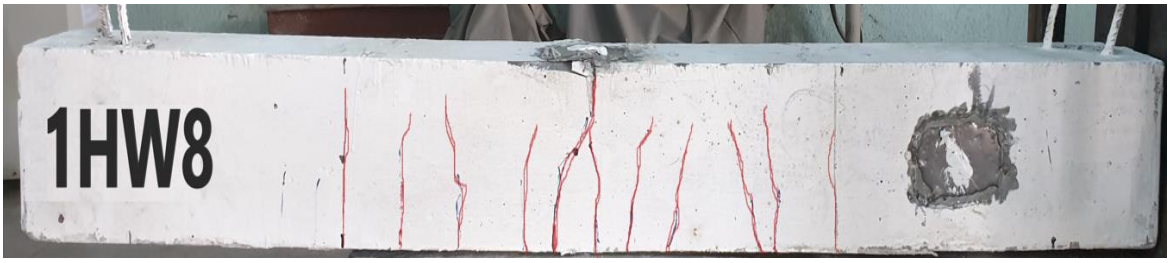

Figure 4.38 Flexural failure for beam 1HW8.

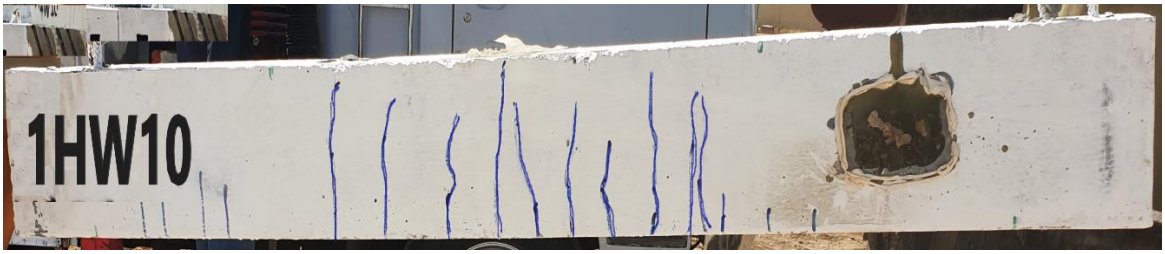

Figure 4.39 Flexural failure for beam 1HW10.

CHAPTER FIVE: CONCLUSIONS AND RECOMMENDATIONS

5.1 General

This study aims to develop understanding of the shear behavior of beams. Based on the experimental work of this study, the following observations can be drawn and recommendations for future works.

5.2 Conclusions

1. The present study found that U-shaped wire mesh effectively enhance the shear capacity of beams and increases the ultimate load with the increase in the number of layers compared to control beams.
2. The shear span to the effective depth ratio is the most critical parameter that controls the behavior and shear capacity of beams. The increase in the shear span to the effective depth ratio leads to a decrease of the ultimate loads and an increase of the mid-span deflection, compared to specimens tested with lower shear span.
3. The high-strength and normal- strength mortar beams tested at (a/d) = 2.5 and containing stirrups showed the highest load at 8 layers with a percentage (60 and 46)%, respectively. While the increase rate reaches 44.44% at 10 layers strengthened beam that has the same high mortar strength, except for (a/d) = 1.8.
4. As for the beams without stirrups of high strength mortar and an amount of (a/d) = 2.5 showed the highest load at 8 layers with a percentage of 66%. While the increase rate reaches 82% at 10 layers for the beam that has the same high strength mortar, except for (a/d) = 1.8.
5. Changing the compressive strength from normal to high strength increased the ultimate load of the beam containing 8 layers of wire mesh by up to 24%.

As for the specimens containing stirrups with wire mesh, the ultimate load improved compared to the specimens without stirrups by up to 24.6%.

6. The addition of the wire mesh with stirrups led to a decrease in the deflection values by up to 20.3%. The decrease of the ultimate deflection of the beams is mainly due to increasing the volume fraction. The use of a larger number of layers leads to an increase in the confining of the zone along shear span, and this in turn contributes to reducing the effective length of the beam due to the increase in stiffness. So the increase of the stiffness reduces the deflection of the beams.
7. The beams with greater shear span show higher ductility than the beams with less shear span by up to 40% where the distance of the load point to the support was greater which increases the deflection and therefore the observed behavior of strengthened beams was more ductility.
8. When comparing specimens made of high-strength mortar with normal - strength mortar, the ductility results show with the presence of transverse reinforcement, high strength mortar becomes more ductility, even more than normal mortar by up to 67%.
9. For beams with 8 and 10 layers of wire mesh had lower ductility index than control beams by up to 13%. Where that increasing the number of mesh layers does not lead to an increase ductility in all beams. The cause of ductility decreasing is due to the members becomes higher stiffness.
10. The initial stiffness increases with increased number of layers compared to control beams by up to 56%.
11. Increase in the energy absorption of beams with an increase in the number of wire meshes compared with control beams by up to 52%.

12. The strains increase the diagonal tensile strain and compressive strain with (a/d) increase by up to (35 and 67)%. That is, the specimens with most ductility shows the more strains.
13. For beams containing 8 and 10 layers of wire mesh, the strains was lower than control beams by up to (19.4 and 24)%. Because the higher the stiffness is, the less deformation of the specimens becomes (That is, have a lower strain).
14. Control beams containing stirrups showed diagonal shear failure. As for beams without stirrups, the diagonal shear failure appears in a brittle manner with the formation of a large diagonal crack of greater width compared to the control beams containing stirrups.
15. Specimens containing stirrups with 4, 8 and 10 layers of wire mesh showed failure to flexural. When The specimens without stirrups containing four layers of wire mesh showed cracks in the shear and flexural zone and eventually the samples failed due to the development of the diagonal crack. As for specimens containing 8 and 10 layers, the flexural failure appeared.

5.3 Recommendations for Future Researchers

1. This study recommends that in order to prevent corrosion in wire meshes, new meshes manufactured of stainless steel, plastic, or any other non-metallic mesh reinforcement may be explored as reinforcement in beam.
2. The theoretical analysis elaborated in this thesis could be used as an indicator of expected values for deflections, strains, loads and crack patterns of the specimens.
3. Fibers may also be incorporated as extra reinforcement in mortar compositions for crack management and resistance to load.

REFERENCES

1. Altoubat, S., Karzad, A. S., Maalej, M., Barakat, S., & Junaid, T. (2020, June). Experimental study of the steel/CFRP interaction in shear-strengthened RC beams incorporating macro-synthetic fibers. In *Structures* (Vol. 25, pp. 88-98). Elsevier.
2. Al-Rousan, R. Z., & Shannag, M. J. (2018, June). Shear repairing and strengthening of reinforced concrete beams using SIFCON. In *Structures* (Vol. 14, pp. 389-399). Elsevier.
3. https://www.researchgate.net/figure/Tested-beam-Pb2-after-shear-failure_fig4_318012919
4. Al-Harbi, E. B. F., Al-Saadi, G. A., & Elragi, A. F. Effect of Different Parameters of U-Concrete Jacketing on Behavior of Strengthened Beam.
5. Iqbal, S., Ali, A., Holschemacher, K., Bier, T. A., & Shah, A. A. (2016). Strengthening of RC beams using steel fiber reinforced high strength lightweight self-compacting concrete (SHLSCC) and their strength predictions. *Materials & Design*, *100*, 37-46.
6. Ahmad, S., Elahi, A., Barbhuiya, S. A., & Farid, Y. (2012). Use of polymer modified mortar in controlling cracks in reinforced concrete beams. *Construction and building materials*, *27*(1), 91-96.
7. Ghai, R., Bansal, P. P., & Kumar, M. (2018). Strengthening of RCC beams in shear by using SBR polymer-modified ferrocement jacketing technique. *Advances in Civil Engineering*, *2018*.
8. Naaman, A. E. (2000). *Ferrocement and laminated cementitious composites* (Vol. 3000, p. 26). Ann Arbor: Techno press.
9. Kondraivendhan, B., & Pradhan, B. (2009). Effect of ferrocement confinement on behavior of concrete. *Construction and Building Materials*, *23*(3), 1218-1222.
10. Batra, A., Ghangas, S., Kumar, L., & Saxena, H. (2017). A Review study of Application of Ferro-Cement. *International Research Journal of Engineering and Technology (IRJET)*, *4*(06).
11. Lalaj, O., Yardım, Y., & Yılmaz, S. (2015). Recent perspectives for ferrocement. *Res. Eng. Struct. Mat*, *1*, 11-23.
12. Pawar, R. (2018). FERROCEMENT TECHNOLOGY. *Maharashtra Engineering Research Institute.*
13. Sharma, P. (2016). Analytical Research on Ferrocement: Design, Strength and Servicibility Aspects.

14. Yardim, Y. (2018). Review of research on the application of ferrocement in composite precast slabs. *Periodica Polytechnica Civil Engineering*, *62*(4), 1030-1038.
15. Al-Sulaimani, G. J., & Basunbul, I. A. (1991). Behavior of ferrocement material under direct shear. *Journal of ferrocement*, *21*(2), 109-117.
16. Al-Sulaimani, G. J., Basunbul, I. A., & Mousselhy, E. A. (1991). Shear behavior of ferrocement box beams. *Cement and Concrete Composites*, *13*(1), 29-36.
17. Mahmood, M. N., & Majeed, S. A. (2009). Flexural Behavior of flat and folded ferrocement panels. *Al-Rafidain Engineering*, *17*(4), 1-11.
18. El-Wafa, M. A., & Fukuzawa, K. (2010). Flexural behavior of lightweight ferrocement sandwich composite beams. *Journal of Science and Technology*, *15*.
19. Savale, M. N., & Alandkar, P. M. (2013). Shear behaviour of ferrocement plates. *International Journal of Innovative Research in Science, Engineering and Technology*, *2*(2).
20. Chkheiwer, A. H., Al-Mazini, M. A., & Zewair, M. S. (2016). Shear Behavior of Slender Ferrocement Box Beams. *Muthana J Eng Technol*, *4*, 1-10.
21. Shaaban, I. G., Shaheen, Y. B., Elsayed, E. L., Kamal, O. A., & Adesina, P. A. (2018). Flexural characteristics of lightweight ferrocement beams with various types of core materials and mesh reinforcement. *Construction and Building materials*, *171*, 802-816.
22. Rafeeqi, S. F. A., Lodi, S. H., & Wadalawala, Z. R. (2005). Behaviour of reinforced concrete beams strengthened in shear. *Journal of Ferrocement*, *35*(1), 479.
23. Zhao, C. Y., Huang, S. M., Yao, Q. L., & Chen, Y. J. (2012). Research on shearing performance of RC beams strengthened with steel wire-polymer mortar. In *Applied Mechanics and Materials* (Vol. 166, pp. 1702-1708). Trans Tech Publications Ltd.
24. Sun, Y. H., Chen, Q. D., Liu, J. W., & Xiong, G. J. (2012). Experimental Research on Shear Property of Steel Bar/Wire Mesh Mortar Strengthening Concrete Beams. In *Applied Mechanics and Materials* (Vol. 204, pp. 3206-3212). Trans Tech Publications Ltd.
25. Hanche, N. (2016). Behaviour and Strength of Ferrocement Rectangular Beams in Shear-A Experimental Study. *J Civil Environ Eng*, *6*(213), 2.
26. El-Sayed, T. A., & Erfan, A. M. (2018). Improving shear strength of beams using ferrocement composite. *Construction and Building Materials*, *172*, 608-617.
27. Elavarasi, D., & Sumathi, A. (2019). Behaviour of Reinforced Concrete Beams with Wire Mesh As Shear Reinforcement. *International Journal of Innovative Technology and Exploring Engineering (IJITEE)*, *8*(12) 781-784.

28. Ojaimi, M. F. (2021). Experimental Study on Shear Strengthening of Reinforced Concrete Beams Using Different Techniques of Concrete Jacketing. *Basrah Journal for Engineering Science*, *21*(2).
29. Ahmed, E., Sobuz, H. R., & Lee, J. B. H. FLEXURAL AND CRACKING PERFORMANCE OF REINFORCED CONCRETE BEAM STRENGTHENED WITH FERROCEMENT LAMINATES.
30. ALAM, M. R., HOSSAIN, M. A., DEY, R. & UDDIN, M. M. (2014). FLEXURAL RETROFITTING OF REINFORCED CONCRETE BEAM USING FERROCEMENT.
31. Fahmy, E. H., Shaheen, Y. B., Abdelnaby, A. M., & Abou Zeid, M. N. (2014). Applying the ferrocement concept in construction of concrete beams incorporating reinforced mortar permanent forms. *International Journal of Concrete Structures and Materials*, *8*(1), 83-97.
32. Ganapathy, L., & Sakthieswaran, N. (2015). Strengthening Of Reinforced Cement Concrete Beam Using Fibrous Ferrocement Laminates. *International Journal of Science and Engineering Research (IJ0SER)*, *3*(5).
33. Ezz-Eldeen, H. A. (2015). An experimental study on strengthening and retrofitting of damaged reinforced concrete beams using steel wire mesh and steel angles. *International Journal of Engineering Research and Technology*, *4*(5), 164-173.
34. Sirimontree, S., Witchayangkoon, B., Leartpocasombut, K., & Thongchom, C. (2019). Flexural Behavior of Reinforced Concrete Beams Strengthened with Ferrocement. *International Transaction Journal of Engineering, Management, & Applied Sciences & Technologies*, *10*(9).
35. Islam, G. S., Haque, M. N., Alam, M. R., Niloy, S. H., & Islam, M. M. (2020). U-shaped ferrocement wrapping with inter-surface locking for flexural strengthening of RC beam. *Australian Journal of Structural Engineering*, *21*(2), 143-153.
36. Al, A. M. İ. N., TAMAL, S., Bari, A. F., Mazumder, M., & Hasan, M. A. (2022). Strengthening of fire damaged reinforced beams by using ferro cement. *Turkish Journal of Engineering*, *6*(3), 206-210.
37. Hughes, B. P., & Evbuomwan, N. F. O. (1993). Polymer-modified ferrocement enhances strength of reinforced concrete beams. *Construction and Building Materials*, *7*(1), 9-12.
38. Fahmy, E., & Shaheen, Y. (1995, March). Use of laminated ferrocement for strengthening and repairing of reinforced concrete beams. In *Civil engineering research magazine* (pp. 589-598).
39. Bansal, P. P., Kumar, M., & Kaushik, S. K. (2008). Effect of wire mesh orientation on strength of beams retrofitted using ferrocement jackets. *International Journal of Engineering*, *2*(1), 8-19.

40. Patil, S. S., Ogale, R. A., & Dwivedi, A. K. (2012). Performances of chicken mesh on strength of beams retrofitted using ferrocement jackets. *Journal of Engineering*, *2*(7), 1-10.
41. Ladi, Y. V., & Mohite, P. M. (2013). Experimental evaluation of reinforced concrete beam retrofitted with ferrocement. *International journal of research in engineering and technology*, *2*(3).
42. A Majeed, S. (2013). Finite Element Analysis of Strengthened Reinforced Concrete Beams. *Al-Rafidain Engineering Journal (AREJ)*, *21*(1), 134-145.
43. Makki, R. F. (2014). Response of reinforced concrete beams retrofitted by ferrocement. *International Journal of Scientific & Technology Research*, *3*(9), 27-34.
44. Al-Rifaie, W. N., Ismaeel, N. N., & Riyad, H. (2017). Rehabilitation of Damaged Reinforced Concrete Beams. *IOSR Journal of Mechanical and Civil Engineering (IOSR-JMCE)*, *14*(6), 58-70.
45. Hassan, R. F. (2018). Flexural and Shear Behavior of RC Concrete Beams Reinforced with Fiber Wire Mesh. *Journal of University of Babylon for Engineering Sciences*, *26*(3), 264-273.
46. Specification, I. (1984b). No. 5, Portland Cement. Iraqi Specif., Iraqi Specifications.
47. Specification, I. (1984a). No. 45, Aggregate from natural sources for concrete and construction. In Iraqi Specif.
48. ASTM C1240-05. 2005. *Standard Specification for Silica Fume Used in Cementitious Mixtures*. West Conshohocken, United States.
49. Imam, A., Kumar, V., & Srivastava, V. (2018). Review study towards effect of Silica Fume on the fresh and hardened properties of concrete. *Advances in concrete construction*, *6*(2), 145.
50. Selvapriya, R. (2019). Silica fume as Partial Replacement of Cement in Concrete. *International Research Journal of Multidisciplinary Technovation (IRJMT), ISSN*, 2582-1040.
51. Shah, A., Khan, S., Khan, R., & Jan, I. U. (2013). Effect of high range water reducers (HRWR) on the properties and strength development characteristics of fresh and hardened concrete. *Iranian Journal of Science and Technology. Transactions of Civil Engineering*, *37*(C), 513.
52. Perenchio, W. F. (1993). Guide for the Use of High-Range Water-Reducing Admixtures (Superplasticizers) in Concrete.
53. ASTM C 494/C 494M – 05a. (2006). In *Standard Specification for Chemical Admixtures for Concrete*[1]. West Conshohocken, United States.
54. ACI Committee 549, "Guide for the Design, Construction, and Repair of Ferrocement", ACI 549.1R-93.

55. ASTM A615/A615M-20. (2020). *Standard Specification for Deformed and Plain Carbon-Steel Bars for Concrete Reinforcement*. United States.
56. ASTM C 109/C 109M– 02. (2002). Standard Test Method for Compressive Strength of Hydraulic Cement Mortars (Using 2-in. or [50-mm] Cube Specimens). *Annual Book of ASTM Standards*, vol 04.01.
57. ASTM C348-02. (2002). *Standard Test method for Flexural Strength of Hydraulic-Cement Mortars*. West Conshohocken, United States.
58. ASTM C780-16. (2016). *Standard Test Method for Preconstruction and Construction Evaluation of Mortars for Plain and Reinforced Unit Masonry*. West Conshohocken, United States.
59. Pam, H. J., Kwan, A. K. H., & Islam, M. S. (2001). Flexural strength and ductility of reinforced normal-and high-strength concrete beams. *Proceedings of the Institution of Civil Engineers-Structures and Buildings*, *146*(4), 381-389.
60. Sullivan, T. J., Calvi, G. M., & Priestley, M. J. N. (2004, August). Initial stiffness versus secant stiffness in displacement based design. In *13th World Conference of Earthquake Engineering (WCEE)* (No. 2888).
61. Erfan, A. M., & El-Sayed, T. A. (2019). Shear Strength of Ferrocement Composite Box Section Concrete Beams. *Int. J. Sci. Eng. Res*, *10*, 260-279.

الخلاصة

نشرت لجنة ACI 549 تعريفا عاما للفيروسمنت نص على ان الفيروسمنت نوع من الخرسانة المسلحة ذات جدران رقيقة يتم بناؤها من مونة الاسمنت الهيدروليكي المقوى بطبقات متباعدة من شبكة سلكية صغيرة الحجم. الفيروسمنت هي مادة بناء تتمتع بصفات فائقة في التحكم بالشقوق، ومقاومة الصدمات، والمتانة ويرجع ذلك إلى التباعد والتشتت المنتظم للشبكات. تهدف الدراسة الحالية إلى التحقق من سلوك القص للعتبات المعرضة لفشل القص مع إضافة عدد من طبقات الشبكة السلكية. يتكون العمل التجريبي من سبعة عشر عتبة بأبعاد (150 × 200 × 1600) مم تم اختبارها تحت تحميل نقطتين. تم فحص متغيرات مختلفة للتنبؤ بتأثيرها على سلوك القص للعتبات. تشمل المتغيرات التي تم فحصها في البرنامج التجريبي من مقاومة الانضغاط (35 و 65) ميجا باسكال، ومدى القص المتغير إلى نسبة العمق الفعال (أ/ د = 1.8 و 2.5)، عدد طبقات الشبكات السلكية (4 ، 8 و 10) ، بالإضافة إلى لتأثير الحلقات. أثناء العمل التجريبي، تم تقسيم العتبات إلى خمس مجاميع حسب متغيرات العمل. تتكون كل مجموعة من ثلاث عتبات باستثناء المجموعة الثالثة والرابعة المكونة من أربع عتبات. المجموعات الأولى والثانية والخامسة لها نفس (أ / د) = 2.5 و نفس عدد الطبقات (4 و 8). متغير المجموعة الثانية والخامسة كمية الحلقات ومقاومة الانضغاط على التوالي. المجموعتان الثالثة والرابعة فلهما نفس (أ / د) = 1.8 نفس عدد الطبقات (4 و 8 و 10) ونفس قوة الانضغاط 65 ميجا باسكال. باستثناء المجموعة الرابعة التي لا تحتوي على حلقات. يتم فحص سلوك العتبات من خلال الحمل النهائي، وحمل الشق الأول، واستجابة انحراف الحمولة، وتوزيع الانفعالات وانماط الفشل. بشكل عام، يزداد الحمل النهائي مع زيادة عدد الطبقات مقارنة بعتبات المرجعية. أدت إضافة الشبكات السلكية إلى تحسين الحمل النهائي بنسب تتراوح من (16 إلى 82)٪. أظهر نتائج الاختبار أيضًا أن الزيادة في مدى القص إلى نسبة العمق الفعال تؤدي إلى انخفاض الحمل النهائي وزيادة انحراف منتصف المدى، مقارنة بالعتبات ذات المدى القص المنخفض. أدى تغيير مقاومة الانضغاط من المقاومة العادية إلى المقاومة العالية إلى زيادة الحمل النهائي للعتبة التي تحتوي على 8 طبقات من شبكة سلكية بنسبة تصل إلى 24٪. أما بالنسبة للعتبات التي تحتوي على حلقات مع شبكة سلكية، فقد تحسن الحمل النهائي مقارنة بالعتبات التي لا تحتوي على حلقات بنسبة تصل إلى 24.6٪. أدت إضافة الشبكة السلكية مع الحلقات إلى انخفاض قيم الانحراف بنسبة تصل إلى 20.3٪. بينما أظهرت العتبات ذات الامتداد الأكبر ليونة أعلى من العتبات ذات امتداد قص أقل بنسبة تصل إلى 32٪. الصلابة الأولية وامتصاص الطاقة تزداد القيم بزيادة عدد الطبقات مقارنة بالعتبات المرجعية بنسبة تصل الى 56٪ و 52٪ على التوالي. حققت عتبات

المحتوية على شبكات سلكية حمل الشق الأول أعلى بنسبة تصل الى 32.3٪ مقارنة بالعتبات المرجعية. أما بالنسبة لفشل العينات، فقد أظهرت العتبات فشل الانحناء عند (4 ، 8 ، 10) للعتبات المحتوية على حلقات مع شبكات مقارنة بالعتبات المرجعية التي فشات بالقص. أما بالنسبة للعتبات التي لا تحتوي على حلقات فقط تحتوي على شبكات، فقد لوحظ فشل القص عند 4 طبقات وفشل الانحناء عند (8 و10) مقارنة بالعتبات المرجعية.

جمهورية العراق
وزارة التعليم العالي والبحث العلمي
جامعة ميسان / كلية الهندسة
قسم الهندسة المدنية

تحسين قابلية تحمل العتبات الخرسانية المسلحة باستخدام الشبكة السلكية الفولاذية كتقوية للقص

من قبل
ساره حسين حميد
بكالوريوس هندسة مدنية 2018

رسالة
مقدمة الى كلية الهندسة في جامعه ميسان
كجزء من متطلبات الحصول على درجة الماجستير في علوم الهندسة المدنية / الإنشاء

حزيران 2022

بأشراف
الاستاذ الدكتور: عبد الخالق عبد اليمة جعفر